LIBRARY

JOURNAL OF THE

# Electrochemical Society

103, No. 10 October 1956

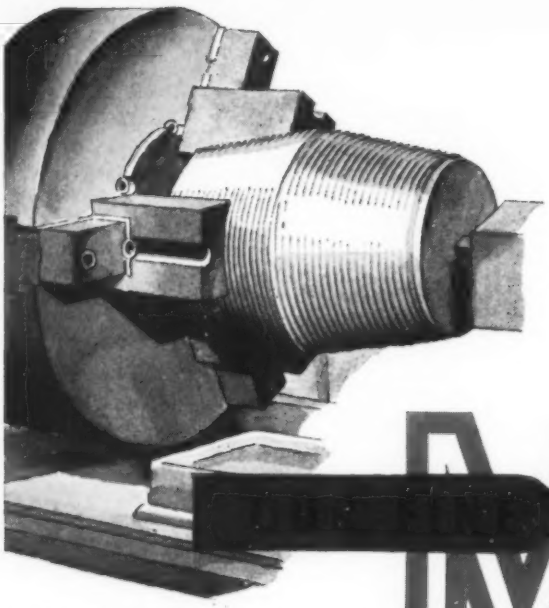

MILLING NIPPLE THREADS

AS PARTNERS IN
YOUR PROGRESS . . .

# MACHINING – is a *plus* factor!

Finishing operations on GLC electrodes, anodes and mold stock are performed with the utmost precision. A strict system of gaging and inspection is required at this stage.

The craftsmanlike spirit of our milling, machining and inspection personnel is a distinctive *plus factor* in the efficiency of GLC carbon and graphite products.

The high degree of integration between discoveries in our research laboratories, refinements in processing raw materials, and improved manufacturing techniques is further assurance of excellent product performance.

ELECTRODE
GLC®
DIVISION

## Great Lakes Carbon Corporation

GRAPHITE ELECTRODES · ELECTRODE BOILERS

ADMINISTRATIVE OFFICE: 18 East 48th Street, New York 17, N.Y. PLANTS: Niagara Falls, N.Y., Morganton, N. C. OTHER OFFICES: Niagara Falls, N.Y., Oak Park, Ill., Pittsburgh, Pa. SALES AGENTS: J. B. Hayes Company, Birmingham, Ala., George O. O'Hara, Wilmington, Cal. SALES AGENTS IN OTHER COUNTRIES: Great Northern Carbon & Chemical Co., Ltd., Montreal, Canada; Great Eastern Carbon & Chemical Co., Inc., Chiyoda-Ku, Tokyo, Japan

EDITORIAL STAFF

R. M. Burns, *Chairman*
Cecil V. King, *Editor*
Norman Hackerman, *Technical Editor*
Ruth G. Sterns, *Managing Editor*
U. B. Thomas, *News Editor*
Natalie Michalski, *Assistant Editor*
Eleanor Blair, *Assistant Editor*

DIVISIONAL EDITORS

W. C. Vosburgh, *Battery*
J. E. Draley, *Corrosion*
John J. Chapman, *Electric Insulation*
Abner Brenner, *Electrodeposition*
H. C. Froelich, *Electronics*
Herbert Bandes, *Electronics—Semiconductors*
Sherlock Swann, Jr., *Electro-Organic*
John M. Blocher, Jr., *Electrothermics and Metallurgy, I*
A. U. Seybolt, *Electrothermics and Metallurgy, II*
W. C. Gardiner, *Industrial Electrolytic*
C. W. Tobias, *Theoretical*

REGIONAL EDITORS

Howard T. Francis, *Chicago*
Joseph Schulein, *Pacific Northwest*
J. C. Schumacher, *Los Angeles*
G. W. Heise, *Cleveland*
G. H. Fetterley, *Niagara Falls*
Oliver Osborn, *Houston*
Earl A. Gulbransen, *Pittsburgh*
A. C. Holm, *Canada*
J. W. Cuthbertson, *Great Britain*
T. L. Rama Char, *India*

ADVERTISING OFFICE

Jack Bain, *Advertising Manager*
545 Fifth Avenue, New York 17, N. Y.

ECS OFFICERS

Hans Thurnauer, *President*
Minnesota Mining & Mfg. Co., St. Paul, Minn.

Norman Hackerman, *Vice-President*
University of Texas, Austin, Texas

Sherlock Swann, Jr., *Vice-President*
University of Illinois, Urbana, Ill.

W. C. Gardiner, *Vice-President*
Olin Mathieson Chemical Corp., Niagara Falls, N. Y.

Lyle I. Gilbertson, *Treasurer*
Air Reduction Co., Murray Hill, N. J.

Henry B. Linford, *Secretary*
Columbia University, New York, N. Y.

*Journal of the*
# Electrochemical Society

**OCTOBER 1956** **VOL. 103 • NO. 10**

CONTENTS

## *Editorial*

Our National Highways ..... 227C

## *Technical Papers*

Some Studies on the Fused Salt Cell, Mg/$LiNO_3$, KCl/Ag. *C. W. Jennings* ..... 531
Association of $Co^{60}$ Ions with Metal Surfaces. *R. T. Foley, B. T. Stark, and C. J. Guare* ..... 534
A Mechanism for the Anodic Dissolution of Magnesium. *J. H. Greenblatt* ..... 539
Properties of Paper Made from Glass Flakes. *T. D. Callinan and R. T. Lucas* ..... 543
Permeation of Gases through Nickel Deposits, I. Determination of the Intrinsic Permeability of Nickel Deposits to Gases. *D. T. Ewing, J. Martin Tobin, and D. G. Foulke* ..... 545
New Design of an Electrolytic Cell for the Study of Electroplating Phenomena. *Roger Gilmont and R. F. Walton* ..... 549
Electron Microscope Studies of Copper Anodes Obtained in Sulfate and Cyanide Baths. *Shinzo Okada, Saburo Magari, and Kentaro Katsui* ..... 553
Electron Microscope Studies on Copper Electrodes in Sulfate Bath Containing Addition Agent. *Shinzo Okada, Saburo Magari, and Kentaro Katsui* ..... 557
Effect of Impurities on the Hardness of Titanium. *T. D. McKinley* ..... 561
Mathematical Studies of Galvanic Corrosion, VI. Limiting Case of Very Thin Films. *J. T. Waber* ..... 567
Oxidation of Alloys Involving Noble Metals. *Carl Wagner* ..... 571
Alternating Current Bridge for Measurement of Electrolytic Conductance. *F. S. Feates, D. J. G. Ives, and J. H. Pryor* 580

## *Technical Feature*

Alaska's Power Resources in Relation to Mineral Development. *Ivan Bloch* ..... 586

## *Current Affairs*

News Notes in the Electrochemical Field ..... 229C
Division News ..... 230C
Section News ..... 230C
Personals ..... 231C
Book Reviews ..... 232C
Announcements from Publishers ..... 232C
New Products ..... 233C
Literature from Industry ..... 234C

Published monthly by The Electrochemical Society, Inc., Mount Royal and Guilford Aves., Baltimore 2, Md., combining the JOURNAL and TRANSACTIONS OF THE ELECTROCHEMICAL SOCIETY. Editorial offices: 216 West 102nd Street, New York 25, N. Y. Statements and opinions given in articles and papers in the JOURNAL OF THE ELECTROCHEMICAL SOCIETY are those of the contributors, and The Electrochemical Society assumes no responsibility for them. Nondeductible subscription to members $5.00; subscription to nonmembers $18.00. Single copies $1.25 to members, $1.75 to nonmembers. Copyright 1956 by The Electrochemical Society, Inc. Entered as second-class matter November 15, 1947, at the Post Office at Baltimore, Md., under the act of August 24, 1912.

# Two Separate Circuits Mean

# Reliable Rectifier Operation

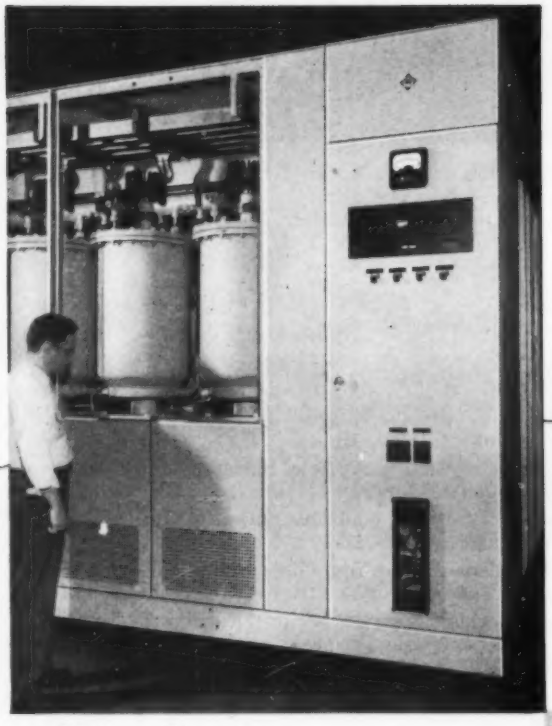

ALLIS-CHALMERS

**Mercury Arc Rectifiers**

One of four metal-enclosed assemblies in a midwestern installation with a total capacity of 15,000 kw at 620 volts, dc.

## 1. Firing Circuit

A small dc excitation arc is automatically ignited only once, when the unit is started. It is then maintained on the mercury cathode of each rectifier tube. It offers advantages similar to a pilot light. Since it is far easier to maintain an arc than to start it, this feature reduces the chance of the excitron losing excitation during power supply disturbances.

## 2. Phase Control Circuit

A separate circuit utilizes the deionizing grid to obtain phase control. Grid-type phase control permits operation in the clean region near the anode where ion density is lowest, instead of on the surface of the cathode mercury pool where there is turbulence and contamination. Reliability of phase control does not depend on the condition of the mercury. This is an exclusive excitron feature.

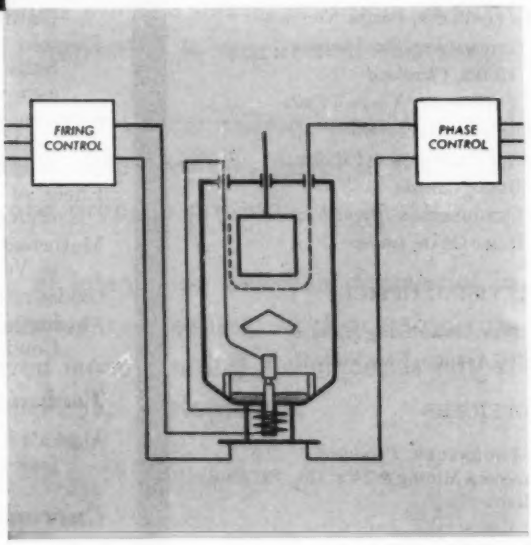


**Only Excitron Rectifiers Provide Separate Circuits**

for these two all-important functions. Improved operation results — one function is never sacrificed for the other—you get optimum operation from each.

**For Complete Information** on rectifier operation, call your nearby A-C office, or write Allis-Chalmers, Industrial Equipment Division, Milwaukee 1, Wisconsin.

# ALLIS-CHALMERS

A-C ALLIS-CHALMERS

A-5136

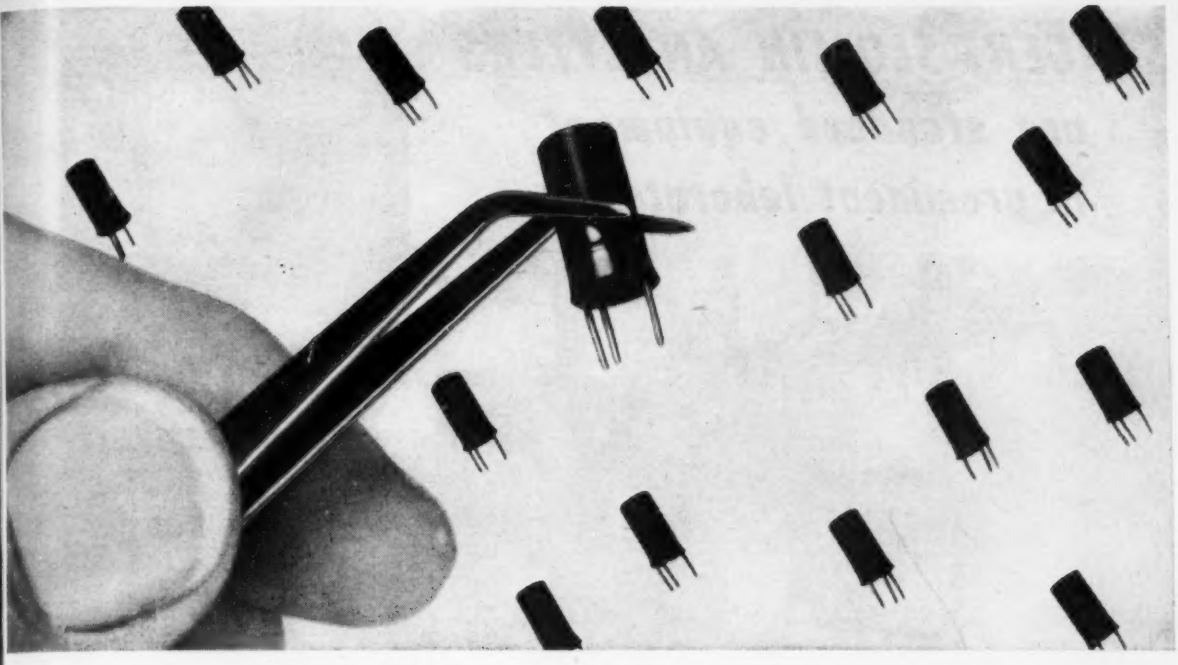

## NOW! From BAKER & ADAMSON...

# A New High in Electronic Chemical Purity for Production of Semiconductors!

### ...Drastic reduction of metallic and other undesirable impurities

Previous standards of chemical purity have been outmoded by the stringent quality requirements of the electronics industry—especially for chemicals used in the production of semiconductor devices.

Baker & Adamson, the country's leading producer of extremely high purity laboratory and scientific chemicals, now meets these demands with "electronic grade" chemicals that establish a new high in chemical purity. Metallic and other undesirable impurities are held to lower limits than ever before.

Listed here is a group of these extremely high purity chemicals made especially for the production of electronic devices—part of B&A's extensive line of electronic grade chemicals. Call or write your nearest B&A sales office today for information on any of the following . . . or other electronic chemicals you may need.

**Acetone**

**Acids**
- Glacial Acetic
- Hydrochloric (Muriatic)
- Hydrofluoric, 48%
- Nitric
- Sulfuric

**Alcohol, Methyl and Propyl**

**Bromine**

**Carbon Tetrachloride**

**Ether**

**Glycerine**

**Hydrogen Peroxide, 3% & 30%**

**Indium Fluoborate**

**Toluene**

**Trichloroethylene**

**Xylene**

**BAKER & ADAMSON®**
**Electronic Grade Chemicals**

**GENERAL CHEMICAL DIVISION**
ALLIED CHEMICAL AND DYE CORPORATION
**40 Rector Street, New York 6, N. Y.**

FINE CHEMICALS
B·A
REAGENTS

Allied Chemical

*Offices:* Albany* • Atlanta • Baltimore* • Birmingham* • Boston* • Bridgeport* • Buffalo* • Charlotte* • Chicago* • Cleveland* • Denver* • Detroit* • Houston* Jacksonville • Kalamazoo • Los Angeles* • Milwaukee • Minneapolis • New York* • Philadelphia* • Pittsburgh* • Providence* • St. Louis* • San Francisco* Seattle • Kennewick* and Yakima (Wash.) **In Canada: The Nichols Chemical Company, Limited • Montreal* • Toronto* • Vancouver*** **Complete stocks carried here.*

# SARGENT-SLOMIN ANALYZERS
## are standard equipment in prominent laboratories

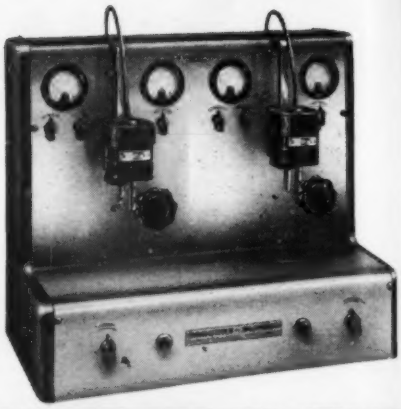

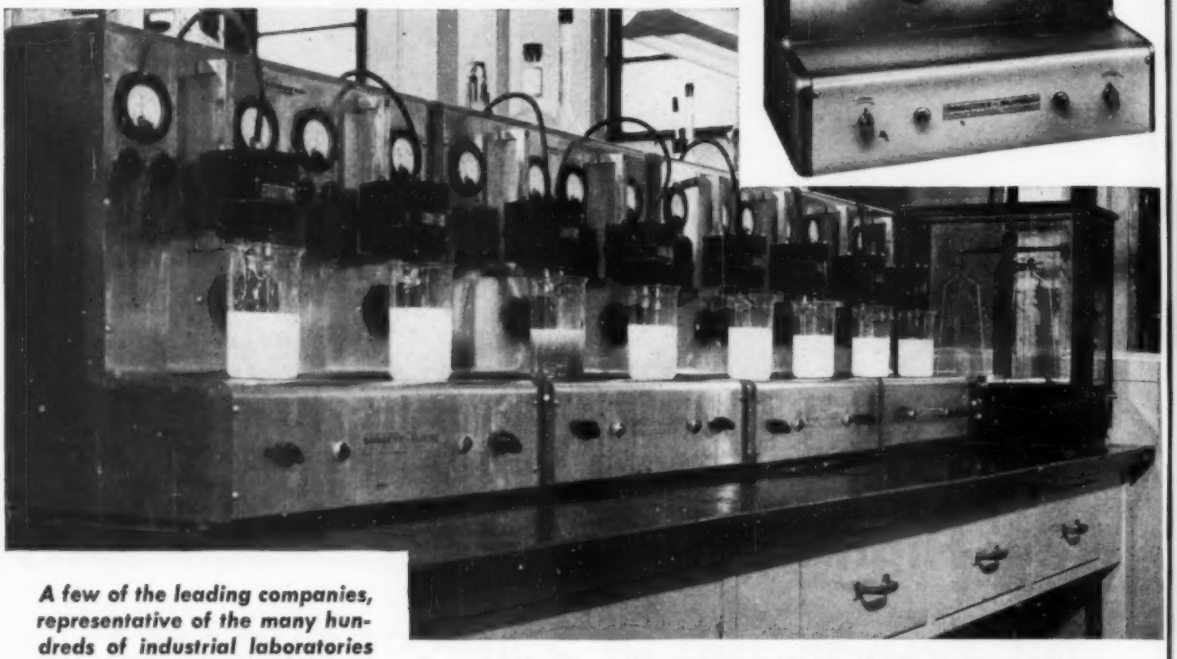

Photo Courtesy INTERNATIONAL HARVESTER COMPANY, Melrose Park, Illinois

***A few of the leading companies, representative of the many hundreds of industrial laboratories using the Sargent - Slomin and Heavy Duty Analyzers for control analyses . . .***

AMPCO METAL, Inc.
ANDERSON LABORATORIES
CALERA MINING COMPANY
EUREKA WILLIAMS COMPANY
THE FEDERAL METAL CO.
FORD MOTOR COMPANY
THE GLIDDEN COMPANY—Chemical, Metal and Pigment Division
HOT POINT CO.
HOWARD FOUNDRY COMPANY
INTERNATIONAL HARVESTER COMPANY
KENNAMETAL Inc.
McQUAY - NORRIS MANUFACTURING CO.
NATIONAL LEAD COMPANY, Fredericktown, Missouri
PIASECKI HELICOPTER CORPORATION
REVERE COPPER & BRASS INCORPORATED
THE RIVER SMELTING & REFINING COMPANY
SILAS MASON COMPANY
THE STUDEBAKER CORPORATION
THOMPSON PRODUCTS, INC.

Sargent-Slomin Electrolytic Analyzers are recommended for such electro analytical determinations as: Copper in—ores, brass, iron, aluminum and its alloys, magnesium and its alloys, bronze, white metals, silver solders, nickel and zinc die castings. Lead in—brass, aluminum and its alloys, bronze, zinc and zinc die castings. Assay of electrolytical copper, nickel and other metals.

Sargent analyzers are completely line operated, employing self-contained rectifying and filter circuits. Deposition voltage is adjusted by means of autotransformers, with meters indicating volts and amperes and controls on the panel. An easily replaceable fuse guards against circuit overload. Maximum D.C. current capacity is 5 to 15 amperes; maximum D.C. voltage available, 10 volts.

Sargent-Slomin Analyzers stir through a rotating chuck operated from a capacitor type induction motor, having a fixed speed of 550 r.p.m. with 60 cycle A.C. current or 460 r.p.m. with 50 cycle A.C. current. Motors are sealed against corrosive fumes and are mounted on cast metal brackets, sliding on ½" square stainless steel rods, permitting vertical adjustment of electrode position over a distance of 4". Pre-lubricated ball-bearings support the rotating shaft. All analyzers accommodate electrodes having shaft diameters no greater than 0.059 inch. Stainless steel spring tension chucks permit quick, easy insertion of electrodes and maintain proper electrical contact. Special Sargent high efficiency electrodes are available for these analyzers. Illustrated above is one model of the five types of Sargent-Slomin and Heavy Duty Analyzers.

**S-29465** ELECTROLYTIC ANALYZER—Motor stirred, Two Position, 5 Ampere. With two adjustable heaters, pilot lights and control knobs. For operation from 115 volt, 50 or 60 cycle A.C. circuits.....**$475.00**

# SARGENT
**SCIENTIFIC LABORATORY INSTRUMENTS • APPARATUS • SUPPLIES • CHEMICALS**

*Catalog No. 100 Now Available*

**E. H. SARGENT & COMPANY, 4647 W. FOSTER AVE., CHICAGO 30, ILLINOIS**
MICHIGAN DIVISION, 8560 WEST CHICAGO AVENUE, DETROIT 4, MICHIGAN
SOUTHWESTERN DIVISION, 5915 PEELER STREET, DALLAS 19, TEXAS
SOUTHEASTERN DIVISION, 3125 SEVENTH AVE., N., BIRMINGHAM 4, ALA.

# Editorial

## Our National Highways

*IN THE* depression days of the early 1930's, a small group in Congress tried to promote a 12-billion-dollar highway program. The proposal was to build six "superhighways" from coast to coast and eight or ten similar north-and-south roads. The purpose was to provide and stimulate wide employment, to "prime the pump"; but also to have something of immediate usefulness, of tangible value, and of lasting economic benefit to show for the billions spent. Of course no one can say how much this program, if it had been adopted and carried out, would have affected automotive transport today; we might have inherited an excellent highway system, or thousands of miles of too-narrow, worn-out country lanes. In any case, the proposal received scant consideration by Congress or Administration.

Under the enormous pressure created by huge numbers of private and commercial vehicles, and the frustration and waste of trying to cope with congested and dangerous roads, the 1956 Congress passed a bill authorizing Federal expenditure of some 34 billion dollars over the next 13 years, for new highways and highway improvement. This will build, at present costs, about the same number of miles as the previous 12-billion-dollar proposal, probably of superior quality. It will be the duty of all of us to insist that the money be spent wisely and properly, for the best in materials and workmanship, and with adequate balance between local needs and the requirements of longer-distance travel.

In the horse-and-buggy days it was natural that the "improved" roads should lead from village to village, and traverse Main Street of every town. Even in the early days of the automobile no great problem was created. By 1920 it was evident that the business streets were inadequate for local and through traffic too; but only in very recent years has the merchant become convinced that the heavy stream of passing traffic will never be a golden asset to him. The diversion to side streets, by-passes, and parkways is not yet complete, but is already antedated. Motorists and truck owners alike are willing to pay, and pay well, to avoid city streets unless they have direct business there.

Obviously, two good highway systems are needed, with easy connection between the two: one for the milk and bakery trucks, the factory workers, and the farmers to use for daily business, the other for quick and safe long-distance travel. Limited-access toll super-highways are no doubt the best solution in the second case. It is difficult to limit access to "free" roads and to prevent them from becoming lined with new housing developments, stores, diners, gas stations, factories. At present they are cluttered with local, low-speed traffic. Since most or all of the highways to be built under the new program will be "free" roads, we hope that these problems will receive the most serious consideration.

The highway program will have a larger impact on chemical and electrochemical industries than appears on the surface. Road-building machinery and road-bed materials will be only the beginning. Much more automotive transportation will be on the roads in future years if only adequate roads are there, and 41,000 miles of new and improved highways will be a strong stimulus to travel and transport. Automobiles, their metals, finishes, fuels, tires, accessories, all require increasing attention from scientific industry and scientific research.

—CVK

# FUTURE MEETINGS OF
# The Electrochemical Society

## Washington, D. C., May 12, 13, 14, 15, and 16, 1957

**Headquarters at the Statler Hotel**

**Sessions probably will be scheduled on**
**Electric Insulation, Electronics (including Luminescence,**
**Semiconductors, Oxide Cathodes, Instrumentation,**
**and possibly Screen Applications),**
**Electrothermics and Metallurgy, Industrial**
**Electrolytics, and Theoretical**
**Electrochemistry (including a special symposium on electrolytes)**

★ ★ ★

## Buffalo, October 6, 7, 8, 9, and 10, 1957

**Headquarters at the Statler Hotel**

★ ★ ★

## New York, April 27, 28, 29, 30, and May 1, 1958

**Headquarters at the Statler Hotel**

★ ★ ★

## Ottawa, September 28, 29, 30, October 1, and 2, 1958

**Headquarters at the Chateau Laurier**

★ ★ ★

Papers are now being solicited for the meeting to be held in Washington, D. C. Triplicate copies of each abstract (*not exceeding 75 words in length*) are due at the Secretary's Office, 216 West 102nd St., New York 25, N. Y., *not later than January 2, 1957* in order to be included in the program. *Please indicate on abstract for which Division's symposium the paper is to be scheduled*. Complete manuscripts should be sent in triplicate to the Managing Editor of the JOURNAL at the same address.

# Some Studies on the Fused Salt Cell

## $Mg/LiNO_3$, KCl/Ag

CHARLES W. JENNINGS

*Department of Chemistry, North Carolina State College, Raleigh, North Carolina*

ABSTRACT

The fused salt cell, $Mg/LiNO_3$, KCl/Ag, was studied at temperatures from 300° to 500°C. Cell characteristics varied with the KCl content. With greater than 20 mole % KCl open-circuit voltages of 1.4–1.6 v were obtained. Cells were discharged at 4–100 ma/cm². Both Ag and Mg reacted directly with the electrolyte. The extent of reaction of Mg varied with the KCl content. Substitution of Pt, Ni, or graphite for Ag increased the open-circuit voltage. A mechanism is proposed in which Ag is involved in the cell reaction.

The literature on fused salt cells relates principally to reversible cells, usually of the type $M/MCl_y$, $XCl/Cl_2$, where $X$ is an alkali metal and $M$ a metal like Pb, Bi, Ag, Zn, Co, Cu, Ni, or Fe (1–3). Similar cells with bromide salts and bromine have also been reported (4). The cells were studied mainly to obtain thermodynamic values; discharge characteristics were not given. Fused salt cells that have been used to furnish electric current have been reported by Hamer and Schrodt (5) and Goodrich and Evans (6), and the general subject of fuel cells in which fused salts have been used has been discussed by Kortum and Bockris (7), Vinal (8), and others.

This investigation was initiated to study fused salt cells that could deliver electrical energy under load at temperatures under 500°C. One such cell, $Mg/LiNO_3$, KCl/Ag, was studied in detail. The work on this cell is largely qualitative in nature, but at the present time it cannot be extended. Because of the scarcity of published data on electrochemical discharges in fused salt systems, it is believed that the results will be of interest to workers in this field.

### EXPERIMENTAL

Negative electrodes were of $\frac{1}{4}$ or $\frac{3}{32}$ in. commercially pure Mg rod. Typical analyses of the rod, obtained from the Dow Chemical Co., gave Al, 0.003; Cu, 0.003; Fe, 0.03; Mn, 0.08; Ni, 0.001; Si, 0.005; and Mg, 99.878% (by difference). The positive electrodes were of rolled silver sheet. Both electrodes were cleaned with $HNO_3$, washed, and dried at 110°C prior to use in the cells. The salts were Merck's or Baker and Adamson's Reagent Grade. For most of the experiments about 50 g of salt mixture was weighed out on a balance (accurate to ±0.02 g) and placed in a Pyrex test tube. The mixture was dried at 110°C for several days and heated in a Hoskins type FD 101 electric furnace. The lower half of the Pyrex tube was in the furnace. An inert gas, helium, was passed through the melt for ½–3 hr. The electrode assembly, shown in Fig. 1, was inserted and the emf of the cell was read with a Heathkit vacuum tube voltmeter. The meter could be read to ±0.01 v and had an input impedance of 11 megohms. The temperature was read to ±2°C with an iron-constantan thermocouple. Unless noted otherwise, an atmosphere of He was maintained above the melt at all times.

Moisture content was controlled by maintaining uniform conditions of operation. Salts were weighed, dried, and heated in the same manner in all experiments. No attempt was made to determine the exact moisture content of the mixtures in the fused state, although it is realized that small amounts of moisture could affect cell behavior. Moisture contents of cells in He atmosphere were not sufficient to account for the large currents obtained during discharge at the temperatures studied.

Distance between electrodes was about 1.5 cm. Discharge characteristics of the cells were obtained by applying external loads of 1, 2, 5, 10, 25, 50, or 100 ohms. Values of current density were obtained by dividing the current obtained after 1 min of cell discharge at a given load by the original surface area of the Mg electrode. This area was from 3 to 4 cm². The Ag electrode had approximately the same surface area as the Mg. Voltage-time characteristics of a number of cells were recorded by inserting a Brush Amplifier, Model BL 932 and Recorder, Model 202/931 in parallel with the vacuum-tube voltmeter. The input impedance of the amplifier was 9 megohms. No measurements were made for cell capacity. Cells were usually discharged for 3 min under each set of conditions.

Open-circuit voltage (OCV) and closed-circuit voltage (CCV) measurements were made on cells with electrolyte compositions of 0–70 mole % KCl in $LiNO_3$. Table I gives the OCV's for five cells, each with a different mole per cent KCl in $LiNO_3$. The cells, contained in small test tubes, were heated simultaneously. He was bubbled alternately through the tubes for 2–3 hr before the Mg and Ag electrodes were added. The temperature was read from a thermocouple outside of, but next to, the tubes. The discharge characteristics of these cells with 100 ohms load at 360°C are given in Table II. The lower values in the table give the recovery of OCV after 1-min discharge. Values in Tables I and II are similar to those obtained from cells heated individually in large test tubes.

The best discharge characteristics with heavy current drains were obtained when an electrolyte of 50 mole % KCl in $LiNO_3$ was used. Table III gives the CCV's for

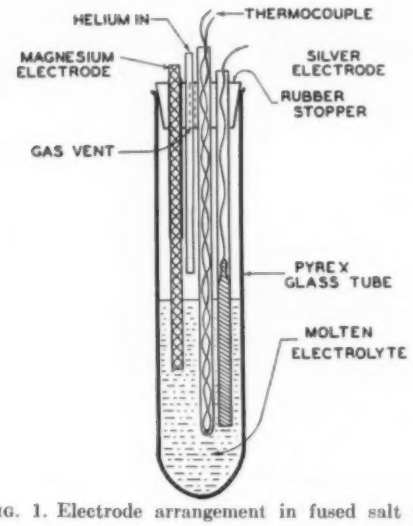


FIG. 1. Electrode arrangement in fused salt cell

TABLE I. *OCV for* $Mg/LiNO_3$, KCl/Ag

| Time (min) | Mole % KCl | | | | | Temp* (°C) |
|---|---|---|---|---|---|---|
| | 0 | 10 | 20 | 30 | 50 | |
| 0 | 1.14 | 1.06 | 1.60 | 1.55 | 1.55 | 366 |
| 10 | 1.14 | 0.94 | 1.56 | 1.59 | 1.52 | 325 |
| 20 | 1.14 | 0.92 | 1.50 | 1.58 | 1.51 | 308 |
| 35 | 1.09 | 0.80 | 1.53 | 1.56 | 1.51 | 323 |
| 50 | 1.06 | 0.75 | 1.57 | 1.57 | 1.52 | 324 |
| 60 | 1.04 | 0.70 | 1.56 | 1.56 | 1.55 | 345 |
| 130 | 0.88 | 0.56 | 1.59 | 1.56 | 1.57 | |
| 160 | 0.55 | 0.51 | 1.60 | 1.58 | 1.57 | |
| 180 | 0.45 | 0.45 | 1.59 | 1.58 | 1.57 | 360 |
| 200 | 0.35 | 0.42 | 1.59 | 1.58 | 1.57 | |
| 240 | 0.26 | 0.45 | 1.56 | 1.56 | 1.57 | 380 |
| 420 | 0.02 | 0.30 | † | † | 1.57 | 384 |

* Outside of tubes.
† Magnesium electrode broke.

this cell at the end of the 3-min discharge period at 475°C. CCV's were averaged at each load from 6 cells, each heated separately. A few cells were discharged at 25 ma/cm² for 15 min or longer at 1.2 v. The voltage changed less than 10% during the discharges. Under loads of 5–100 ohms the magnitude of polarization at the Mg electrode was of the same order as at the Ag electrode. Polarization was measured by comparing an operating electrode with an idle electrode in the same electrolyte.

The electrical output from cells containing less than 20% KCl was poor. The reason for the poor performance of cells with low chloride contents is not known, but appears to be related to film formation on the Mg electrode. Analysis of the system was complicated by side reactions, the principal ones being the direct or corrosion reactions of the Mg and Ag electrodes with the electrolyte.

The characteristics of the cells varied with the proportion of KCl to $LiNO_3$. Cells with only $LiNO_3$ had initial OCV's of 1.0–1.4 v at 300°–370°C. OCV's decreased appreciably with time at any temperature (*see* Table I). In cells with 10% KCl and 90% $LiNO_3$, OCV decreased

TABLE II. *Discharge of* $Mg/LiNO_3$, KCl/Ag *at 100 ohms load at 360°C*

| Time (sec) | Mole % KCl | | | | | | | | | |
|---|---|---|---|---|---|---|---|---|---|---|
| | 0 | | 10 | | 20 | | 30 | | 50 | |
| | V (v) | I (ma) | V (v) | I (ma) | V (v) | I (ma) | V (v) | I (ma) | V (v) | I (ma) |
| 0 | 0.28 | | 0.54 | | 1.57 | | 1.57 | | 1.58 | |
| 5 | 0.24 | 2.0 | 0.43 | 3.8 | 1.42 | 12.5 | 1.50 | 13.2 | 1.49 | 13.2 |
| 15 | 0.23 | 2.0 | 0.41 | 3.5 | 1.42 | 12.6 | 1.48 | 13.1 | 1.48 | 13.2 |
| 30 | 0.22 | 1.9 | 0.41 | 3.3 | 1.42 | 12.6 | 1.48 | 13.1 | 1.48 | 13.2 |
| 45 | 0.22 | 1.9 | 0.41 | 3.2 | 1.41 | 12.6 | 1.47 | 13.1 | 1.48 | 13.2 |
| 60 | 0.22 | 1.9 | 0.41 | 3.2 | 1.41 | 12.6 | 1.47 | 13.1 | 1.48 | 13.2 |
| 3 | 0.26 | | 0.40 | | 1.50 | | 1.54 | | 1.55 | |
| 15 | 0.30 | | 0.50 | | 1.52 | | 1.55 | | 1.56 | |
| 30 | 0.31 | | 0.50 | | 1.53 | | 1.56 | | 1.57 | |
| 60 | 0.34 | | 0.48 | | 1.54 | | 1.56 | | 1.57 | |

TABLE III. *Discharge characteristics for the cell* $Mg/50LiNO_3$-50KCl/Ag *at 475°C*

| OCV (v) | CCV (v) | Current density (ma/cm²) |
|---|---|---|
| 1.45 | 1.40 | 4 |
| | 1.34 | 12 |
| | 1.25 | 25 |
| | 1.15 | 50 |
| | 0.9 | 100 |

with time at all temperatures up to 450°C. Mg corroded rapidly in the electrolyte. With electrolytes of 15% KCl the OCV was stable with time, its value being 1.5 v above 360°C and 0.5 v below 300°C. Somewhere between 300° and 360°C, the OCV changed abruptly, about 1 v, within a few degrees. A fresh Mg electrode inserted in the melt at 300°C region had an initial OCV of 1.4–1.5 v, but decreased with time to 0.5 v. The OCV did not decrease with time above 360°C. With electrolytes containing more than 20 mole % KCl (and less than 80 mole % $LiNO_3$) the OCV did not change abruptly with temperature or KCl content and was from 1.5 to 1.6 v between 300° and 400°C. As the KCl content of the electrolyte was increased, cells could be operated at higher temperatures without excessive electrolyte decomposition or Mg corrosion. Minimum temperature of operation, the melting point of the mixture, also increased with KCl content. The difference between OCV and CCV for a given load decreased as temperature was increased.

The corrosion reaction of Mg with the electrolyte, in which gas was evolved, was greatest between 10 and 30 mole % KCl. Mg reacted much less in $LiNO_3$ than in $LiNO_3$-KCl mixtures. At KCl concentrations of greater than 30 mole %, the corrosion reaction decreased with increasing KCl content. Rate of corrosion reaction increased in an exponential-like manner with temperature; at any given chloride concentration the extent of corrosion increased slowly with temperature up to a certain temperature region and then accelerated. Gas samples analyzed with the mass spectrometer contained $N_2O$, $N_2$, NO, and $NO_2$. Alkali oxide and nitrite were found in the solidified residues. Ag was oxidized in all electrolytes in which $LiNO_3$

TABLE IV. Mg/50$LiNO_3$–50KCl/M

| | Ni | Ag | Pt | C | °C |
|---|---|---|---|---|---|
| Initial OCV | 1.70 | 1.55 | 2.14 | 1.86 | 366 |
| After 10 min | 1.82 | 1.55 | 2.14 | 1.85 | 364 |
| After 2 hr | 1.85 | 1.54 | 2.12 | 1.80 | 362 |
| After 4 hr | 1.75 | 1.52 | 1.85 | 1.66 | 372 |
| CCV (30 sec after load applied*) | 1.50 | 1.41 | 1.32 | 1.36 | 372 |
| OCV (30 sec after load removed) | 1.57 | 1.55 | 1.55 | 1.51 | 372 |
| OCV (30 min after load removed) | 1.65 | 1.55 | 1.70 | 1.65 | 368 |

* Load of 100 ohms was applied for 1 min.

was present. In the absence of Mg [1] about 12 % of the Ag electrode reacted in 1 hr at 400°C in an electrolyte containing 50% $LiNO_3$ and 50% KCl. About the same amount of Ag reacted in a 70$LiNO_3$–30KCl mixture. Less reaction occurred with 100% $LiNO_3$.

Analysis of the reactions in which Ag and Mg were oxidized was complicated by subsequent reactions that could occur between products, for example, a reaction between $Li_2O$ and $NO_2$ to form $LiNO_2$ and $LiNO_3$ (9). Decomposition of $LiNO_3$ offered a further complication, although the cells were usually operated at temperatures well below the region at which gas evolution could be observed.

In cells with electrolytes containing no $LiNO_3$, but only LiCl and KCl, OCV's of 1.45–1.65 v were obtained at 360°–500°C. The cells polarized badly in comparison with cells containing $LiNO_3$. Gas was evolved at both the Ag and Mg under load but only at the Mg when no load was applied. As there was no apparent oxidizing agent, the discharge reactions that were obtained are attributed to the presence of moisture, or other impurity like $NH_4Cl$, in the salts. Salts taken directly from the reagent bottles showed better discharge characteristics than those given the usual drying treatment. A cell made up to contain 1% $NH_4Cl$, a better acid than $H_2O$ in the LiCl-KCl electrolyte, had good discharge characteristics. There was evidence for $NH_3$ in the evolved gases in this cell. In cells with a LiCl-KCl electrolyte, that is, no $LiNO_3$ present, AgCl was not found.

### Positive Electrodes Other Than Ag

The OCV's for different positive electrodes were compared in the cell, Mg/50$LiNO_3$–50KCl/*M*, where *M* was Ni, Ag, Pt, or graphite (Table IV). The OCV was highest for the Pt and lowest for the Ag electrode. The Ag and Ni electrodes were etched in the electrolyte. The cell Mg/85 $LiNO_3$-15 KCl/Pt gave an OCV of 2.19 v at 340°C. Under load this cell polarized badly, and there was a very long recovery period. When a Ni electrode was used in place of Ag, with an electrolyte of 90$LiNO_3$–10KCl, the OCV was 0.3–0.4 v higher, but as with the Ag electrode, the initial OCV decreased with time to around 0.5 v. In cells with an electrolyte containing only LiCl and KCl, that is, no $LiNO_3$ present, Pt positives were similar to Ag positives.

[1] Mg reacts with $LiNO_3$ producing reduction products of $LiNO_3$, such as $LiNO_2$, $NO_2$, and NO. In addition to the Ag-$LiNO_3$ reaction, a reaction could occur between Ag and the reduction products of $LiNO_3$.

### Discussion

In cells with a Mg electrode and $LiNO_3$-KCl electrolyte, lower OCV's were obtained with Ag or Ni positive electrodes than with Pt. This indicated that Ag and Ni were not inert, but took some part in the cell reaction. This is further confirmation of the results obtained by Selis (10) and Rubin (11) on the behavior of different metal positives in fused salt cells.

One explanation that can be offered for the behavior of the Ag positive is based upon the continuous oxidation of the Ag by nitrate. The Ag compound formed in the oxidation covered the metal, preventing direct access of the nitrate. The film never became thick, as the Ag compound was soluble in the electrolyte. When current was drawn from the cell, the Ag compound was reduced in preference to the nitrate. The oxidizing action of nitrate on Ag could account for the Ag compound always found in the electrolyte of cells containing nitrate. Such a film was not formed on Pt and the nitrate had direct access to the Pt metal. Pt acted as an inert electrode. The large amount of polarization observed in the cells with Pt indicated a slow electrode reduction of nitrate at an inert electrode. The electrochemical reduction of the Ag compound is considered to be much faster than the electrochemical reduction of the nitrate at an inert electrode.

An electrochemical reaction for this postulated mechanism is: $Li_2O + Mg + 2AgCl = MgO + 2Ag + 2LiCl$. $LiO_2$ would be produced in the reduction of nitrate. Solubility of MgO was not appreciable and it accumulated at the bottom of the melts during cell activation.

### Acknowledgments

This research was supported by the Diamond Ordnance Fuze Laboratories, Dept. of the Army, formerly a part of the National Bureau of Standards.

Manuscript received May 9, 1955. This paper was prepared for delivery before the Cleveland Meeting, September 30 to October 4, 1956.

Any discussion of this paper will appear in a Discussion Section to be published in the June 1957 Journal.

### REFERENCES

1. J. H. Hildebrand and G. C. Ruhle, *J. Am. Chem. Soc.*, **49**, 722 (1927).
2. E. J. Salstrom, *ibid.*, **55**, 2426 (1933).
3. S. I. Rempel and I. N. Ozeryanya, *Zhur. Fiz. Khim.*, **25**, 1181 (1951).
4. J. H. Hildebrand and E. J. Salstrom, *J. Am. Chem. Soc.*, **54**, 4257 (1932).
5. W. J. Hamer and J. P. Schrodt, *ibid.*, **71**, 2347 (1949).
6. R. B. Goodrich and R. C. Evans, *This Journal*, **99**, 207 (1952).
7. G. Kortüm and J. O'M. Bockris, "Electrochemistry," Vol. II, p. 479, Elsevier Co., Amsterdam (1951).
8. G. W. Vinal, "Primary Batteries," p. 324, John Wiley & Sons, Inc., New York (1950).
9. T. Oza, *J. Indian Chem. Soc.*, **22**, 180 (1945).
10. S. M. Selis, Private communication.
11. B. Rubin, Private communication.

# Association of $Co^{60}$ Ions with Metal Surfaces

R. T. Foley, B. T. Stark, and C. J. Guare

*General Engineering Laboratory, General Electric Company, Schenectady, New York*

ABSTRACT

The radiochemical technique for the study of surface reactions has been investigated. This technique readily demarks on the metal surface areas that are cathodic to adjacent areas. The steel-copper and aluminum-copper couples were observed and the strong attraction of radiocobalt to the cathode member of the couple was measured. The sorption of radiocobalt ions on surface films is a complicating effect in the employment of this technique if not considered and understood. The extent of this effect varies with the surface film under consideration, being considerable for oxide and sulfide films on copper and small for oxide films on alloy steels and anodized films on aluminum.

The sorption of ions from solution has a great significance in so far as corrosion mechanism is concerned as it would appear that ion concentration cells are common occurrences when part of a metal surface is covered with an oxide film and part is bare.

The fact that atoms on a metal surface may exchange with ions of the same metal in solution has been known for a number of years and has been of particular interest to those working on the theoretical aspects of corrosion, catalysis, and other applications of surface chemistry. Recently pickup of radioactive ions from solution by metals has been used to study electrode reactions (1), adsorption processes (2), and corrosion mechanisms (3, 4).

In this laboratory there has been a critical appraisal of the radiochemical technique with respect to its usefulness in studying corrosion mechanisms. There are several possible mechanisms by which tracers, as radiocobalt ions, may be transferred from solution to a metal surface: (*a*) exchange between metal ions on surface and in solution; (*b*) sorption; (*c*) electrolytic action.

The more recent publications on this technique have contained experiments interpreted in terms of the electrolytic action mechanism. However, some of the authors' earliest experiments demonstrated that the cobalt ion tracer was rather loosely held on the surface, suggestive of a sorption mechanism.

If this technique is to be of value for the study of corrosion processes there should be no ambiguity in the interpretation of the results obtained. The objective of this work was to contribute to the understanding of the mechanism and interpretation of the technique.

## Experimental

All the radiochemical studies were carried out using solutions containing tracer concentrations of the radioactive isotope, cobalt-60. This isotope has a half-life of 5.27 years and emits $\beta$-radiation of 0.306 mev energy as well as 1.33 mev and 1.17 mev $\gamma$-rays. The original solution was obtained from Oak Ridge National Laboratory and was in the form of $CoCl_2$ (7.1 mg Co/ml) in 0.34*N* HCl solution. Separate dilutions of this solution were used for each of the metals investigated. Concentrations of cobalt ion and $H^+$ after dilution are shown in Table I. This table also records the activity of each solution. In all cases the metal samples in strip form were immersed in the tracer solution for 10 min at a constant temperature of 30°C. Usually a volume of 500 ml was taken. The size of the samples varied, 1.2 cm x 1.2 cm squares being used most frequently. In some of the experiments with aluminum 5.1 cm x 5.1 cm samples were used. In a typical experiment a large number of samples would be prepared in an identical manner and 10 from the group would be carried through the experiment and given similar treatment. The use of a large number of samples compensated for the small size of each sample. All activity figures were normalized to unit area.

Autoradiographs were made by placing the samples directly in contact with Kodak No-Screen x-ray film. Exposure time varied with the activity of the samples, but in most cases it was possible to obtain sufficient contrast in 3–4 hr. During preliminary experiments the samples were dipped in a 2% solution of VYNS (vinylite) in acetone to prevent fogging of the film by the bare metal (5, 6), but this was subsequently discontinued since no fogging was observed from dry, untreated control samples.

Radioactivity measurements were made using a thallium activated sodium iodide scintillation crystal coupled to a photomultiplier tube as a detector. The observed data were corrected for physical geometry and detector efficiency by direct comparison with a standard cobalt-60 source.

## Influence of Surface Films on Pickup of Radiocobalt

In the study of a corrosion process the influence of surface films on the pickup of radiocobalt from solution would be an important factor. The influence of surface films would also be suggestive of the mechanism by which Co became attached to the surface. If only the potential differences existing on the surface account for the pickup of activity, then the pickup would be expected to remain constant or decrease with increase in film thickness. It would seem reasonable to assume that as the film increased in thickness anode sites would be covered up. On the other hand, if adsorption accounted for the pickup, one would expect an increase in pickup of radiocobalt ions with increased weight of sorbent. The location of Co on

TABLE I. Co *solutions*

| Solution | Calculated total conc. of Co | Calculated conc. of $H^+$ | Measured activity (Co) |
|---|---|---|---|
| | μg/ml | *N* | d/min/ml* |
| #1-Used with Al samples | 0.8 | $4 \times 10^{-5}$ | $3.4 \times 10^6$ |
| #2-Used with Cu samples | 0.5 | $2.5 \times 10^{-5}$ | $2.0 \times 10^6$ |
| #3-Used with steel samples | 0.7 | $3.5 \times 10^{-5}$ | $2.6 \times 10^6$ |

* Disintegrations per minute per milliliter of solution.

TABLE II. *Activity pickup as related to oxide film thickness on* Cu

| Surface treatment—Oxidized at 400°C for: | Weight of oxide† (mg/cm²) | Co pickup—(d/min/cm²) | |
|---|---|---|---|
| | | Prior immersion in $H_2O$ | Prior immersion in NaCl solution |
| Experiment 1 | | | |
| min | | | |
| 0 | 0.00 | 278 | 642 |
| 5 | 0.010 | 529 | 1,840 |
| 10 | 0.062 | 10,200 | 4,170 |
| 20 | 0.194 | 8,450 | 6,710 |
| Experiment 2 | | | |
| 0 | 0.00 | 210 | |
| 5 | * | 178 | |
| 10 | 0.128 | 4,420 | |
| 20 | 0.190 | 5,530 | |
| 30 | 0.401 | 6,620 | |

* Less than experimental error.
† Found by stripping after oxidation.

the metal surface, whether it was attached to the basis metal or the surface film, would be of interest. Association with the surface film would not argue entirely for adsorption as opposed to electrochemical action as the surface film may be the cathode in the electrolytic cell. The influence of surface film thickness on Co pickup was studied with oxide and sulfide films on Cu, oxide films on Al, and oxide films on alloy steels.

### *Oxide Films on Copper*

The oxide films were developed on strips of copper[1] by oxidizing in air at 400°C for various lengths of time. Samples (1.25 cm x 1.25 cm x 0.064 cm thick) were used for the radiochemical experiments, ten samples being taken for each variation. To characterize the film layer, samples (3.8 cm x 3.8 cm x 0.064 cm thick) were oxidized along with the squares that would be later exposed to radiocobalt. The oxide strips were immersed in distilled water for 10 min, in radiocobalt solution for 10 min, and rinsed for 30 min. After drying, the samples were counted to determine the radioactive pickup and autoradiographs were made. Variation in this procedure included substituting a 10-min immersion in NaCl solution (5 g/l) for the prior immersion in distilled water. Following the completion of these operations, the samples were immersed for a short time in $H_2SO_4$ solution (5 ml of concentrated $H_2SO_4$ diluted to 100 ml) and again counted. This $H_2SO_4$ reagent is known to strip oxide films from Cu without attacking the Cu itself. Results of two experiments with oxide films are summarized in Table II. Another set of experiments confirmed these results in a qualitative manner. These experiments demonstrate that with increased thickness (or amount) of oxide on the surface the pickup of Co increases. Treatment with the oxide stripping reagent removes all of the activity. This indicates that the activity is associated with the oxide film rather than firmly attached to the basis metal.

[1] Analysis 99.90% copper, 0.04% oxygen.

TABLE III. *Activity pickup related to copper sulfide film thickness*

| Surface treatment—Exposure time to polysulfide solution | Weight gain (mg/cm²) | Co pickup (d/min/cm²) |
|---|---|---|
| hr | | |
| 3.5 | 0.023 | 1,160 |
| 8 | 0.051 | 5,680 |
| 15 | 0.113 | 11,500 |
| 27.5 | 0.186 | 16,200 |

### *Sulfide Films on Copper*

Films of copper sulfide were developed on copper by holding Cu strips over a polysulfide solution (1 ml of Baker's dark ammonium polysulfide solution diluted to one liter) in a closed desiccator-type jar. Subsequent treatment was similar to that given the oxidized copper strips and described above. Results of a typical experiment are summarized in Table III. The Co pickup relative to the increase in film thickness is pronounced.

The autoradiographs of this series of filmed samples demonstrated that the variation of activity along the surface of the individual sample was similar to the distribution of the surface film itself. This comprised qualitative confirmation of the influence of surface film.

### *Aluminum Oxide Films*

Oxide films of varying thickness were developed on aluminum[2] by means of an anodic treatment in $H_2SO_4$ solution (15% by weight). A current density of 1.3 amp/dm² and 16 v were used at 25°C. Strips of aluminum 5.1 cm x 5.1 cm x 0.064 cm thick were treated for various lengths of time. The anodic film thicknesses for the individual panels were characterized by the weight loss through stripping in chromic-phosphoric acid reagent. In one series of experiments the strips were immersed in NaCl solution for 30 min before immersion in the Co tracer. In another series the prior immersion was in distilled water. Experimental results are given in Tables IV and V. From these results it may be concluded that the thicker anodic films show very little tendency to pick up the Co tracer. Co was picked up by strips which were not anodized or which were anodized to produce thin films to produce a strong activity. This pickup is interpreted as electrodeposited. Even in distilled water, sites of different potential are set up over the surface accounting for the electrochemical action. Autoradiographs confirmed the results set down in Tables IV and V.

[2] Analysis 99.0% Al; Fe and Si 1.0%.

TABLE IV. *Activity pickup as related to aluminum oxide film thickness*
(After activation in NaCl solution)

| Thickness of oxide (by stripping) (mg/cm²) | Activity (d/min/cm²) |
|---|---|
| 0.0 | 5,633 |
| 0.0 | 9,546 |
| 0.14 | 7,353 |
| 0.26 | 3,557 |
| 0.84 | 601 |
| 0.84 | 988 |
| 0.91 | 2,842 |
| 1.28 | 968 |
| 1.28 | 556 |
| 1.38 | 558 |
| 2.34 | 432 |
| 2.47 | 427 |

TABLE V. *Activity pickup and aluminum oxide film thickness*
(After activation in distilled water)

| Thickness of oxide (by stripping) (mg/cm²) | Activity (d/min/cm²) |
|---|---|
| 0.00* | 11,414 |
| 0.00* | 13,860 |
| 0.00* | 15,089 |
| 0.00† | 8,514 |
| 0.88 | 116 |
| 0.93 | 885 |
| 0.98 | 679 |
| 1.11 | 183 |
| 4.87 | 198 |

* Annealed strip.
† As rolled strip.

TABLE VI. *Activity pickup and oxide film thickness on stainless steel*

| Weight gain on oxidation (mg/cm²) | Activity (d/min/cm²) |
|---|---|
| 0.00 | 9 |
| 0.00 | 12 |
| 0.008 | 84 |
| 0.008 | 33 |
| 0.012 | 34 |
| 0.012 | 65 |
| 0.016 | 33 |
| 0.020 | 33 |
| 0.031 | 33 |

### *Oxide Films on Alloy Steel*

Stainless steel strips[3] were oxidized at 1000°C to develop oxide films of varying thickness. These oxidized samples were allowed to stand in NaCl solution for 30 min along with unoxidized controls. Results are given in Table VI.

The cleaned surface of the stainless steel picks up a negligible amount of Co during the immersion period. There is a slight increase in pickup of activity with increase in oxide film thickness as would be suggested by the adsorption mechanism. However, stainless steel surfaces appear to be passivated and equipotential surfaces appear to have been developed even with air-formed oxide films. In some experiments, oxidized stainless steel panels were scribed before immersion in the tracer solution. Considerable Co was attracted to the scratch. Results obtained with this alloy steel were different from those obtained during experiments with an Fe-Ni alloy containing 42% Ni and 58% Fe. In the latter case a great deal of activity was attracted to the alloy surface possessing only the room temperature air-formed film.

[3] Type 302, 18% Cr, 9% Ni.

### Study of Worked Surfaces

One method of introducing cold work into the surface is by abrasion. Cleaned strips of Cu (1.25 cm x 1.25 cm x 0.064 cm thick) were abraded in air, under acetone and under benzene. Strips were stored under benzene before and after the abrasion. They were rinsed in acetone and activated for 30 min in NaCl solution before immersion in the tracer solution. After rinsing for 30 min in running water the samples were counted.

| Surface treatment | Activity—(d/min/cm²) |
|---|---|
| Abraded in air | 5,542 |
| Abraded under acetone | 1,185 |
| Abraded under benzene | 2,429 |

A further experiment checked this effect and also the retention of the activity after rinsing.

| Surface treatment | Activity—(d/min/cm²) | |
|---|---|---|
| | After 30 min rinsing | After 18 hr rinsing |
| Abraded in air | 3,996 | 2,014 |
| Abraded under benzene | 996 | 440 |

Autoradiographs from this last experiment reveal increased activity when abrasion is carried out in air as well as the fact that much of the activity is confined to the edges of the sample. In both cases some of the activity is loosely held and is lost on prolonged rinsing. Increase in activity through abrasion in air is attributed to adsorption on the oxide film that must be formed. When only a portion of the strip is abraded, radioactivity is restricted to the abraded area.

Further experiments were performed to estimate the competitive influence of the presence of an abraded area and a filmed area on the same sample. Strips of Cu (3.8 cm x 3.8 cm x 0.064 cm) were treated in the following ways:

(*A*) The entire side of the sample was coated with a sulfide layer by exposure over an ammonium sulfide solution.

(*B*) One half of the area was abraded with 2/0 emery under benzene. This abraded area was masked by painting with a paraffin wax solution in benzene, then the whole strip was exposed above the sulfide solution. Thus, one-half the face was abraded, the other half filmed.

(*C*) One-half the area was abraded.

(*D*) No treatment was given the sample, and it was carried through as a control.

Duplicate samples with these treatments were allowed to stand for 30 min in NaCl solution, then immersed in the Co tracer solution.

Autoradiographs of this series of samples demonstrated how the activity is drawn to the sulfide covered area when

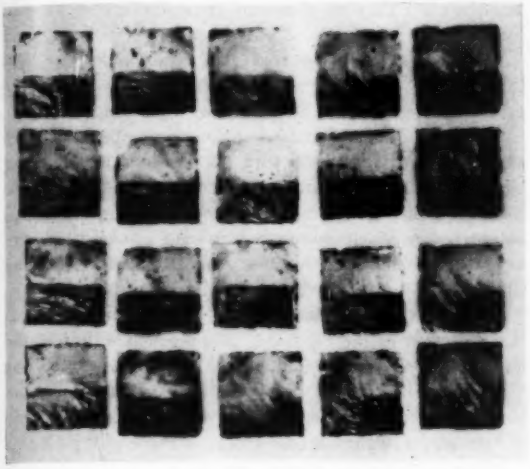

FIG. 1. Co activity pickup on the copper-steel couple. These samples were rinsed in running tap water for varying lengths of time. Starting with right column and proceeding to the left, rinsing times of 30 min, 2.5 hr, 4 hr, 5.5 hr, and 22.5 hr, respectively.

it is adjacent to an area which represents an acknowledged worked area. The activity associated with the filmed area would obscure the effects of the worked surfaces. When abrasion is carried out in air the pickup of the tracer is enhanced. While the greater amount of activity is associated with the filmed area the worked area is also quite distinct.

### EXAMINATION OF GALVANIC COUPLES

Several cases were considered that would represent obvious galvanic couples. The object was to compare the behavior of galvanic couples with the behavior of those systems characterized by adsorption on surface films.

A Cu-Fe couple was prepared by the displacement plating of Cu from copper chloride solution. The steel[4] panel (2.5 cm x 2.5 cm x 0.050 cm) after being annealed and pickled was painted with a solution of paraffin in benzene so that only one half of one side was left exposed. This exposed area was covered with a few drops of a solution of copper chloride (5 g of $CuCl_2 \cdot 2H_2O$ dissolved in 100 ml of concentrated HCl) and allowed to stand for a few minutes. After rinsing the strip in water the wax was removed by standing first in benzene and then in acetone. The sample was allowed to stand in NaCl solution (1 g NaCl/100 ml), rinsed, and immersed in the cobalt tracer solution. Autoradiographs in Fig. 1 illustrate the cathode-anode relationship of this couple. In this particular experiment four samples were taken for each of five different rinsing periods. Retention of activity during rinsing is described below. This couple is characterized by the deposition of a high activity which is associated with the Cu member of the cell.

In a similar manner a Cu-Al cell was prepared. The

[4] This was A1S1 Type 1020 Analysis; Carbon = 0.12%; Mn—0.30–0.60%.

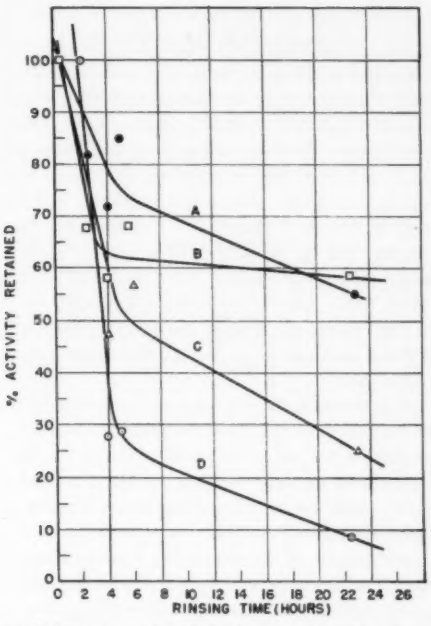


FIG. 2. Effect of continual rinsing on retention of activity. A = Cu plated on Al; B = Cu plated on steel; C = thin copper sulfide film; D = thick copper sulfide film.

autoradiograph showed that while most of the activity was concentrated on the cathode copper area there was some distributed over the rest of the surface. Distribution was not as clear cut as in the Fe-Cu case. The experiments did, however, demonstrate the ability of the technique to outline the areas of different potential as has been described by other investigators.

It is well known that inert matter, as silica residing on a surface, sets up a concentration cell which leads to corrosion. An attempt was made to simulate this sort of cell. A colloidal sol was prepared by suspending very finely divided silica in water, spreading the colloidal material of Fe, Cu, and Al and allowing to dry over night. The strips were allowed to stand in NaCl solution for 1 hr and then transferred to the Co tracer.

From autoradiographs prepared it was evident that metal surfaces acted differently. It was noticed that the silica on Cu and steel attracts the Co and thus would be termed the cathode area. On Al the Co was attached to the Al surface not covered by the silica. The area covered was relatively free of activity. If the period of activation in NaCl solution is reduced from 60 to 15 min slightly different results are obtained. With Al the activity is still associated with the metal proper rather than the silica. However, upon examining the steel and copper samples subjected to a shorter exposure to chloride solution it was observed that the activity resided with the metal surface rather than the silica.

The effect of silica on influencing the direction in which the Co goes is difficult to interpret, but it is apparent that the technique can outline areas of different potential on the metal surface.

### Retention of Activity as Influenced by Method of Deposition

During the preliminary work with this technique it was observed that the time of rinsing following the Co immersion step required control if reproducible results were to be obtained. Previous workers on exchange reactions indicated that there was no appreciable drop in activity if the rinsing was longer than a few minutes. The degree of retention of Co would suggest the mechanism by which Co was attached to the surface. If Co ions were adsorbed, one would expect desorption with continued rinsing. On the other hand, electrodeposited Co would be tightly bound and moreover should be electrochemically protected from dissolution by the anodic elements immediately adjacent.

In the present work, the activity associated with the copper sulfide film has been termed "adsorbed." The greater part of that associated with systems like the Cu-Al couple has been termed "electrolytically deposited." Loss of activity with continual rinsing is depicted in Fig. 2. In these experiments a large number of samples were taken and groups of six rinsed for various times. Thus, the points on the curve represent the behavior of separate groups of samples rather than the same group carried through the whole experiment. This explains why apparently the activity does not always drop continually with continued rinsing. The copper-steel couple and the Al-Cu couple lose about 30–40% of their activity within the first few hours. After 24-hr rinsing time 40–50% has been lost.

About 60–70% of the activity associated with the copper sulfide film is lost in the first few hours. After 24-hr rinsing, as much as 92% may be removed by running water. In cases wherein the activity was slight at the start the retained activity may be 25% after the 24-hr rinsing time. Retention of active Co is apparently a means of differentiating between the two mechanisms involved in the collection of the activity on the surface.

### Discussion and Conclusions

These experiments have demonstrated that the tracer Co may be picked up from solution by two processes: (*a*) adsorption, and (*b*) electrolytic deposition.

Both mechanisms probably are involved to some degree as discussed by King (2). When porous films lacking in density are studied, the major contribution is from adsorbed Co. With galvanic couples, as for example, the Fe-Cu couple, the electrolytic effect predominates. It appears that the adsorption may be either on the metal or on the oxide film. The two types of deposition are distinguished by the higher intensity and the greater retention associated with electrolytically deposited Co. Most of the adsorbed Co may be removed from the metal by prolonged rinsing.

It has been demonstrated that when a surface film exists along side of a worked area on a given sample the greater portion of the activity may be attracted to the filmed area. This may not be entirely a competitive effect as the activity associated with the worked area may not be great. It had been pointed out by previous investigators that polished or abraded surfaces picked up the radioactive tracer much more readily than annealed or unworked surfaces. Some of this pickup is contributed by the oxide film developed by polishing in air.

Various oxide films act in a different manner insofar as the collection of the Co tracer is concerned. Films of the nature of copper oxide and copper sulfide adsorb a great deal of cobalt whereas films like the oxide on aluminum produced by anodizing or the oxide of stainless steel adsorb only a negligible amount.

When a particular mechanism is under investigation consideration must be given to this adsorption by oxide films. For example, in the pitting of Al one of the products situated near the cathode products is the hydrated oxide of Al. It seems likely that Co is attracted to the site not only because of the cathode nature of the site but also because of the adsorptive ability of the hydrated oxide.

The attraction of ions from solution to the oxide films covering a surface would appear to have a broader significance from the standpoint of corrosion mechanisms. If the oxide films represent sites whereon clusters of cations may be accumulated, it is logical to conclude that oxide films of varying thickness represent in themselves the sites for concentration cells on metal surface.

### Acknowledgment

The authors wish to express their appreciation to Dr. A. H. Bushey, Dr. H. R. Schmidt, and Mr. M. B. Leboeuf for their suggestions and stimulating discussion of this radiochemical technique.

Manuscript received December 22, 1955.
Any discussion of this paper will appear in a Discussion Section to be published in the June 1957 Journal.

### REFERENCES

1. M. Haissinsky, *Z. Elektrochem.*, **59**, 750 (1955).
2. C. V. King, *Ann. N. Y. Acad. Sci.*, **58**, 910 (1954).
3. M. T. Simnad, "Properties of Metallic Surfaces," p. 23, Institute of Metals, London (1953).
4. P. M. Aziz, *This Journal*, **101**, 120 (1954).
5. H. Yagoda, "Radioactive Measurements with Nuclear Emulsions," John Wiley & Sons, Inc., New York (1949).
6. G. C. Towe, H. J. Gomberg, and J. W. Freeman, *Nucleonics*, **13**, 54 (1955).

# A Mechanism for the Anodic Dissolution of Magnesium

J. H. GREENBLATT

*Naval Research Establishment, Dartmouth, Nova Scotia*

ABSTRACT

Magnesium anodes were electrolyzed in 3% NaCl solution in a simple electrolysis cell. Mg in the anolyte, Mg in the corrosion product, total hydrogen evolved, and weight loss were determined. It was found that the quantities soluble Mg, insoluble Mg, Mg calculated from the current passed were in approximate one to one relationship with each other and all of these quantities are roughly half of the total weight loss. Hydrogen evolved was always slightly less than the soluble and insoluble Mg. These facts are explained and integrated into existing knowledge of the behavior of Mg anodes by postulating that Mg dissolves in the solution investigated mainly as a univalent ion followed by reaction of this univalent ion with water.

The problem of hydrogen evolution at a magnesium anode during electrolysis is an old one with literature references dating back to the work of Beetz (1) and Elsoesser (2). Recently, the problem has been reconsidered by Petty, Davidson, and Kleinberg (3), who measured the apparent valence of Mg anodes in a variety of aqueous electrolytes and found that their results could be explained by postulating the presence of both uni- and divalent Mg during electrolysis at a Mg anode. Hydrogen evolution was explained as being a reduction product of the reaction between univalent Mg ions and water. Other substances, such as $KMnO_4$, $ClO_3^-$, introduced into the anolyte compartment of their apparatus were also reduced, and in a recent paper by Kleinberg and co-workers (4), where measurements of apparent valence in organic liquids are described, reductions of such test liquids that were electron acceptors were obtained.

The existence of univalent Mg has been postulated at various times, and in the earlier work (1, 2, 5) the continued evolution of hydrogen after current shut-off, and the ability of the grayish-black corrosion product that had accumulated on the Mg to evolve hydrogen from water were ascribed to the existence of a suboxide in the corrosion product. However, all efforts to isolate and identify such a compound failed. More recently, Faivre and Michel (6) have shown by x-ray analysis that the grayish product formed on oxidation of Mg in humid air is $Mg(OH)_2$ with Mg atoms inserted in the lattice. Brouchere (7) and Huber (8) claim that x-ray and electron diffraction of corrosion films on Mg indicate that the films are mainly MgO with Mg atoms in the lattice.

Insofar as none of the work to date has given a clear picture of the mechanism of solution of Mg at an anode, the work described was undertaken with the purpose of attempting to obtain the necessary information to accomplish this.

## EXPERIMENTAL

Mg of 99.92% purity with an iron content of 0.0001–0.0005% was used as the anode material. Anodes were of varying lengths and were 16.5 mm in diameter, except for a short portion that was machined slightly smaller to fit inside the untapered portion of a 19/38 ground joint. Before use, the anodes were cleaned by immersion in 5% $HNO_3$ and then inserted in the apparatus shown in Fig. 1.

All experiments were conducted in 3% reagent grade NaCl solutions. A silver-silver chloride cathode was used, and the driving voltages, in all except the high current density experiments, was that of the magnesium, silver-silver chloride couple. For the high current density experiments, an impressed d-c source was used. The procedure followed was to electrolyze at constant current, collecting the gas during electrolysis. At the end of the electrolysis, current was shut off, the cathode removed, and the electrolyte quickly run out. After a quick rinse, the electrolysis vessel was filled with hot 5% chromic acid containing 0.5% silver chromate. This cleaning solution was left in contact with the Mg cylinder for 10 min, after which it was run out, the electrolysis vessel was rinsed, and the rinsings were added to the chromic acid. All gas evolved during cleaning of the Mg cylinder was also collected. After cleaning, the Mg cylinder was removed from the apparatus, washed in distilled water, dried, and weighed.

The electrolysis solution was filtered to remove any solid particles of corrosion product that had spalled off the cylinder during electrolysis, and Mg was determined in the filtrate by the standard oxime method. The solid particles of corrosion product on the filter were dissolved by washing with a portion of the hot chromic acid cleaning solution. The washings were then combined with the main portion of the chromic acid cleaning solution and the Mg was separated from chromium by precipitation in excess NaOH after first oxidizing with bromine water. The precipitated $Mg(OH)_2$ was then redissolved in acid, and titrated with versene after buffering. The collected gases were analyzed for hydrogen by absorption by hot cupric oxide after first analyzing for oxygen by absorption in alkaline pyrogallate. Blanks run by immersing uncorroded Mg cylinders in chromic acid cleaning solution gave average weight losses of 3 mg.

The effect of surface area, current density, and temperature on the anodic dissolution of Mg were studied. The effect of varying anode area was studied only at room temperature and anodes of 16.5 mm diameter and

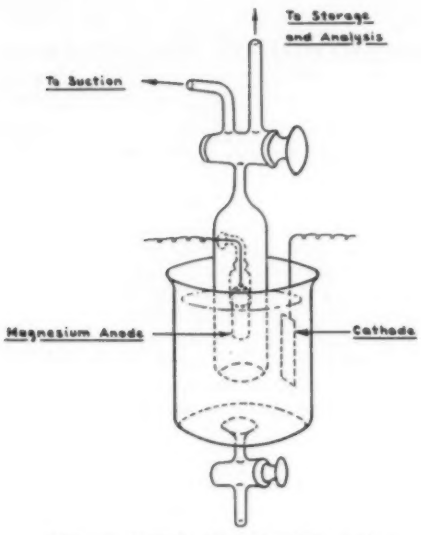


FIG. 1. Sketch of electrolysis cell

exposed lengths of 51, 38, and 25 mm were used. At all other temperatures, anodes 51 mm long were used, and, in the set of experiments with varying current densities, anodes 25 mm long were used. The volume of solution in the electrolysis vessel was the same in all cases, approximately 500 ml. In the usual experiments, the current density was 0.0035 amp/cm², except for those shown in Fig. 3, where the area was varied, and for some of the experiments in Fig. 2 at 75°C where current densities of 0.0017, 0.0023, and 0.0026 amp/cm² were also used. In the experiments with varying current density, this variable was varied over the range 0.0196–0.369 amp/cm², the total number of coulombs during each experiment being kept constant.

## RESULTS

The data obtained are shown graphically in Fig. 2 and in Table I. Examination of the data obtained at room temperature shows that the quantities: Mg soluble in the electrolyte, insoluble Mg retained on the surface of the test cylinder as corrosion product, and the magnesium calculated from the current passed (coulombs × 12)/$F$ bear an approximate 1:1 ratio to each other. Moreover, all these quantities are approximately half the total weight loss. These relationships persist over the

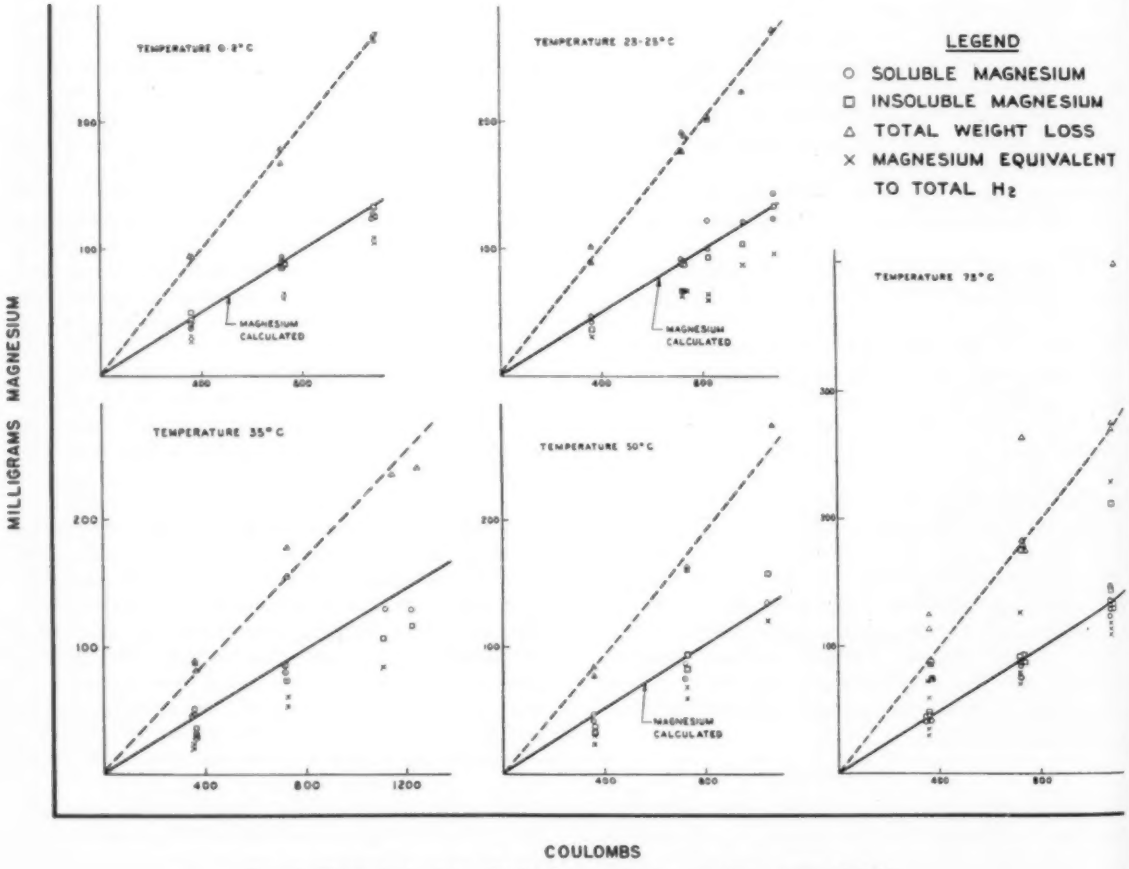


FIG. 2. Electrolysis data obtained over the temperature range 0°–75°C

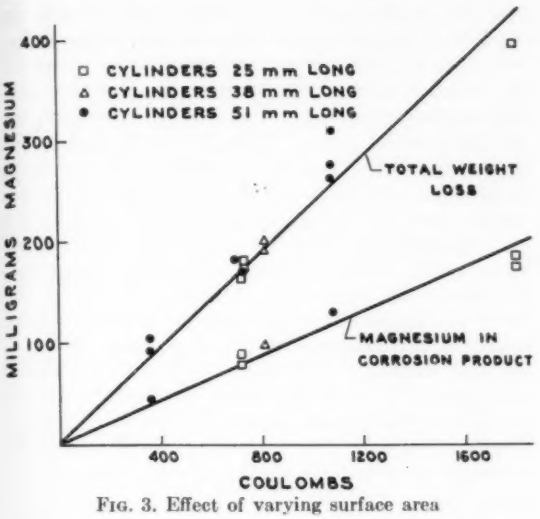


FIG. 3. Effect of varying surface area

TABLE I. *Effect of varying current density*

| Current density (amp/cm²) | Soluble Mg (mg) | Insoluble Mg (mg) | Magnesium equivalent to $H_2$ (Evolved mg) | Total weight loss (mg) |
|---|---|---|---|---|
| 0.0196 | 553 | 413 | 365 | 978 |
| 0.0196 | 542 | 419 | 358 | 976 |
| 0.0922 | 506 | 309 | 276 | 831 |
| 0.0922 | 475 | 354 | 278 | 825 |
| 0.102 | — | — | 314 | 891 |
| 0.102 | — | — | 311 | 846 |
| 0.115 | 529 | 365 | 299 | 892 |
| 0.148 | 520 | 324 | 292 | 849 |
| 0.184 | — | — | 321 | 897 |
| 0.184 | — | — | 314 | 906 |
| 0.278 | — | — | 318 | 902 |
| 0.278 | — | — | 321 | 910 |
| 0.369 | — | — | 320 | 901 |
| 0.369 | — | — | 312 | 895 |

Total quantity of electricity = 4500 coulombs in all experiments.

range of temperatures 0°–75°C as seen from the data. At 75°C, however, it can be seen that there are scattered experiments in which the insoluble Mg is considerably greater than both the soluble and calculated Mg. Where this occurs, it can also be seen that the total weight loss and hydrogen evolved are correspondingly greater than in so-called normal experiments. The total hydrogen evolved expressed in milligrams of equivalent Mg is also plotted. This is somewhat lower than the quantities soluble Mg, insoluble Mg, and calculated Mg, except for the instance already mentioned at 75°C where amounts of hydrogen greater than one-half the total weight loss were obtained.

It can also be seen from the graphs under consideration that the quantities soluble Mg, insoluble Mg, total hydrogen evolved, and total weight loss give reasonable linear relationship with the number of coulombs passed. This relationship persisted in spite of variations in surface area, as can be seen from Fig. 3; also, the data of Fig. 2 at 75°C includes variations in current density at constant surface area and quantity of electricity. These

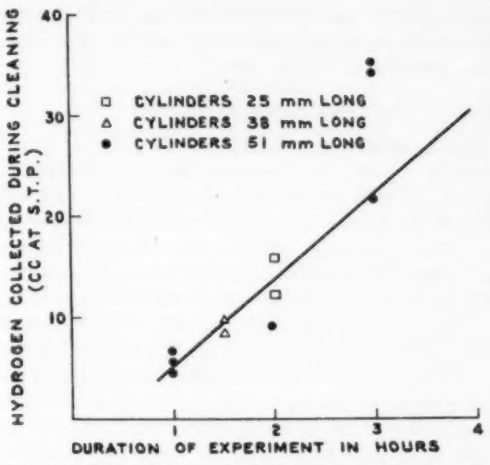


FIG. 4. Relation between hydrogen evolved during cleaning and time of experiment.

variations were made when scattered unusual weight losses and quantities of hydrogen evolved were obtained. None of these experiments with slight changes in current density (¼, ⅔, ¾ normal) showed abnormal behavior, and they are all included in the graph for 75°C. This linearity could be evidence that soluble Mg, insoluble Mg, total hydrogen evolved depend on a primary current carrying reaction.

The effect of varying current density is shown in Table I. There is an indication of a small decrease in weight loss, insoluble Mg, and total hydrogen evolved, but decreases are small and do not indicate any great change of mechanism. Petty, Davidson, and Kleinberg (3) report similar results in their study of the variation of apparent valance with current density in dilute solutions.

Total hydrogen was obtained by adding the quantities collected during cleaning and during electrolysis. At 0° and at room temperatures, the amount of hydrogen evolved during cleaning was about ½ the amount obtained during electrolysis. As the temperature increased, the amount obtained decreased, and at high temperatures practically none was obtained. Also, in experiments with varying current densities, where a large number of coulombs (4500) were passed, practically no hydrogen was obtained during cleaning. At room temperatures, the hydrogen obtained during cleaning was found to be linearly dependent on the time during which current had been passing, as can be seen from Fig. 4. Deviation from linearity at the longer times occurred due to spalling off of the corrosion product as it thickens with the fragments lost falling outside the gas collecting bell. This explanation also accounts for the small amounts of hydrogen obtained on cleaning in the experiments with varying current densities, since in these cases the experiments were of long duration and most of the insoluble Mg spalled off the cylinders and fell outside the gas collecting bell.

A few blank experiments were made in which Mg cylinders were allowed to remain in the electrolyte without any current being passed. The amount of hydrogen

evolved at 75° was equivalent to 3 mg of Mg during a 2-hr period. At room temperature, less than this amount was recovered in a 24-hr period.

## Discussion of Results

The significant fact from the data given is that the quantities soluble Mg, insoluble Mg, and calculated Mg all bear an approximate 1:1 relationship to each other and are all approximately equal to half the total weight loss. This relationship persists over a range of temperature, current density, and surface area. To ascribe the 50% efficiencies of Mg anodes to self-corrosion requires acceptance of the fact that the self-corrosion reaction, which does not occur when the anode remains uncoupled in the electrolyte, is by fortuitous circumstances proceeding at the same rate as the current carrying reaction, and is linked to the latter in such a way that this constancy is maintained through all conditions studied. A more satisfactory explanation from the kinetic point of view would be to postulate a series of consecutive reactions all dependent on the current carrying reaction as the primary step. The following series of reactions are proposed to explain the data obtained.

$$Mg \rightarrow Mg^{+} + e \qquad \text{(I)}$$

$$2Mg^{+} + H_2O \rightarrow [Mg^{+}O^{Mg^{+}}_{H_2}] \rightarrow MgO + Mg^{++} + H_2 \qquad \text{(II)}$$

$$2Mg^{+} \rightarrow Mg^{++} + Mg \qquad \text{(III)}$$

$$Mg \rightarrow Mg^{++} + 2e \qquad \text{(IV)}$$

$$Mg + H_2O \rightarrow MgO\ H_2 \qquad \text{(V)}$$

The above reaction scheme is in accord with all the data obtained. Reaction (I), followed by reaction (II), would lead to the one to one ratio of soluble to insoluble Mg and would also give values of soluble, insoluble, and calculated Mg that are half the weight loss. Reaction (III) would account for the accumulation of Mg in the MgO lattice with time, and this Mg when dissolved in the chromic acid cleaning bath would account for the hydrogen evolved there. Reaction (II) also predicts one mole of hydrogen for each mole of soluble or insoluble Mg. Examination of the data shows that the amount of hydrogen evolved is considerably less than that predicted. There are several reasons for this discrepancy. The occurrence of (IV) to any extent would decrease the amount of hydrogen produced. The occurrence of (III) should not do so, as the removal of $Mg^{+}$ from the system would be compensated for by the production of hydrogen from the dissolution during cleaning of the Mg trapped in the corrosion product. Loss of hydrogen could occur during the changing of solutions in the electrolysis vessel, since hydrogen is evolved continuously from the wet Mg surface during this operation.

Reaction (I) is favored over reaction (IV) on energy consideration (9, 10), as the heat of hydration of Mg is 33 kcal less than the ionization potential of $Mg^{++}$ (g). However, the relative occurrence of (I) and (IV) can be changed by factors which influence this energy difference, such as electrolyte and concentration, as shown by the variation of apparent valence with electrolyte and concentration reported by Kleinberg and co-workers (3) and by the earlier work of Beetz (1) and Turrentine (5). Beetz found that the sum of the quantities: Mg equivalent to hydrogen evolved and the Mg calculated from the current passed were sometimes less than the total weight loss, indicating that (IV) was occurring to some extent. With sodium sulfate solutions, Turrentine found that the ratio of Mg equivalent to hydrogen evolved at the anode to Mg calculated from the current passed varied from ½ to 1, indicating that (IV) could occur to an appreciable extent. Robinson (11) has reported similar variations of Mg anode efficiencies while Bodforss (12), on the basis of potential measurements over a range of *p*H's, postulates (I) and (IV) co-existing over the range he investigated, with (IV) existing almost exclusively at high *p*H's.

Self-corrosion, which does not appear to any great extent at low temperatures, appeared significantly in scattered cases at 75°C. The self-corrosion reaction (V) is written as shown because, where self-corrosion occurred, the excess Mg appeared as insoluble Mg and such a reaction is analogous to that postulated by Lepin, Tetere, and Schmitt (13) for the reaction between colloidal aluminum and water. Where self-corrosion occurred, the amount of hydrogen evolved was always large and both the hydrogen evolved and the insoluble Mg were greater than the calculated weight loss, when (V) occurred to a significant extent.

The occurrence of (IV) to any extent should lead to values of soluble Mg greater than insoluble. Examination of the data shows many cases where this is so, but no unequivocal conclusions can be drawn from the data. In experiments of long duration, there is more definite evidence that the amount of soluble Mg obtained is greater than the insoluble Mg. Also, the ratio of calculated weight loss to total weight loss, i.e., the efficiency, is greater than half. Both these factors indicate occurrence of (IV) to some extent and this occurrence of (IV) may be due to the fact that the solution close to the anode surface in these experiments is separated from the bulk of the electrolyte by a reasonably thick layer of corrosion product on the anode, and thus the anode surface may be in contact with an electrolyte differing from that in the bulk of the solution for a longer time than in the shorter experiments. As electrolyte composition and concentration influences the ratio of (I) to (IV), it is possible that a change in the relative amount of reactions (I) and (IV) can occur under the conditions described.

The occurrence of (III) also explains the linear dependence of the hydrogen evolved during the cleaning on duration of current passage. One would expect that the number of Mg atoms trapped in the corrosion product lattice would increase with duration of the experiment.

There is room for considerable speculation as to the nature of the reaction complex in (II). Since the zone from which gas bubbles come was extremely narrow, it is

likely that (II) occurs at the surface between an adsorbed water molecule and univalent Mg ions.

## Conclusions

Study of the electrolysis of magnesium in 3% NaCl solutions shows that the data obtained can be explained and integrated into existing knowledge of the behavior of Mg as an anode by postulating that Mg dissolves predominately as a univalent ion and then the univalent ion reduces water forming an insoluble oxide film, divalent Mg, and hydrogen.

## Acknowledgment

The author wishes to acknowledge permission of the Defence Research Board to publish. The work described was carried out as part of Defence Research Board Project D-12-75-10-21.

Manuscript received November 7, 1955.
Any discussion of this paper will appear in a Discussion Section to be published in the June 1957 Journal.

## References

1. W. Beetz, *Pogg Ann*, **27**, 115 (1866); *Phil. Mag.*, **4**, C32, 269 (1866); *Ber.*, **10**, 118 (1877).
2. E. Elsoesser, *Ber.*, **9**, 1818 (1876).
3. R. L. Petty, A. W. Davidson, and J. Kleinberg, *J. Am. Chem. Soc.*, **76**, 363 (1954).
4. M. D. Rausch, W. E. McEwen, and J. Kleinberg, *ibid.*, **77**, 2093 (1955).
5. J. W. Turrentine, *J. Phys. Chem.*, **12**, 448 (1908).
6. R. Faivre and A. Michel, *Compt. rend.*, **208**, 1008 (1939).
7. C. Brouchere, *J. Inst. Metals*, **71**, 131 (1943).
8. K. Huber and H. Fluckiger, Comte International de Thermodynamique and de Cinetique Electro Chemiques Comptes Rendus, p. 123 (1951).
9. H. J. Emeleus and J. S. Anderson, "Modern Aspects of Inorganic Chemistry," pp. 43 and 46, Routledge & Kegan Paul, London (1952).
10. J. O'M. Bockris, "Modern Aspects of Electro Chemistry," p. 52, Butterworths, London (1954).
11. H. A. Robinson, *Trans. Electrochem. Soc.*, **90**, 49 (1946).
12. S. Bodforss, *Z. physik. Chem.*, **A153**, 101 (1931); *ibid.*, **124**, 81 (1926).
13. L. Lepin, A. Tetere, and A. Schmitt, *Doklady Akad. Nauk SSSR*, **88**, 871 (1953).

# Properties of Paper Made from Glass Flakes

T. D. Callinan and R. T. Lucas

*U. S. Naval Research Laboratory, Washington, D. C.*

## ABSTRACT

The preparation and properties of paper made from glass flakes are described. The electrical properties of a capacitor made from this paper are presented. Glass flake paper was impregnated with varnishes and became mechanically strong and water resistant.

Glass is now available commercially in the form of transparent colorless flakes. The flakes vary in size and shape but average 0.25 in. x 0.25 in. x 0.0003 in. A number of patents have described the process for manufacturing such flakes (1–3). Each entails the formation of a thin film of molten glass which, on cooling rapidly, shatters into fine pellicles.

The glass flakes employed in this work are described by the manufacturer as being a borosilicate glass, Type "E" (10% boron oxide, 54% silicon dioxide, 16% calcium oxide, 16% aluminum oxide, and 4% sodium and potassium oxide), which softens at 840°C. The density of such glass is 2.56 g/cm$^3$; refractive index, 1.549; tensile strength, 200,000 psi, and modulus of elasticity 11 $\times$ 10$^6$ psi. The material has been suggested as a filler for inorganic plastics and molding compounds. The electrical properties of such glass have been reported (4).

The preparation and properties of a paper-like product made from these flakes is described. As a class, such paper-like products have been made from flakes other than glass; thus, mica flake has been successfully made into paper and is now commercially available from several sources. The process by which this valuable item is manufactured (5) entails separating the thin leaves of naturally occurring books of mica either mechanically or chemically and depositing the pulp on the rapidly moving wire of a Fourdrinier paper machine.

At present, such a paper can be used in transformers and motors as slot armor, segment insulators, and spacers. By incorporating varnishes and impregnants, these papers can be strengthened enormously to yield laminates and plates. Again, by backing the paper with fabrics, yarns, or cellulose papers, tapes have been produced that have sufficient mechanical strength to permit use as wire and cable insulation.

As part of the continuing interest of this laboratory in inorganic papers (6), laboratory handsheets have been prepared from glass flakes. While machine runs yielding continuous sheets have not been possible because no such facilities are available here, it is thought that data summarized in this article suggest the value of industrial trials.

## Laboratory Handsheet Preparation

Handsheets were prepared by dispersing 3 g of glass flakes in 500 ml of water ($p$H 3.5), with vigorous agitation in a Waring blendor for 30 sec. $H_2SO_4$ was used to adjust the $p$H. The flakes dispersed readily and remained sus-

TABLE I. *Properties of 100% glass-flake paper*

| Physical | | Electrical | |
|---|---|---|---|
| Appearance: Transparent sheet | | Dielectric constant | |
| Glass content % | 100 | (a) 60 cps | 1.45 |
| Binder, % | 0 | (b) 1000 cps | 1.36 |
| Thickness, in. | 0.010 | (c) 10,000 cps | 1.35 |
| Tensile strength, psi | 86 | Power factor (%) | |
| Density, g/cc | 0.75 | (a) 60 cps | 0.68 |
| Mullen burst number | 1 | (b) 1000 cps | 0.66 |
| Elmendorf tear, lb | 20 | (c) 10,000 cps | 0.66 |
| Voids, % | 61 | Dielectric loss factor | |
| Uniformity | Very high | (a) 60 cps | 0.0098 |
| Dirt count | 0 | (b) 1000 cps | 0.0090 |
| Basis weight (25 × 40–500) | 150 | (c) 10,000 cps | 0.0089 |
| | | Volume resistivity $2 \times 10^{11}$ ohm-cm | |
| | | Dielectric strength 90 v/mil | |
| | | Conducting particles | 0 |

TABLE II. *Properties of varnish impregnated glass-flake paper*

| Characteristics | Alkyd (GE 1202) | Phenolic (DuPont 8995) | Polysiloxane (D-C 993) |
|---|---|---|---|
| Physical | | | |
| Color | Tan | Brown | Colorless |
| Transparency, % | 85 | 80 | 95 |
| Thickness, mils | 10.1 | 9.0 | 9.4 |
| Build, mils | 1.0 | 1.0 | 0.9 |
| Tensile strength, psi | 900 | 1800 | 700 |
| Density, g/cc | 1.14 | 1.16 | 1.74 |
| Resin content, % | 39 | 40 | 55 |
| Fold strength, psi | 0 | 0 | 0 |
| $H_2O$ absorption, % | 0.4 | 1.5 | 0.0 |
| Electrical | | | |
| Dielectric constant | | | |
| (a) 60 cps | 2.45 | 1.93 | 1.91 |
| (b) 1000 cps | 2.32 | 1.70 | 1.82 |
| (c) 10,000 cps | 2.30 | 1.69 | 1.80 |
| Power factor, % | | | |
| (a) 60 cps | 1.99 | 1.26 | 0.96 |
| (b) 1000 cps | 1.70 | 0.36 | 0.24 |
| (c) 10,000 cps | 1.69 | 0.24 | 0.20 |
| Volume resistivity, ohm-cm | $10^{13}$ | $10^{13}$ | $10^{13}$ |
| Dielectric strength, v/mil | 100 | 120 | 105 |

pended under gentle agitation. Depending on the time and degree of beating, a finer and more dispersed pulp was secured; the number of larger sized flakes was necessarily reduced.

The slurry was then added to a standard sheet mold and the wet web couched from the 200-mesh screen. Drainage time was 42 sec. The white water was clear enough to show the filtering action of the web. A uniform transparent sheet approximately 10 mils thick was obtained. Reflected light gave the sheet a silvery sheen.

The properties found are listed in Table I. The sheet was uniform, porous, brittle, and transparent. In thinner sheets it was more flexible, albeit weaker mechanically. Without a binder it would be difficult to handle in common production techniques, although the product was self-supporting. It possessed a finite although extremely low tear strength. It is thought that this might be associated with the thickness of the presently available flakes.

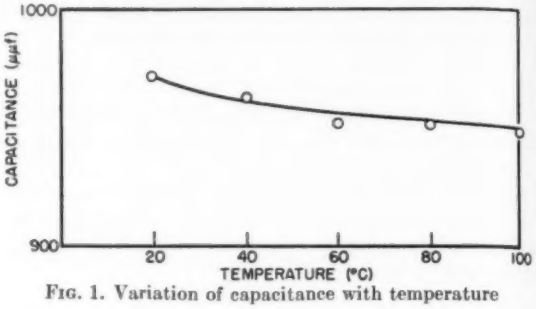


FIG. 1. Variation of capacitance with temperature

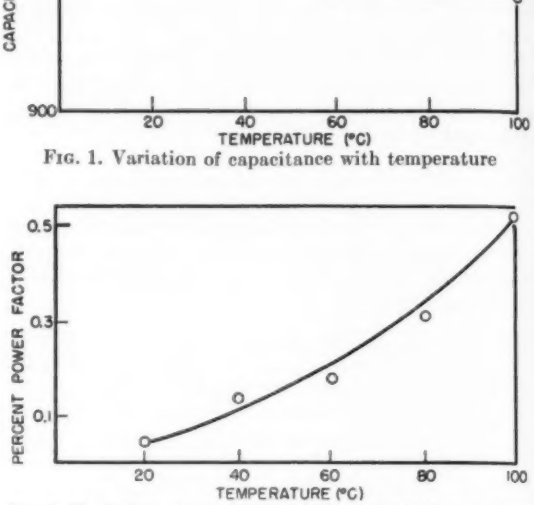


FIG. 2. Variation of per cent power factor with temperature

Thus, thin flakes (less than 4μ) might be expected to yield both stronger and more flexible glass-flake papers.

## IMPREGNATED GLASS-FLAKE PAPER

Three varnishes were studied as impregnants for glass-flake paper and the properties obtained are listed in Table II. In all cases the paper was found to saturate readily and to yield, on drying, mechanically strong, water resistant, transparent dielectric sheets. No effort was made to produce either the most highly saturated item or the highest in strength. Requirements vary so widely that each problem would require its discrete solution. From the data collected, the practicing engineer may judge the degree of saturation to satisfy his own need.

In these studies an alkyd varnish (GE 1202), an enamel used in motor insulation (Du Pont 8995 Formvar), and a silicone (Dow-Corning 993) were employed. A handsheet of glass-flake paper was dipped into a varnish and allowed to remain there (1 min) until no air bubbles or discontinuities were visible. Each impregnated sample was then permitted to air dry for 16 hr, after which it was subjected to a temperature of 125°C for 8 hr. At this point the alkyd-impregnated paper and the formvar-impregnated paper were tested. The silicone was heated 16 hr longer at 200°C to effect cure before it was tested.

All samples were found to have increased substantially in tensile strength, density, dielectric constant, and water resistance. Differences in the degree of impregnation are attributable to the viscosity of the impregnating varnishes and the techniques employed, rather than to any specific absorptivity characteristic of the glass-flake paper. The dielectric constants and the dielectric loss factors of the impregnated papers are seen to be low; greater resin content might be expected to result in higher values of both.

### Glass-Flake Paper Capacitor

A capacitor was prepared by sandwiching a piece of glass-flake paper (4 in. x 6 in. x 0.010 in.) between two aluminum electrodes (3 in. x 3 in.) held together by sheet glass clamped securely. After drying at 210°C for 24 hr, the specimen was evacuated and impregnated with silicone oil (GE SF 81/40). The capacitor was found to have the characteristics shown in Fig. 1 and 2. While glass-flake paper is not now of sufficient quality to permit it being made into tissues (0.0003 in.), the characteristics obtained on the relatively thick specimens suggest the value of studies on developing such items.

### Conclusions

From the foregoing tests, it would appear that a useful paper product can be prepared experimentally from glass flakes and that the characteristics of the items justify pilot and mill trials.

Preparation of thinner sheets containing binders deposited *in situ* seems likely from what is common knowledge of this art. It has been proved that mechanically strong and electrically good impregnated structures can be prepared in laboratory equipment; this is probably also true of continuous mill made glass-flake paper.

Tissue paper made from glass flakes, 8 $\mu$ in thickness, does not seem feasible; a sheet 0.003 in. thick would consist of flakes stacked only six high. It would appear, however, that when thinner flakes are made available, thinner as well as stronger paper will be practicable.

Manuscript received August 29, 1955. This paper was prepared for delivery before the Cincinnati Meeting, May 1 to 5, 1955.

Any discussion of this paper will appear in a Discussion Section to be published in the June 1957 Journal.

### References

1. (To Corning Glass Works) British Pat. 503,369, April 5, 1939.
2. E. H. Wellech and W. C. Weber (to Corning Glass Works), U. S. Pat. 2,251,726, Aug. 5, 1941.
3. E. H. Wellech and W. C. Weber (to Corning Glass Works) U. S. Pat. 2,251,727, Aug. 5, 1941.
4. T. D. Callinan, *This Journal*, **100**, 141 (1952).
5. H. George and L. Metzger, *Rev. gen. elec.*, **59**, 514 (1950).
6. T. D. Callinan, R. T. Lucas, and R. C. Bowers, *Elec. Mfg.*, **48**, 94 (1951).

# Permeation of Gases Through Nickel Deposits

## I. Determination of the Intrinsic Permeability of Nickel Deposits to Gases

D. T. Ewing[1] and J. Martin Tobin[2]

*Michigan State College, East Lansing, Michigan*

and

D. Gardner Foulke

*Hanson-Van Winkle-Munning Company, Matawan, New Jersey*

### ABSTRACT

Values have been obtained for permeability constants of Ni electrodeposits to hydrogen and helium with a good degree of reproducibility, the values for 0.0001 in. deposits being of the order of 9 and 6 $\times$ $10^{-8}$, respectively. Electrodeposited Ni has a porosity, in contrast to rolled Ni for which no permeability could be measured. Data show that the pores present in sound Ni electrodeposits are extremely small and that flow occurs by molecular streaming, probably at grain boundaries.

Ni electrodeposits subject to corrosive conditions may become perforated to the base metal at certain discrete points. The failure of Ni from the standpoint of protective coating is not wholly understood. A number of theories have been postulated to explain such failures (1) and a number of tests have been devised to measure either the tendency to fail or the porosity of Ni deposits.

Thon and associates discovered a structural porosity or gas permeability characteristic of Ni deposits based on the fact that, when a difference in pressure is established across a detached deposit, gas atoms or molecules flow through these "pores" or "capillaries" which extend through the deposit. Difficulty in obtaining reproducible results by this method (2) led to attempts to develop other methods, such as the passage of light rays or low energy particles, to measure the porosity of Ni deposits.

The procedure used by the authors to study this characteristic of Ni electrodeposits is similar in most respects to that used by Thon with certain modifications which have resulted in highly reproducible gas permeability data.

[1] Deceased.

[2] Present address: General Electric Co., Richland, Wash.

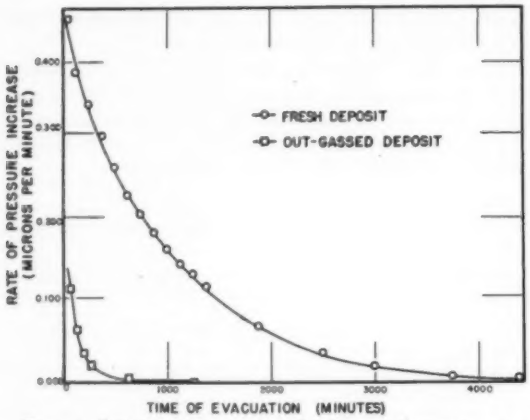


FIG. 1. Instantaneous rate of pressure increase as a function of time of evacuation at constant low pressure.

The modifications fall into two categories. Certain correctable errors were reduced to small reproducible values by improvements in technique such as the use of gases with constant moisture content, controlled out-gassing of the apparatus, and vacuum out-gassing of the foils. Second, a greater degree of reproducibility from sample to sample was attained by careful selection of samples, even though all were prepared and plated with great care.

## METHOD

The apparatus and method used were in principle the same as those already described by Thon (3). For most of the permeation measurements, Ni deposits were produced on a passive, buffed Ni base metal from which they were readily detached.

Ni deposits were prepared under controlled conditions of bath composition, temperature, current density, etc. They were then cut through to the base metal and detached. The foil was tested for "photographable" pores according to the procedure described by Ogburn (2). Deposits which were carefully prepared showed no photographable pores. When an occasional photographable pore was detected, however, that part of the deposit was not used for the permeability test.

The mean thickness of the deposit was estimated from the area of the deposit sample (a circle of $\frac{5}{8}$ in. diameter) and the weight of the sample as determined on a semimicro balance. The density of the deposit was assumed to be 8.90 g/cm$^3$.

Six circular disk samples were cut from each deposit panel and numbered according to a definite pattern. Deposit samples were then examined under a low power microscope, using transmitted light, as a further precaution against using a sample with a gross defect.

Ni deposits studied were found to be relatively impervious to the flow of gas through the deposit. Consequently, the increase in pressure in the evacuated system on the one side of the deposit which was caused by gas flowing through the deposit was of the same order of magnitude as the increase of pressure in the system caused by other effects. Correction must be made for these other effects in order to obtain the rate of permeation of gas through the deposit.

One effect is the desorption of gases from the walls of the system. This effect was controlled to a large extent by the use of compressed gases, which had a more constant composition than the dry air prepared in the laboratory.

The other effect of importance is the removal of dissolved or occluded gases and vapors from the Ni deposit itself. This effect can be very large for a freshly deposited sample. The amount of gas and vapor in a freshly deposited sample of Ni from a Watts' bath at a *p*H of 2.2 was determined in the following manner. The rate of dissolution of gas was followed as the instantaneous rate of pressure increase per unit of time and recorded as a function of time of evacuation at 25°C under a constant pressure of 1$\mu$. Correction for pressure increase caused by desorption was made by testing a sample treated in the same manner, except that it was previously out-gassed in a vacuum (Fig. 1).

A graph of the instantaneous rate of pressure increase as a function of the time of evacuation at a constant, low pressure is shown in Fig. 2. The area between the two curves was obtained by graphical integration, and is approximately $3.4 \times 10^{-5}$ atm. From the known volume of the high vacuum side and the temperature, the number of moles of gas can be calculated.

$$n = \frac{PV}{RT}$$

$$= \frac{3.40 \times 10^{-5} \text{ atm} \times 1.45 \text{ liters}}{8.20 \dfrac{\text{liter-atm}}{\text{mole-degree}} \times 298^\circ}$$

$$= 2.02 \times 10^{-8} \text{ moles}$$

A very simple qualitative test to determine the proportion of the pressure indicated by a McLeod gauge which was due to vapor was to cool the capillary tip of the gauge. In the McLeod gauge, the absolute pressure of the gas in the tip of the capillary was approximately equal to the difference in height of the two mercury

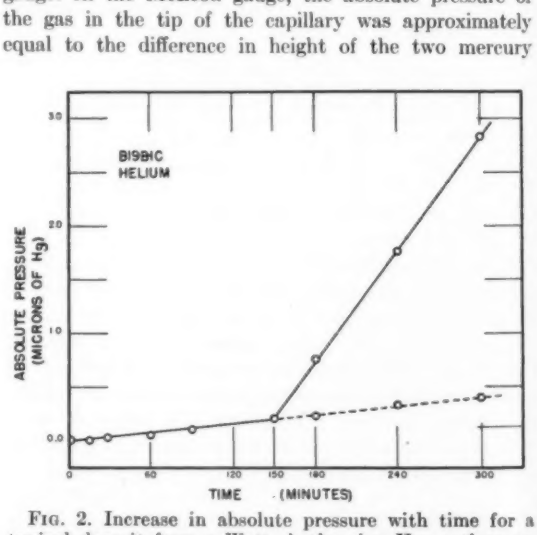


FIG. 2. Increase in absolute pressure with time for a typical deposit from a Watts bath using He as the permeating gas.

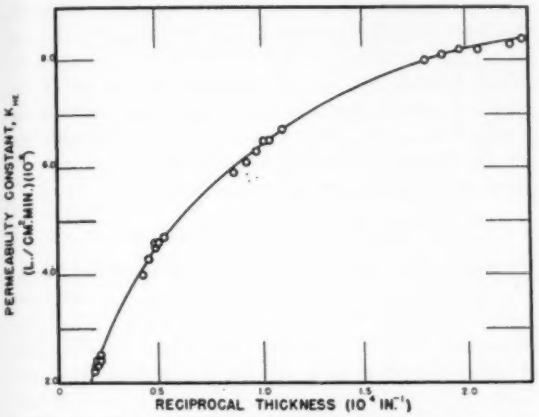


FIG. 3. Change in permeability constant, $K_{He}$, for deposits from a Watts' bath of varying thicknesses.

columns, and was easily measured in millimeters of mercury of pressure. When the tip was cooled, vapors in the tip condensed and the pressure indicated by the gauge was that caused by the permanent gases. When the tip was cooled after out-gassing a fresh deposit into the vacuum, most of the gas given off by the deposit was found to be a vapor, presumably water vapor.

Assuming the gas to be all water vapor, the per cent of water in the deposit was calculated to be as follows:

$$\% H_2O = \frac{\text{Wt } H_2O}{\text{Wt Ni}} \times 100 = \frac{2.02 \times 10^{-8} \times 18.0 \times 10^2}{4.5 \times 10^{-3}}$$

$$= 0.00809\%$$

Rise in absolute pressure as a function of time was measured by a triple scale McLeod gauge. Adjustments were made for the increase in pressure caused by the two effects previously mentioned in order to obtain the increase in pressure caused by permeation of the gas through the deposit.

Typical data with He as the permeating gas are plotted in Fig. 3. The curve of pressure as a function of time was established over a long period with a vacuum on both sides of the deposit; it was essentially linear in the range which was studied.

When a gas was admitted to the system on one side of the deposit to provide an overpressure, 1 atm in this work, a sharp inflection occurred. The increase in rate, the difference between the slopes of the two curves, was caused by gas permeating through the deposit.

The permeability constant, a measure of the flow rate at a constant overpressure, as defined by Thon, is calculated from the following equation:

$$K = V/F \times 1/P \times \Delta P/\Delta t$$

where $K$ = permeability constant, liter/cm²-min, $V$ = volume of vacuum system on the low pressure side of the deposit (1.45 l), $F$ = area of deposit being measured (0.375 cm²), $P$ = overpressure in mm Hg, $\Delta P$ = change in pressure in the evacuated system in mm Hg, and $\Delta t$ = time interval in minutes.

Thus, if the overpressure is kept constant for a series of foils, the ratio of the permeability constants is the same as the ratio of the rates of diffusion.

## RESULTS

Using a Watts' bath at 60°C, a current density of 40 asf at a *p*H of 2.2, four series of six samples of electrodeposits were prepared varying in thickness from 0.00005 in. to 0.0005 in.

Rates of flow of helium and nitrogen through these deposits with 1 atm overpressure were measured. Values of the permeability constant $K_{He}$ were calculated from the rates of flow as shown in Fig. 3. $K$ values for nitrogen were not plotted because the increase in rate of flow for this gas is smaller than the error involved in reading the McLeod gauge.

TABLE I. *Effect of deposit thickness on permeability*

| Deposit sample | Mean thickness (in.) | Inverse mean thickness ($10^4$ in.$^{-1}$) | $K_{H_2} \times 10^8$ (l/cm²min) | $K_{He} \times 10^8$ l/cm²min. |
|---|---|---|---|---|
| B16A-1A | 0.00055 | 0.18 | — | 2.2 |
| B16A-1B | 0.00051 | 0.20 | — | 2.4 |
| B16A-1C | 0.00047 | 0.21 | — | 2.4 |
| B16A-2A | 0.00057 | 0.18 | — | 2.3 |
| B16A-2B | 0.00053 | 0.19 | — | 2.3 |
| B16A-2C | 0.00048 | 0.21 | — | 2.5 |
| B16B-1A | 0.00022 | 0.45 | — | 4.3 |
| B16B-1B | 0.00021 | 0.48 | — | 4.5 |
| B16B-1C | 0.00020 | 0.50 | — | 4.6 |
| B16B-2A | 0.00024 | 0.42 | — | 4.0 |
| B16B-2B | 0.00021 | 0.48 | — | 4.6 |
| B16B-2C | 0.00019 | 0.53 | — | 4.7 |
| B19A-1A | 0.000107 | 0.93 | 8.7 | 6.1 |
| B19A-1B | 0.000102 | 0.98 | 9.0 | 6.3 |
| B19A-1C | 0.000096 | 1.04 | 9.2 | 6.5 |
| B19A-2A | 0.000115 | 0.87 | 8.5 | 5.9 |
| B19A-2B | 0.000099 | 1.01 | 8.9 | 6.5 |
| B19A-2C | 0.000093 | 1.08 | 9.4 | 6.7 |
| B19B-1A | 0.000053 | 1.88 | — | 8.1 |
| B19B-1B | 0.000049 | 2.06 | — | 8.2 |
| B19B-1C | 0.000045 | 2.22 | — | 8.3 |
| B19B-2A | 0.000055 | 1.80 | — | 8.0 |
| B19B-2B | 0.000051 | 1.97 | — | 8.2 |

TABLE II. *Conformity with Graham's law*

$$\frac{K_{H_2}}{K_{He}} = \sqrt{M_{He}/M_{H_2}}$$

| Sample | Ratio $K_{He}/K_{H_2}$ |
|---|---|
| B30-1A | 1.43 |
| B30-1B | 1.41 |
| B30-1C | 1.43 |
| B30-2A | 1.41 |
| B30-2B | 1.41 |
| B30-2C | 1.50 |
| B19-1A | 1.43 |
| B19-1B | 1.43 |
| B19-1C | 1.41 |
| B19-2A | 1.44 |
| B19-2B | 1.37 |
| B19-2C | 1.40 |
| Mean Value | 1.42 |

It should not be assumed that the foils were impermeable to nitrogen. Instead, the permeability of the foils to nitrogen was consistently less than the sensitivity of the measurement. The correction applied to the data (Fig. 2) depends on the permeating gas. He gas was adsorbed on the walls of the system to a lesser extent than nitrogen and the correction for out-gassing was smaller. As a result, the lower limit for measurement of the permeability constant for both hydrogen and helium was about $8 \times 10^{-9}$, while the lower limit for nitrogen was $5 \times 10^{-8}$.

The permeability of a substance which is uniform throughout its thickness is inversely proportional to its thickness. Many substances follow this relationship linearly, including metallurgically prepared Ni sheet at high temperature. However, when values for the permeability constant, $K_{He}$, of electrolytically prepared Ni deposits from the Watts' bath were plotted against the reciprocal thickness, this simple relationship was not obtained (Fig. 3). Apparently, the microstructure of the Ni deposit changed with increasing thickness in such a way that the thicker deposits were less permeable to gases than would be expected.

The rate of flow of hydrogen through the series of deposits approximately 0.0001 in. thick was determined and compared with the rate of flow for helium (Table I).

Comparison of the flow rates for hydrogen and helium with this series shows that the mean value of the ratio of the hydrogen flow rate to the helium flow rate is 1.42 as predicted from Graham's law of diffusion when both permeability constants are obtained at the same temperature and overpressure (Table II).

Agreement of the experimentally measured ratio of flows with that predicted from Graham's law is an indication that the pores are so small that the flow through any one pore occurs by molecular streaming and not by turbulent flow. According to Barrer (4), this type of diffusion takes place when the size of the capillary is less than the mean free path of the gas molecule at that pressure. Since the pore or capillary must also be larger than the diameter of the gas atom or molecule, the pores through which the gas flows in the electrolytic Ni deposit must be of the order of 1–1000 Å (size of atom or molecule and mean free path at entrance of pore at 1 atm pressure) and the flow must occur along grain boundaries, crystal defects, etc. They must also extend through the deposit. The same reasoning would hold for a large number of such pores in parallel.

### Effect of the Base Metal

Much of the early work on gas permeability of Ni deposits was done using buffed stainless steel as the base metal. In order to eliminate the possibility that the substitution of Ni for stainless steel would yield deposits of different permeabilities a series of measurements were made on electrodeposits prepared from a 2.2 *p*H Watts' bath with stainless steel as the base metal. Resultant values were nearly identical with values obtained for electrodeposits from the same bath with a buffed Ni base.

Rolled Ni of about the same thickness as the electrodeposits studied were reported impermeable when air was used. This was confirmed on an 0.0001 in. thick rolled Ni sample kindly supplied by August Mendizza of the Bell Telephone Laboratories. No measurable gas flow could be noted for nitrogen, hydrogen, or helium.

Manuscript received December 5, 1955. This paper was prepared for delivery before the Boston Meeting, October 3 to 7, 1954.

Any discussion of this paper will appear in a Discussion Section to be published in the June 1957 Journal.

### REFERENCES

1. N. Thon and E. T. Addison, *Monthly Rev. Am. Electroplaters' Soc.*, **34**, 831 (1947).
2. F. Ogburn and A. Benderly, *Plating*, **41**, 61, 169 (1954).
3. N. Thon, *et al.*, *ibid.*, **36**, 362 (1949).
4. R. M. Barrer, "Diffusion In and Through Solids," p. 53–5, Cambridge Press at the University, Cambridge (1951).

# New Design of an Electrolytic Cell for the Study of Electroplating Phenomena

ROGER GILMONT

*Manostat Corporation, New York, N. Y., and Polytechnic Institute of Brooklyn, Brooklyn, New York*

AND

ROBERT F. WALTON

*Tube Department, RCA Laboratories, Radio Corporation of America, Harrison, New Jersey*

ABSTRACT

By means of the theory of the electropotential, the geometrical shape of a new electroplating cell was deduced in which the current density along the cathode is linear and can be calculated directly from the total current and voltage of the cell.

The new cell consists of a container with two straight sides intersecting at 45° and two curved sides consisting of rectangular hyperbolic cylinders orthogonal to each other, and each in turn orthogonal to one of the straight sides. One of the straight sides and its opposite curved surface are insulators, the other straight side is the cathode while the remaining curved surface is the anode.

The new cell may not only be used for current density studies, but may also be used to determine the total polarization directly from simple measurements on the cell combined with the electrical conductivity of the solution.

The use of the Hull cell (1) for making plating tests is well known. It consists of a small trapezoidal cell in which the two parallel sides are insulators, the third side perpendicular to the parallel sides is the anode, and the fourth side inclined to the parallel sides is the cathode. Because the cathode is inclined, the current density varies along its length. Thus, the cell permits studies to be made of the interrelation between plating characteristics and current density in a single plating experiment.

As simple as the construction of the Hull cell is, the theoretical analysis of the variation of current density along its cathode leads one to an almost insurmountable barrier of higher mathematics. Thus, Kasper (2) pointed out that, although a mathematical solution does exist for the Hull cell, it is of such complexity that it is of no practical use to the electroplater, although to the theoretical mathematician it is a brilliant advance in the theory of the potential. Hull was able to surmount the mathematical difficulties by the simple expedient of empirically determining the current density along the inclined cathode. By a series of ingenious experiments, he measured the current density variation for a number of important electroplating solutions.[1]

Kasper maintained that the proper choice of electrode geometry would yield sufficiently simple mathematical solutions so as to eliminate the need for empirical methods. This paper attempts to show that by proper choice of geometry, it was possible to construct a simple electrolytic cell in which the current density function along the cathode could be predicted by simple mathematics and what is more, this function could be made proportional to distance, that is, linear.

## THEORY

The correct geometry was obtained by utilizing one of the fundamental principles of the theory of potential, namely, that the current density lines must be orthogonal to the equipotential surfaces. Many geometrical arrangements were considered until the desired result was obtained. But, for purposes of clarity, it will be shown how the theory of the potential may be used to derive the proper geometrical shapes to give the desired linear relationship of current density along the cathode.

In the following derivation, use is made of the four basic conditions as defined by Kasper (2):

1. The electrolyte obeys Ohm's law, namely, that the rate of dissipation of potential energy (current) is proportional to the potential energy gradient (voltage change).

2. The electrolyte is homogeneous, that is, electrically isotropic.

3. Voltage change along an electrode is negligible, so that it may be considered as an equipotential surface.

[1] The senior author of this paper had the good fortune to make the acquaintance of Kasper at the National Bureau of Standards in Washington, D. C., where both were employed in the Chemistry Division. At that time Kasper was engaged in his studies of the theory of the potential in relation to electroplating. His main thesis was that electroplaters were seriously neglecting the application of this theory to their problems. He believed that simple application of the theory would lead to the solution of the most baffling problems in electroplating and warned against the continued use of intuition and so-called "common sense" in dealing with these problems. His classic example was the Hull cell, because in all its apparent simplicity was hidden a complexity of mathematics that would frighten away the most stouthearted.

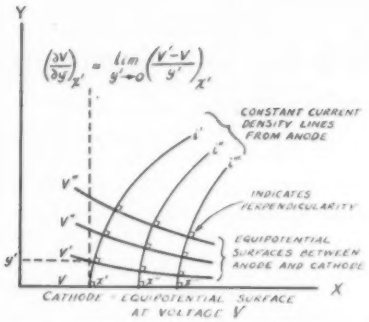
Y
$\left(\frac{\partial V}{\partial y}\right)_{x'} = \lim_{y'\to 0}\left(\frac{V'-V}{y'}\right)_{x'}$
CONSTANT CURRENT DENSITY LINES FROM ANODE
INDICATES PERPENDICULARITY
EQUIPOTENTIAL SURFACES BETWEEN ANODE AND CATHODE
CATHODE = EQUIPOTENTIAL SURFACE AT VOLTAGE V
X

FIG. 1. Equipotential surfaces are cylinders with axes perpendicular to the $x$-$y$ plane, that is, parallel to the $z$-axis. The cathode lies in the $x$-$z$ plane. Thus, current density does not vary with the $z$-coordinate, which is perpendicular to the plane of the paper.

4. A discontinuity in potential between the electrode and the solution (polarization) may exist, but it must be uniform over the electrode surface.

Since Ohm's law generally holds for electrolytes, condition 1 is a good assumption. But, condition 2 normally does not hold for electrolytes since the flow of current sets up inhomogeneities in the electrolyte. However, by vigorous stirring of the electrolyte and avoiding extremely high current densities, these inhomogeneities can be made negligible. The specific resistance of the electrode is usually negligible compared to that of the electrolyte so that condition 3 is also a good assumption. Condition 4 cannot be readily shown to hold. In fact, since the current density usually varies along the electrode surface, polarization would vary accordingly. However, experiments with the new cell have verified the fact that polarization is uniform along an equipotential surface, such as an electrode.

Thus, for a fixed geometry the polarization may be expressed as a function of the total voltage, which is constant over the electrode. In order to compare this polarization with that produced on electrodes of uniform current density and voltage, the average current density on the variable electrode is used. Although the polarization is fundamentally a function of current density, for a fixed geometry, the current density is a function of the total voltage. Since the former varies over the electrode surface in question, it is more convenient to utilize the latter as the independent variable. This procedure is equivalent to expressing the polarization as a function of the average current density on the electrode. [See equations (XIV) and (XVIII)].

Condition 1 may be expressed mathematically as follows:

$$i = -\kappa\left(\frac{\partial V}{\partial y}\right)_x \qquad \text{(I)}$$

where $i$ = current density along the cathode, $\kappa$ = conductivity in consistent units, $V$ = potential, and $(\partial V/\partial y)_x$ = potential gradient along the cathode. The minus sign indicates that the flow of current is in the direction of decreasing potential. In equation (I) the positive $x$-axis is considered to be the cathode. Since the constant current density lines are normal to an equipotential surface, the potential gradient along the cathode is given by the rate of change of voltage with respect to the $y$-coordinate at constant $x$. This condition is shown in Fig. 1.

It is desired to select the anode in such manner that the current density along the cathode is proportional to the distance from the origin. Mathematically stated:

$$i = -bx]_{y=0} \qquad \text{(II)}$$

where $b$ = proportionality constant. Again the minus sign indicates that the current flows opposite to increasing potential gradients. Combining equations (I) and (II) gives:

$$\left(\frac{\partial V}{\partial y}\right)_x = \frac{b}{\kappa}x$$

or

$$dV = \frac{b}{\kappa}x\,dy\Big]_{\text{constant } x} \qquad \text{(III)}$$

Condition 2 implies that $\kappa$ is constant so that equation (III) may be integrated at constant $x$, from the limits of $V = 0$ at $y = 0$, to give,

$$V = \frac{b}{\kappa}xy \quad \text{or} \quad xy = \frac{\kappa V}{b} \qquad \text{(IV)}$$

Equation (IV) proves that the equipotential surfaces are rectangular hyperbolic cylinders. These appear as rectangular hyperbolas in the $x$-$y$ plane with the $x$- and $y$-axes as asymptotes.

Similarly for the cathode as negative $x$-axis:

$$xy = -\frac{\kappa V}{b} \qquad \text{(V)}$$

From equations (IV) and (V), the potential of the $y$-axis (both positive and negative parts) is also at zero potential.

The equation of the current lines may now be derived from the fact that these lines must be orthogonal with the equipotential surfaces, that is, the tangents to the line and surface at their point of intersection are perpendicular. In the $x$-$y$ plane, this means that the slopes of the current lines are the negative reciprocals of the slopes of the constant voltage lines. Differentiating equation (IV) gives the slope of the constant voltage lines,

$$\frac{dy}{dx} = -\frac{y}{x}\Big]_{V=\text{constant}} \qquad \text{(VI)}$$

Thus, the slopes of the current lines become,

$$\frac{dy}{dx} = \frac{x}{y}\Big]_{i=\text{constant}}$$

or

$$x\,dx - y\,dy = 0]_{i=\text{constant}} \qquad \text{(VII)}$$

Integrating differential equation (VII), from the limits of equation (II), gives,

$$x^2 - y^2 = \frac{i^2}{b^2} \qquad \text{(VIII)}$$

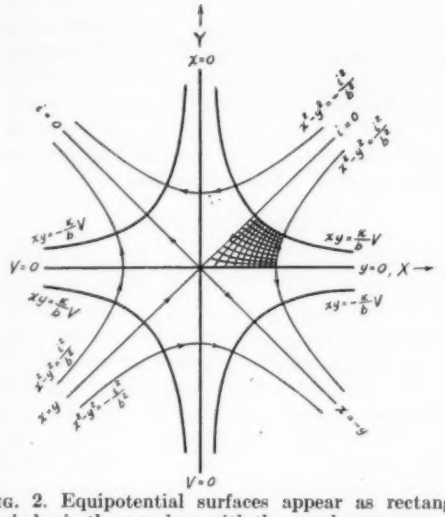


FIG. 2. Equipotential surfaces appear as rectangular hyperbolas in the $x$-$y$ plane with the $x$ and $y$ axes as asymptotes. The current lines are also rectangular hyperbolas in the $x$-$y$ plane, but with the lines $x = \pm y$ as asymptotes. Both sets of hyperbolas are mutually orthogonal in accordance with the theory of the potential.

For no current flow, i.e., $i = 0$,

$$x^2 = y^2 \quad \text{or} \quad x = \pm y \tag{IX}$$

The constant current lines are, thus, rectangular hyperbolas, but with asymptotes $x = \pm y$ (the 45° lines through the origin).

The desired result is then obtained by choosing a cell in which the equipotential surfaces are rectangular hyperbolic cylinders and the current lines are the corresponding orthogonal rectangular hyperbolas. In Fig. 2, the plating cell is a portion of the first quadrant shown by cross-hatching which simulates the current and voltage lines. Two such cells may be selected from each of the four quadrants; in the first cell, the cathode lies in the $x$-axis, in the second, the cathode lies in the $y$-axis (they are mirror images). All of the eight cells are geometrically equivalent. Those in the first and third quadrant have the cathodes in the $x$- and $y$-axes, while those in the second and fourth quadrant have the anodes in the $x$- and $y$-axes.

## CELL DESIGN

The cell was designed with two straight sides of equal length intersecting each other at 45°. The other two sides are rectangular hyperbolas orthogonal to each other and to the straight sides which each intersects (Fig. 3). The anode is placed on one of the hyperbolic sides and made to conform to its shape. The cathode is placed on the straight side opposite the anode. The remaining sides are insulators. The electrodes may be reversed in those cases where the anode is the electrode of interest such as in anodizing or electropolishing.

If the length of the cathode is made equal to $L$ and a potential difference equal to $V$ is placed across the electrodes causing a current equal to $I$ to flow between them, then it is possible to calculate the current density distribution along the cathode and evaluate the conductivity factor, $\kappa$, as follows.

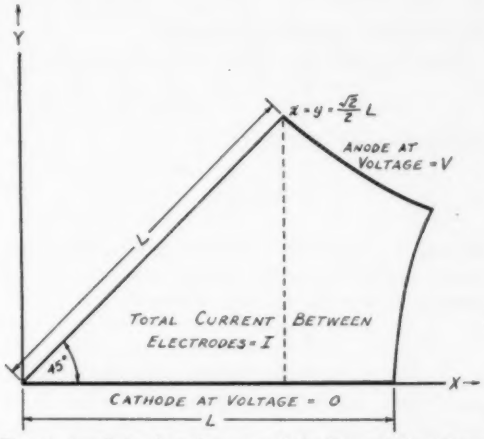


FIG. 3. Anode is placed on one of the hyperbolic sides and the cathode is placed on the opposite straight side of the cell. The length of the cathode is $L$, the voltage drop across the electrodes is $V$, and the total current flowing between them is $I$.

From equation (II),

$$b = -\frac{i}{x} = \frac{2I}{LA} \tag{X}$$

where $A$ = area of cathode receiving current. This follows from the fact that the average current density, $(-I/A)$, occurs at the midpoint of the cathode, $(x = L/2)$, which in turn is true because the current density is proportional to distance along the cathode. Substituting equation (X) in (II) gives,

$$i = -\frac{2I}{LA}x \tag{XI}$$

Taking the cathode along the positive $x$-axis, the coordinates of the point of intersection between the anode and the straight insulating side are,

$$x = y = \frac{\sqrt{2}}{2}L \tag{XII}$$

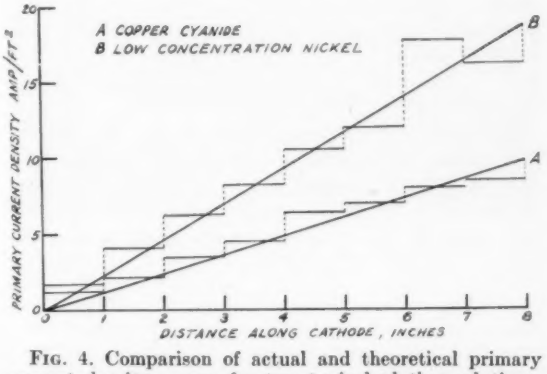


FIG. 4. Comparison of actual and theoretical primary current density curves for two typical plating solutions. Actual data are plotted as horizontal segments, while the theoretical curve is plotted as a straight line through origin.

Substituting in equation (IV) gives,

$$\frac{L^2}{2} = \frac{\kappa V}{b} \quad \text{or} \quad \kappa = \frac{b}{V}\left(\frac{L^2}{2}\right) \tag{XIII}$$

Substituting (X) in (XIII),

$$\kappa = \frac{IL}{VA} \tag{XIV}$$

If there is no polarization at the electrodes, this value of $\kappa$ should correspond to the specific conductivity of the electrolyte used in the cell, represented by $\kappa_e$.

### Polarization

If polarization does occur, condition 4 (above) may be applied. Thus, the total voltage drop, $V$, may be considered as the sum of a uniform polarization voltage, $V_p$, and the voltage drop due to resistance of the electrolyte, $V_e$, giving for the fixed geometry:

$$V = V_p + V_e \tag{XV}$$

In the absence of polarization, equation (XIV) may be written as

$$\kappa_e = \frac{IL}{V_e A} \quad \text{or} \quad V_e = \frac{IL}{\kappa_e A} \tag{XVI}$$

In the presence of polarization, equation (XVI) is a measure of the voltage drop due to electrolytic resistance only. Combining equations (XV) and (XVI) yields

$$V_p = V - \frac{IL}{\kappa_e A} \tag{XVII}$$

Adding equation (XIV) gives

$$V_p = V\frac{\kappa_e - \kappa}{\kappa_e} \tag{XVIII}$$

Equation (XVII) permits evaluation of the total polarization voltage (anode plus cathode) from simple measurements taken on the cell combined with the specific conductivity of the electrolyte. Equation (XVIII) shows that the ratio of polarization voltage to total voltage is given by the fractional loss in conductivity due to the polarization. Thus, the new cell affords a simple, rapid means of determining polarization voltage at the same time that it is used for current density studies of electroplated films.

### Cell Construction

Full details of the construction of the new cell for experimental purposes will be published elsewhere. In order to verify the theoretical basis for the cell, provisions were made to divide the cathode into vertical segments. The segments were then individually wired so that the average current to each segment could be measured and compared against the theoretical values. In addition the weight of metal deposited on each segment could also be checked against the theoretical secondary current densities. Since it is the purpose of this paper merely to develop the theoretical basis of the design of the new cell, only representative data are given here.

### Representative Data

Experimental data taken on the new cell for several key electrolytes amply verify the linear variation of current density along the cathode. In Fig. 4 are shown two typical curves of experimental data compared against theory for plating solutions with relatively high polarization. The small apparent intercept can be explained by a slight plating behind the electrode segments. Experimental error also appeared to be larger at higher current densities, although most of this error could be correlated with appearance of the plate. These examples were selected to illustrate the average extent of agreement; some were better, others were worse. On the whole, maximum deviation from theory did not exceed 10% of the maximum current density.

Total polarization voltages calculated from the data check with literature values well within the experimental error. For example, the calculated value for copper sulfate was 0.3 v compared to the literature value of 0.2 v. For copper cyanide the calculated values varied from 2.0 to 2.5 v compared to the literature value of 2.1 v. The best agreement was found with silver cyanide where both calculated and literature value were approximately equal at 0.4 v. The worst agreement was with the nickel sulfate baths, both regular and low concentration, where calculated values of 1.4 to 1.6 v compared against literature values of 0.9 to 1.1 v. This agreement must be considered excellent in light of the fact that literature values themselves were found to differ by several tenths of a volt in some cases.

### Acknowledgment

The authors wish to express their thanks to Miss Anne Michalko of the Manostat Corp. for her assistance in preparing the manuscript and drawings.

Manuscript received December 2, 1955. This paper was prepared for delivery before the Cleveland Meeting, September 30 to October 4, 1956, and was submitted to the Polytechnic Institute of Brooklyn in partial fulfillment of the degree of Master of Chemical Engineering by R. F Walton.

Any discussion of this paper will appear in a Discussion Section to be published in the June 1957 Journal.

### REFERENCES

1. R. O. Hull, *Proc. Am. Electroplaters' Soc.*, 52 (1939).
2. C. Kasper, *Trans. Am. Electrochem. Soc.*, **77**, 353 (1940).

# Electron Microscope Studies of Copper Anodes Obtained in Sulfate and Cyanide Baths

SHINZŌ OKADA, SABURŌ MAGARI, AND KENTARŌ KATSUI

*Engineering Research Institute, Kyoto University, Kyoto, Japan*

ABSTRACT

Copper anodes in sulfate and cyanide plating baths, at low current densities, were studied by the use of the electron microscope and it was found that the appearance of the microstructure of the surface formed during electrolysis varied with the electrolytes, but the same crystal planes were developed in both baths and in a number of etching solutions. The microstructure was characteristic for a given crystal face at the surface. {210} planes were developed.

Much work has been done on the etch structure developed on single-crystal and polycrystalline copper, and it is believed that, with a single crystal of copper, the {111} and {100} planes, and sometimes the {210}, {311}, {310}, and {511} planes, are developed by etching (1, 2).

In this study, the microstructure of the surface of the copper anode formed during electrolysis in sulfate and cyanide plating baths, at low current densities, was examined by the electron microscope. In addition, the orientation of the microstructure of the anode was determined.

## EXPERIMENTAL

The sulfate bath contained 150 g/l copper sulfate pentahydrate and 40 g/l sulfuric acid. The cyanide bath contained 22.5 g/l copper cyanide, 30.0 g/l sodium cyanide, and 10.0 g/l sodium carbonate. Electrolysis was carried out, without agitation, at 30°C in all experiments. Cathodes were 2 x 2 cm² rolled copper plates, while the anodes were copper plates, the characteristics of which varied for different experiments. One side of each anode and cathode was coated with polyvinyl formal.

The two-step replica method was used for electron microscopy. A benzol solution of polymethyl methacrylate was poured on the anode before electrolysis and allowed to dry. The resin was then carefully removed from the anode, placed in a vacuum evaporator, coated with aluminum, and shadowed with chromium. After electrolysis the anode was rinsed with distilled water, dried, and again treated with polymethyl methacrylate as outlined above. The technique outlined previously was used to locate the identical spot on the anode under the electron microscope before and after electrolysis (3).

Orientation of facets developed on the surface during electrolytic etching was determined by combined x-ray transmission analysis and light reflections.

## RESULTS

*Dissolution in copper sulfate electrolyte.*—The electropolished surface of a rolled copper anode, 2 x 2 cm² in area and 0.5 mm thick, was electrolyzed at between 1.6 and 20 ma/cm². Plate I shows the surface after electrolysis for 12 min at 3 ma/cm².

Electrolysis was also carried out between 1.6 and 20 ma/cm² on a rolled copper anode etched with 10% ammonium persulfate solution. Electrolysis for 24 min at 1.6 ma/cm² gave the surface shown in Plate II.

PLATE I. Electropolished rolled copper anode in sulfate bath. 3000×.

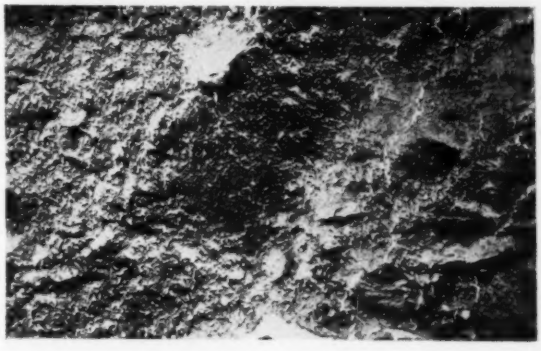

PLATE II. Chemically etched rolled copper anode in sulfate bath. 3000×.

In order to determine whether or not the facets that developed on the polycrystalline anode were related to a crystallographic plane in the crystals on which they formed, an electropolished anode composed of two single crystals of known orientation was electrolyzed at 1 ma/

PLATE III(a). Single-crystal copper anode in sulfate bath, initial surface. 3000×.

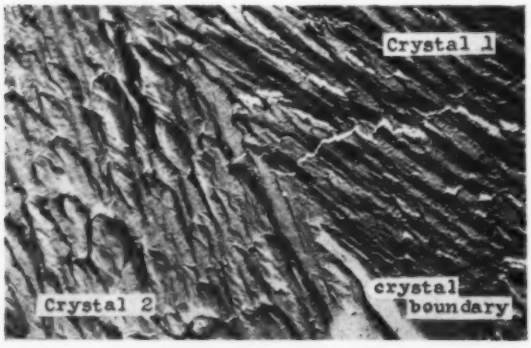


PLATE III(b). Single-crystal copper anode in sulfate bath after electrolysis for 20 min. 3000×.

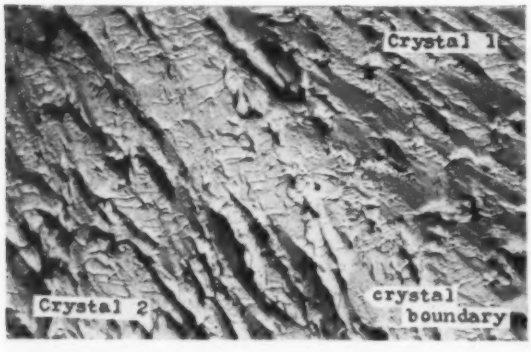


PLATE III(c). Single-crystal copper anode in sulfate bath after 40 min additional electrolysis. 3000×.

cm². Plate III(a) shows the initial surface, preparing for electrolysis. After 20 min the surface shown in Plate III(a) became rougher as shown in Plate III(b). An additional 40 min gave the surface shown in Plate III(c). Plate V shows the surface corresponding to Plate III(c) under greater magnification.

Optical reflecting data are recorded in Table I.

*Dissolution in copper cyanide electrolyte.*—Rolled copper

TABLE I

| | Crystal 1 | | Crystal 2 | |
|---|---|---|---|---|
| | $\delta°$ | $\theta°$ | $\delta°$ | $\theta°$ |
| Optical | −135 | 76 | −122 | 75 |
| | ($a_1$) | | ($b_1$) | |
| X-ray | −142 | 76 | −130 | 76 |
| | (021) | | (120) | |
| Optical | 25 | 70 | 78 | 68 |
| | ($a_2$) | | ($b_2$) | |
| X-ray | 28 | 68 | 80 | 65 |
| | ($\bar{1}20$) | | ($02\bar{1}$) | |

$\delta$: angle between a reference plane including the normal to the surface of the specimen and the plane including this normal and the normal to the crystallographic plane or facets in question.

$\theta$: angle between the normal to the crystallographic plane or facets and the normal to the surface of the specimen.

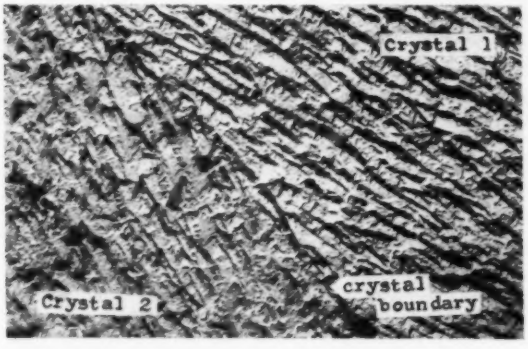


PLATE IV(a). Single copper anode in cyanide bath after electrolysis for 60 min. 3000×.

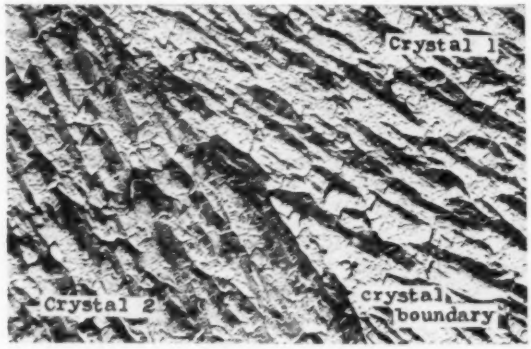


PLATE IV(b). Single copper anode in cyanide bath after 60 min additional electrolysis. 3000×.

anodes were electrolyzed at current densities between 10 ma/cm² and 1.6 ma/cm².

To determine whether dissolution in a cyanide electrolyte would show a characteristic plane on a single-crystal anode, the electropolished bi-crystal anode was electrolyzed at 1 ma/cm². Plate IV(a) shows the surface

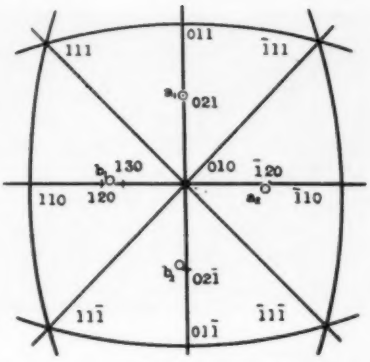


FIG. 1. $a_1$ and $a_2$ represent the normals to the optical reflecting facets for electrolyzed crystal 1, and $b_1$ and $b_2$ represent the corresponding facets for crystal 2.

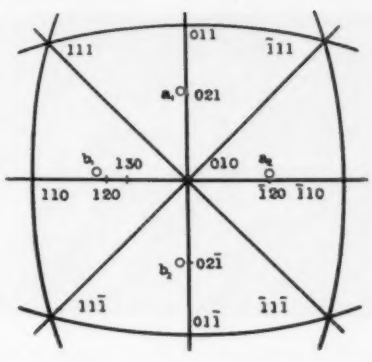


FIG. 2. $a_1$ and $a_2$ represent the normals to the optical reflecting facets for electrolyzed crystal 1, and $b_1$ and $b_2$ represent those for crystal 2.

after electrolysis for 60 min and further electrolysis for another 60 min gave the surface shown in Plate IV(b).

Optical analysis was carried out on the surface.

*Dissolution in etching solutions.*—To learn the relation between the dissolution in copper plating baths and that in etching solutions for metallography, the bi-crystal copper plate was etched in the following manner: (*a*) immersed in aqua regia for 2 min, then in 10% ammonium persulfate solution for 15 min; (*b*) anodically etched with 1 part nitric acid ($d$ = 1.38) to 5 parts water at 20 ma/cm² for 5 min; (*c*) anodically etched with 10% ammonium persulfate solution at 20 ma/cm² for 5 min.

## DISCUSSION

*Dissolution in copper sulfate electrolyte.*—Dissolution of electropolished rolled copper anodes was almost uniform over the surface at higher current densities. The lower the current density, the more uneven the surface was left. Nonuniform dissolution is seen in Plate I, and further electrolysis accentuated the unevenness. Unevenness of the surface at lower current densities is believed to be due to the difference of the solutional potential of each crystal in the anode.

In the case of chemically etched rolled copper anode, nonuniformity of dissolution was not observed at any current density and indeed the surface became smoother than the initial one. No characteristic dissolution was revealed as shown in Plate II. It is possible that the orientation formed by chemical etching of the facets on the anode might be the same as that formed by electrolysis.

In the case of the electropolished bi-crystal anodes, the crystal boundary is discernible after electrolysis as shown in Plate III(b), while on the initial surface the boundary was not evident [Plate III(a)]. The boundary became accentuated after further electrolysis as shown in Plate III(c). The ability to distinguish the boundary after electrolysis shows that the orientation of the microstructure of the surface on the two crystals was different.

The data of Table I are summarized stereographically in Fig. 1. It is considered that $a_1$, $a_2$, $b_1$, and $b_2$ correspond to the (021), ($\bar{1}$20), (120), and (02$\bar{1}$) planes of the base crystal, respectively.

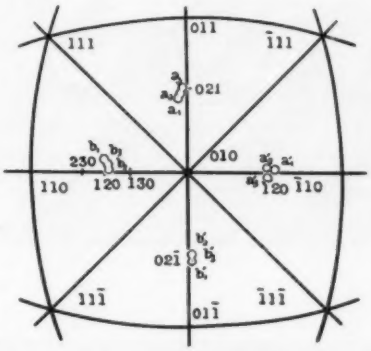


FIG. 3. $a_1$, $a_2$, $a_3$, $a_1'$, $a_2'$, and $a_3'$ represent the normals to the optical reflecting facets for electrolyzed crystal 1, respectively, and $b_1$, $b_2$, $b_3$, $b_1'$, $b_2'$, and $b_3'$ represent the corresponding facets for crystal 2.

It is concluded that the dissolution of a single copper crystal in a sulfate bath occurs with the development of {210} planes of the base crystal.

*Dissolution in copper cyanide electrolyte.*—Regardless of whether the rolled anode had been electropolished or chemically etched, no characteristics of the microstructure of the surface was observed at any current density.

The initial surface of electropolished bi-crystal anode again did not reveal the crystal boundary. After electrolysis, however, the boundary became evident and additional electrolysis made it much more pronounced. This is shown more clearly by the greater magnification of Plate VI. It is clear from the evidence presented that the orientation of the base crystal has an influence on that of the microstructure of the surface.

Optical data are summarized stereographically in Fig. 2. As before, the reflecting facets are {210} planes of the base crystal.

It is concluded that the dissolution of a single copper crystal in a cyanide bath also shows {210} planes of the base crystal.

*Dissolution in etching solutions.*—Optical data are summarized stereographically in Fig. 3. The normals to the optical reflecting facets are near the normals to {210} planes of the base crystal.

PLATE V. Enlargement of Plate III(c). 5500×.

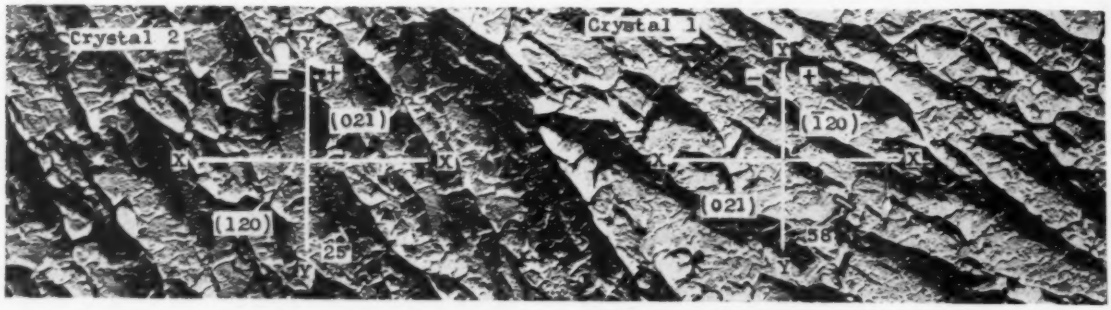


PLATE VI. Enlargement of Plate IV(b). 5500×.

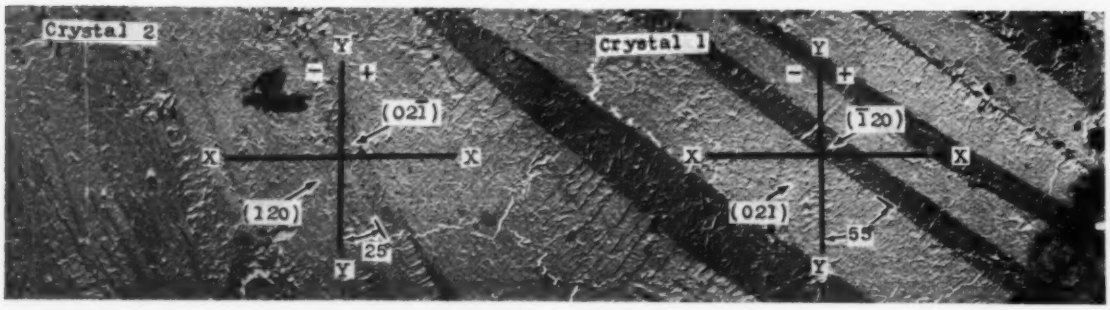


PLATE VII. Etched with 10% ammonium persulfate solution for 15 min. 5500×.

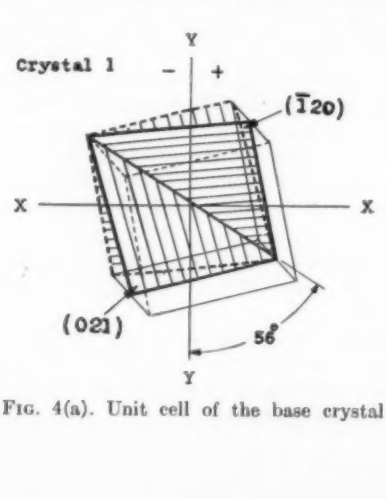


FIG. 4(a). Unit cell of the base crystal

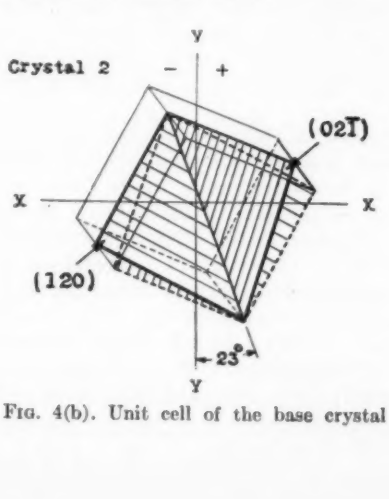


FIG. 4(b). Unit cell of the base crystal

It is concluded that the dissolution of a single crystal in etching solution also shows {210} planes of the base crystal.

Fig. 4(a) and (b) show a unit cell of base crystals 1 and 2, as determined from x-ray examinations, corresponding to Plate V, Plate VI, and Plate VII. The lightly shadowed planes in the electron micrographs are (021) planes of base crystal 1 and (120) planes of crystal 2, while the heavily shadowed planes are $(\bar{1}20)$ planes of crystal 1 and $(02\bar{1})$ planes of crystal 2, respectively.

Analysis of the data of x-ray and optical reflection and electron micrographs showed that the facets in the surface were parallel to {210} planes and that the ridges were nearly parallel to the line of intersection on the {210} planes that were parallel to the facets. This was a [212] direction.

ACKNOWLEDGMENT

The authors are deeply indebted to Dr. J. Takamura, Faculty of Engineering, Kyoto University, for supplying copper single crystals and for his valuable advice.

Manuscript received June 3, 1955.
Any discussion of this paper will appear in a Discussion Section to be published in the June 1957 JOURNAL.

REFERENCES

1. S. TAKEYAMA, *Mem. Coll. Sci. Univ. Kyoto*, **13**, 353 (1930).
2. H. LEIDHEISER AND A. T. GWATHMEY, *Trans. Electrochem. Soc.*, **91**, 95 (1947).
3. S. OKADA AND S. MAGARI, *Bull. Eng. Research Inst. Kyoto Univ.*, **3**, 59 (1953).

# Electron Microscope Studies on Copper Electrodes in Sulfate Bath Containing Addition Agent

SHINZŌ OKADA, SABURŌ MAGARI, AND KENTARŌ KATSUI

*Engineering Research Institute, Kyoto University, Kyoto, Japan*

ABSTRACT

Thiourea, gelatin, or glue in a copper sulfate bath at low current densities prevent development of facets in the surface parallel to the {111} planes of a single-crystal cathode but have no influence on the facets of the deposit parallel to the {010} planes. Thiourea gave the smoothest deposits, in which the facets of the deposit were parallel to the {120} planes of the base crystal. At a single-crystal anode, planes developed parallel to the {010} planes of the crystal when gelatin or glue was present, but thiourea did not cause development of a characteristic plane. Aging the electrolyte did not influence the orientation of facets on the anodes, but did increase the smoothness of its surface.

In the absence of addition agents, facets in the surface parallel to the {111}, {010}, and {120} planes of a single-crystal cathode are developed during electrodeposition from a copper sulfate bath at low current densities (1). At the anode, facets in the surface parallel to the {120} planes of the base crystal were developed. The present study was made to determine the influence of addition agents on the orientation of the facets on the electrode surfaces, if the addition of thiourea, gelatin, and glue to the electrolyte influences the character of the new surface developed on large copper crystals during electrolysis.

## EXPERIMENTAL

The electrolytic bath contained 150 g/l copper sulfate pentahydrate, 40 g/l sulfuric acid ($d$ = 1.84) and the desired amount of addition agent (gelatin, glue, or thiourea). In all experiments, the current density was 1 ma/cm$^2$, the electrolyte was unstirred. Gelatin or glue were dissolved in the bath at 35°C after which the temperature was reduced to 30°C, at which temperature electrolysis occurred in all experiments.

Electrodes to be examined with the electron microscope were 1 cm x 2 cm bi-crystal (denoted as crystals 1 and 2) copper plates of known orientation. (Orientation was determined by transmitted x-ray analysis.) Other electrodes were 2 cm x 2 cm rolled copper sheet. One side of each anode and cathode was coated with polyvinyl formal.

The 2-step replica method was used for electron microscopy. A benzol solution of polymethyl methacrylate was poured on the surface of each electrode before electrolysis and allowed to dry. The resin film was then carefully removed and placed in a vacuum evaporator, where it was coated with aluminum and shadowed with chromium in the usual way. The procedure was repeated after electrolysis. The technique outlined previously (2) was used to locate the identical spot on the electrode under the microscope before and after electrolysis.

Orientation of the facets on the electrode surface was determined by reflection of light from the surface passed through a 0.5 mm slit to establish the position of the facets relative to an arbitrary set of axes. Then, with the crystal in the same position, orientation of the original

single crystal was determined with transmitted x-rays. By comparison of the two sets of data, it was possible to determine which planes of the base crystal were parallel to the facets on the electrode surface.

TABLE I. *Optical and x-ray data for deposits and for anodes after electrolysis for 120 min in the presence of gelatin*

| Gelatin, % | 0.1 | | | | 0.3 | | | | 1.0 | | | |
|---|---|---|---|---|---|---|---|---|---|---|---|---|
| Cathode crystal | 1 | | 2 | | 1 | | 2 | | 1 | | 2 | |
| | $\delta°$ | $\theta°$ | $\delta°$ | $\theta°$ | $\delta°$ | $\theta°$ | $\delta°$ | $\theta°$ | $\delta°$ | $\theta°$ | $\delta°$ | $\theta°$ |
| Optical | −41 | 70 | 142 | 66 | −40 | 68 | 143 | 66 | −43 | 68 | 147 | 69 |
| X-ray | −40 | 68 | 145 | 65 | −40 | 68 | 145 | 65 | −40 | 68 | 145 | 65 |
| | (010) | | (010) | | (010) | | (010) | | (010) | | (010) | |
| Optical | −140 | 78 | −128 | 76 | | | | | | | | |
| X-ray | −140 | 76 | −130 | 78 | | | | | | | | |
| | (021) | | (120) | | | | | | | | | |
| Anode crystal | 1 | | 2 | | 1 | | 2 | | 1 | | 2 | |
| Optical | −145 | 74 | −130 | 75 | 30 | 67 | 76 | 65 | −42 | 70 | 140 | 68 |
| X-ray | −142 | 76 | −130 | 76 | 28 | 68 | 80 | 63 | −40 | 68 | 145 | 65 |
| | (021) | | (120) | | (120) | | (021) | | (010) | | (010) | |
| Optical | | | | | −140 | 74 | −128 | 74 | | | | |
| | | | | | −142 | 76 | −130 | 76 | | | | |
| | | | | | (021) | | (120) | | | | | |

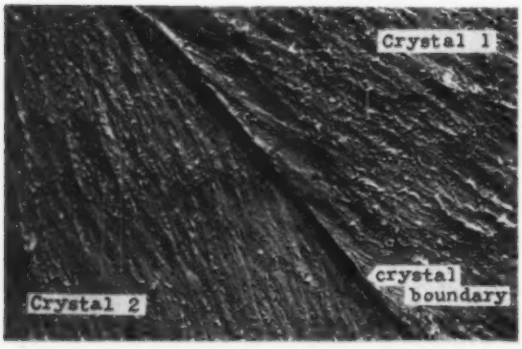


Plate I(a). Deposit from fresh bath containing 1% gelatin after 120-min electrolysis. 3000×.

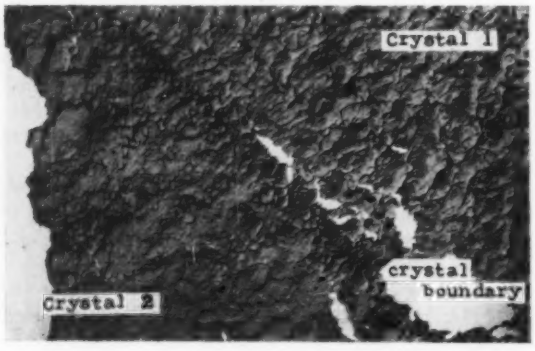


Plate I(b). Anode in fresh bath containing 1% gelatin after 120-min electrolysis. 3000×.

## Results

*Gelatin as addition agent.*—In Table I are recorded the average angular coordinates of the normals to facets in the new surfaces of electrodes and the angular coordinates of the normals to crystallographic planes of low indices in the electrodes that are nearly parallel to the facets. X-ray data give only the index of the plane of the facets on the electrode determined by back reflection of light. $\theta$ is the angle between normal to surface and normal to facet and is also used as the angle between normal to surface and normal to crystallographic plane. $\delta$ is the angle between a reference line in the surface examined and the plane including the surface and facet normals, measured in clockwise and counter clockwise relations. It is used in a similar way for the crystallographic planes.

Prior to the experiments with 1% gelatin, no boundary was evident between cathode crystals 1 and 2, but the boundary was discernible after electrolysis [Plate I (a)], which indicates that the deposits on the two crystals were different. The surface of the anode after electrolysis in the presence of 1% gelatin is shown in Plate I (b).

Aging the electrolyte containing 1% gelatin gave results shown in Table II. The data of treatment C in the table were obtained with copper crystals which had been electropolished and showed no boundaries prior to electrolysis. However, after 20 min of electrolysis the boundaries on both cathode and anode were revealed. The cathode surface resembled that in Plate I (a). After the electrolyte had aged for 8 days, and electrolysis resumed for 100 min, the surface of the cathode [Plate II (a)] became quite different from that of Plate I (a), although the total time of electrolysis was the same. Similarly, the surface of the anode was smoother [Plate II (b)] than that shown in Plate I (b).

*Glue as addition agent.*—Electrolysis for 120 min in fresh electrolyte containing 0.5% glue gave a cathode surface [Plate III (a)] rougher than that obtained with gelatin. The corresponding anode surface [Plate III (b)] had a blocky mosaic structure.

Electropolished crystals, which again showed no boundaries, developed boundaries at both cathode and anode after 20 min electrodeposition in fresh electrolyte containing 0.5% glue. This boundary became accentuated after 40-min electrolysis when the electrolyte had been allowed to age for 4 days. With 60 min additional electrolysis after the electrolyte had aged for 8 days, the cathode surface of Plate IV(a) and the anode surface of Plate IV(b) were obtained; the cathode was smoother than that with gelatin in similar circumstances [Plate II (a)], while the anode surface was rougher than that in a new bath [Plate II(b)]. The optical and x-ray data are shown in Table III.

*Thiourea as addition agent.*—Electrodeposition for 120 min in fresh electrolyte containing 0.04 g/l thiourea revealed the boundaries between the crystals [Plate V(a) and V(b)] although the reflected light was weak from the cathode and insufficient from the anode to permit characterization of the surface. Optical and x-ray data for the cathode were recorded in Table IV.

TABLE II. *Effect of aging the electrolyte on cathode deposits and on anodes in the presence of 1.0% gelatin*

| Treatment | | Cathode crystal | | | | Anode crystal | | | |
|---|---|---|---|---|---|---|---|---|---|
| | | 1 | | 2 | | 1 | | 2 | |
| | | $\delta°$ | $\theta°$ | $\delta°$ | $\theta°$ | $\delta°$ | $\theta°$ | $\delta°$ | $\theta°$ |
| A. Aged 2 days, electrolyzed 120 min | Optical | −41 | 70 | 145 | 69 | | | | |
| | X-ray | −40 | 68 | 145 | 65 | | | | |
| | | (010) | | (010) | | | | | |
| | Optical | −141 | 77 | | | | | | |
| | X-ray | −142 | 76 | | | | | | |
| | | (021) | | | | | | | |
| B. Aged 3 days, electrolyzed 120 min | Optical | −41 | 68 | 142 | 68 | | | | |
| | X-ray | −40 | 68 | 145 | 65 | | | | |
| | | (010) | | (010) | | | | | |
| | Optical | −140 | 76 | −128 | 77 | | | | |
| | X-ray | −142 | 76 | −130 | 78 | | | | |
| | | (021) | | (120) | | | | | |
| C. Electrolyzed 20 min, aged 8 days, electrolyzed further for 100 min | Optical | −40 | 68 | 142 | 65 | 25 | 66* | | |
| | X-ray | −40 | 68 | 145 | 65 | 28 | 65 | | |
| | | (010) | | (010) | | ($\bar{1}$20) | | | |
| | Optical | −143 | 77 | −130 | 78 | −40 | 72 | 144 | 69 |
| | X-ray | −142 | 76 | −130 | 78 | −40 | 69 | 145 | 65 |
| | | (021) | | (120) | | (010) | | (010) | |

* Weak.

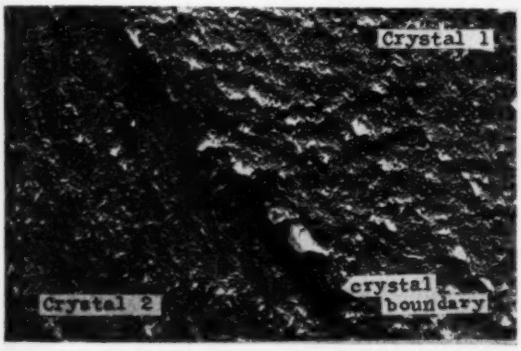


Plate II(a). Deposit from aged bath containing 1% gelatin after 120-min electrolysis. 3000×.

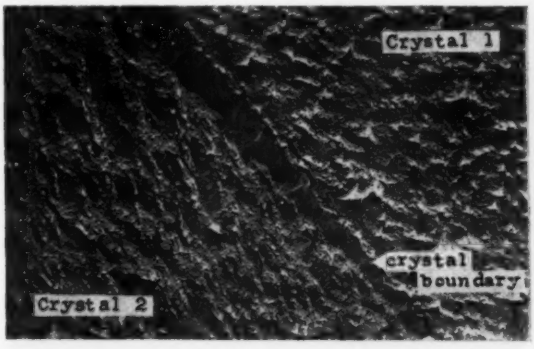


Plate III(a). Deposit from fresh bath containing 0.5% glue after 120-min electrolysis. 3000×.

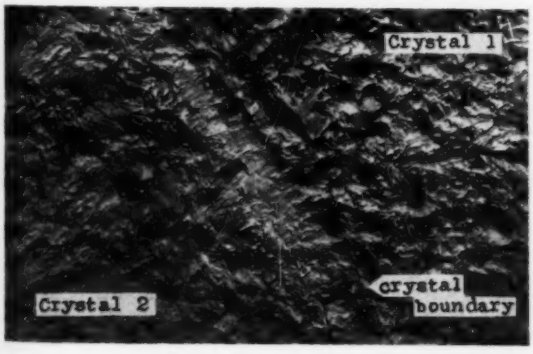


Plate II(b). Anode in aged bath containing 1% gelatin after 120-min electrolysis. 3000×.

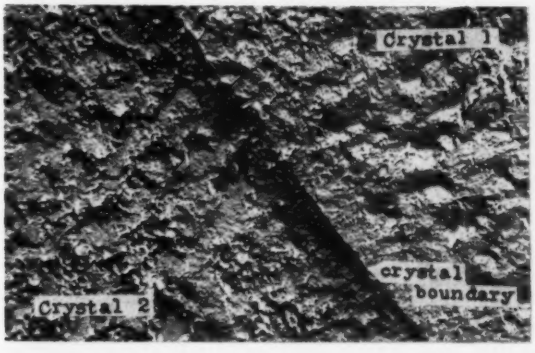


Plate III(b). Anode in fresh bath containing 0.5% glue after 120-min electrolysis. 3000×.

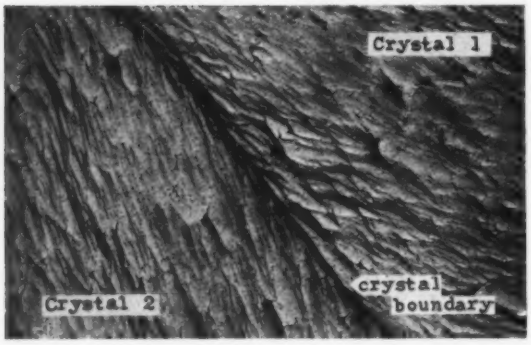


Plate IV(a). Deposit from aged bath containing 0.5% glue after 120-min electrolysis. 3000×.

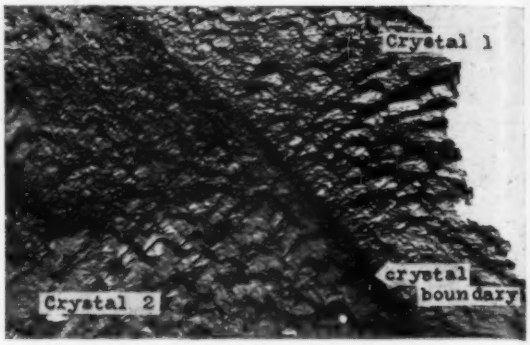


Plate IV(b). Anode in aged bath containing 0.5% glue after 120-min electrolysis. 3000×.

TABLE III. *Effect of glue on fresh and aged electrolyte on cathode deposit and on anode*

| Treatment | | Cathode crystal | | | | Anode crystal | | | |
|---|---|---|---|---|---|---|---|---|---|
| | | 1 | | 2 | | 1 | | 2 | |
| | | $\delta°$ | $\theta°$ | $\delta°$ | $\theta°$ | $\delta°$ | $\theta°$ | $\delta°$ | $\theta°$ |
| Electrolysis for 120 min in fresh electrolyte | Optical | −38 | 72 | 144 | 69 | −42 | 68 | 140 | 69 |
| | X-ray | −40 | 68 | 145 | 65 | −40 | 69 | 145 | 65 |
| | | (010) | | (010) | | (010) | | (010) | |
| | Optical | −140 | 76* | −132 | 78* | | | | |
| | X-ray | −142 | 76 | −130 | 78 | | | | |
| | | (021) | | (120) | | | | | |
| Electrolysis for 20 min in fresh electrolyte, 40 min after 4 days aging, and 60 min after 8 days aging | Optical | −37 | 68 | 145 | 69 | −40 | 70 | 141 | 68 |
| | X-ray | −40 | 68 | 145 | 65 | −40 | 69 | 145 | 65 |
| | | (010) | | (010) | | (010) | | (010) | |
| | Optical | −144 | 75* | −129 | 78* | | | | |
| | X-ray | −142 | 76 | −130 | 78 | | | | |
| | | (021) | | (120) | | | | | |

* Weak.

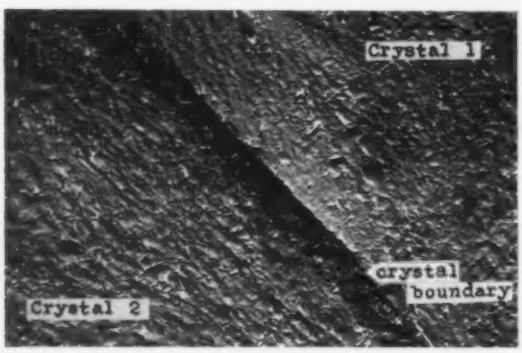


Plate V(a). Deposit from fresh bath containing 0.04 g/l thiourea after 120-min electrolysis. 3000×.

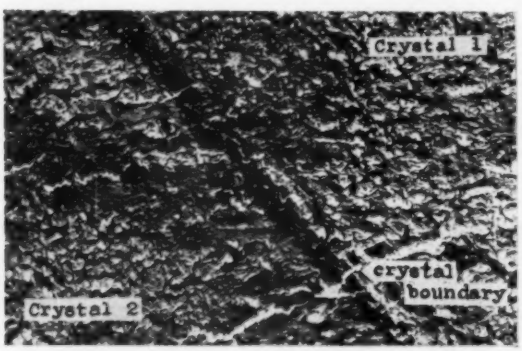


Plate V(b). Anode in fresh bath containing 0.04 g/l thiourea after 120-min electrolysis. 3000×.

## Discussion

The effect of gelatin on orientation of the facets in the cathode deposit changed with concentration; with 0.1% gelatin, facets corresponded to the {120} and {010} planes of the base crystal, but with 0.3% and 1% gelatin the orientation changed to that of the {010} planes. A strong spot in the center indicates that a large portion of the new surface remained parallel to the initial surface, that is, the deposition or dissolution did not completely cover the surface with facets parallel to crystallographic planes. Aging the electrolyte affects the orientation of the facets on the cathode corresponding to {120} planes of the base

TABLE IV. *Optical and x-ray data for deposits after electrolysis for 120 min in the presence of thiourea*

| | Cathode crystal | | | |
|---|---|---|---|---|
| | 1 | | 2 | |
| | $\delta°$ | $\theta°$ | $\delta°$ | $\theta°$ |
| Optical | 25 | 68 | 78 | 68 |
| X-ray | 28 | 65 | 80 | 65 |
| | ($\bar{1}$20) | | (02$\bar{1}$) | |
| Optical | −142 | 75 | −133 | 78 |
| X-ray | −142 | 76 | −130 | 78 |
| | (021) | | (120) | |

crystal, probably because the life of gelatin as an addition agent is very short. At the anode, the presence of 0.1% and 0.3% gelatin had no influence on the orientation of the facets, and the {120} planes of the base crystal developed in the bath without addition agent, while in the 1% bath those corresponding to the {120} planes disappeared. Aging the electrolyte appeared to have no influence on the orientation of the facets, but seemed to affect the evenness of the anode surface.

With glue as the addition agent in fresh electrolyte, the behavior was different from that observed with gelatin. Strong development corresponding to the {010} planes of the base crystal occurred in the cathode, together with weaker development corresponding to the {120} planes. The reverse occurred in aged electrolyte, which yields a smoother deposit than fresh electrolyte. At the anode, glue promoted development of the {010} planes in both fresh and aged electrolyte, although the anode was smoother in the aged than in the fresh.

Thiourea gave a very smooth cathode, with weak development of facets corresponding to the {120} planes of the base crystal, and a strong center spot. At the anode, uniform solution of each crystal would account for the optical data and electron micrographs, but the existence of a boundary between the crystals suggests that they dissolved at different rates.

Manuscript received October 13, 1955. This paper was prepared for delivery before the Pittsburgh Meeting, Oct. 9 to 13, 1955. Any discussion of this paper will appear in the June 1957 Discussion Section.

REFERENCES

1. S. Okada and S. Magari, *This Journal*, **102**, 580 (1955).
2. S. Okada and S. Magari, *Bull. Eng. Research Inst. Kyoto Univ.*, **3**, 59 (1953).

# Effect of Impurities on the Hardness of Titanium

T. D. McKinley

*Research Division, Pigments Department, E. I. du Pont de Nemours & Company, Wilmington, Delaware*

ABSTRACT

The individual effects of 15 impurities on the as-cast hardness of Ti buttons prepared under reproducible conditions have been determined. The data presented allow the estimation of oxygen in unalloyed Ti from a hardness measurement and a few conventional chemical analyses with an error of less than 10% from the value as determined by vacuum fusion analysis.

Numerous experimenters (1–15, 17, 18) have studied the effect of impurities on the hardness of Ti. In general, correlations were obtained using Ti that had been mechanically worked. Since the hardness of a metal is a function of thermal and mechanical history as well as of impurity level, it is not surprising that reported values have considerable variance.

Determination of the as-cast hardness of arc melted Ti has been and continues to be a primary measure of Ti quality for both sponge producers and fabricators. The primary object of the present work is to correlate the individual effects of varying amounts of some 15 impurities on the as-cast hardness of Ti buttons prepared under reproducible conditions. These correlations show the relative hardening effect of the impurities and allow estimation of variation of hardness with impurity level. Above and beyond the obvious applications of such correlations, the data presented also allow the estimation of oxygen in unalloyed Ti from a hardness measurement and a few conventional chemical analyses, that is, without recourse to an actual oxygen determination. Estimation of oxygen can be made in this manner with an expected error of less than 10% from the value as determined by vacuum fusion analysis. A further result of this work, and one having a direct bearing on the accuracy of the data, is the development of a simple, reproducible procedure for preparing homogeneous Ti buttons.

## Preparation of Samples

Ti buttons were prepared in a furnace with water-cooled copper crucible and water-cooled tungsten electrode (Fig. 1). Direct current was supplied by either a motor-generator or a rectifier. For melting 100-gram buttons, the standard weight used throughout this study, the maximum power requirement is 200 amp at 25 v. Melting was performed under pure helium at 650–800 mm absolute pressure.

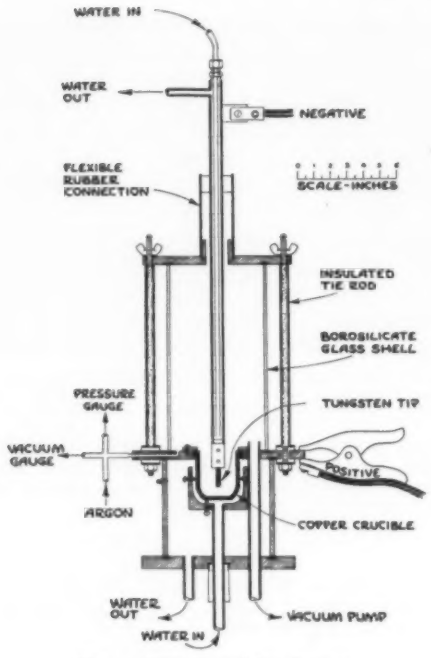


FIG. 1. Button melting furnace

For the work on all impurities, except oxygen, buttons were prepared by a triple melting process:

1. The base sponge and measured quality of impurity were thoroughly mixed and formed into a cylindrical compress. This compress was then melted in the furnace.
2. The button so formed was placed on edge in the crucible and remelted.
3. The button was turned over and melted a third time.

Approximately 80% of the button was fully molten in each step.

Contamination by tungsten from the electrode is negligible. Analyses of several buttons showed an average tungsten content of 0.005% with none over 0.01%.

Contamination by atmospheric oxygen and nitrogen is also negligible. Buttons remelted 10 to 12 times showed no measurable increase in Brinell hardness.

Most of the contaminants were prepared as master alloys and homogenized by this triple melting process. The master alloy buttons were then broken up and added to the base sponge in measured quantities and buttons were prepared from this mixture. In a few cases it was found expedient to add metallic impurities directly and in one case (vanadium) the impurity was added both directly and as a master alloy.

Buttons were prepared for hardness measurement by grinding parallel flat surfaces, about 1 in. in diameter, on both top and bottom by means of a belt grinder. Since the buttons had a shallow elliptical cross section, only a small amount of metal needed to be removed to provide these flat surfaces. Water cooling between short grinding periods precluded contamination by atmospheric oxygen or nitrogen. For hardness measurement the surface was given a smooth finish by application of successively finer abrasive papers. The finished buttons were approximately 50 mm in diameter and 12 mm in thickness between parallel faces. Hardness measurements were made on a standard Brinell machine using a 1500 kg load on a 10 mm steel ball for 20 sec. The hardness of each button was determined as the average reading of two impressions.

### *Oxygen and Nitrogen*

The effect of oxygen and nitrogen was first established by treating the two impurities as a single impurity. Data in Fig. 2 were collected from routine analyses of early sponge products; each point represents a different sponge. Buttons were prepared by single melting and Brinell hard-

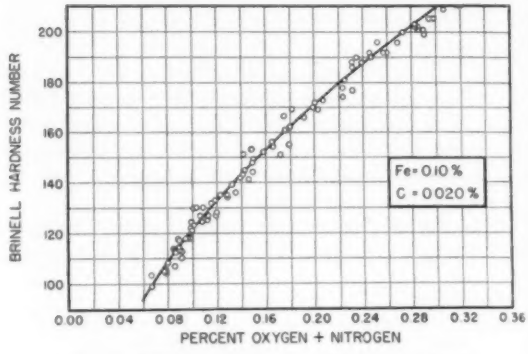


FIG. 2. BHN vs. oxygen + nitrogen content

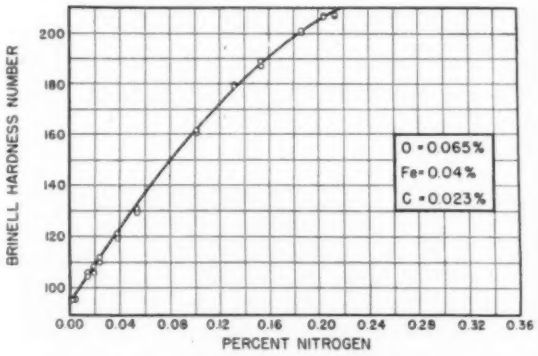


FIG. 3. BHN vs. nitrogen content

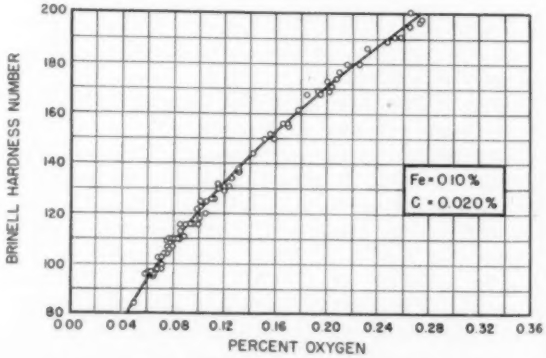


FIG. 4. BHN vs. oxygen content

ness was determined. These buttons were then analyzed for oxygen by the vacuum fusion method using the Walter technique (16). Drillings of the buttons were analyzed for nitrogen, iron, and carbon by conventional methods. Commercial sponge contains, beside oxygen and nitrogen, variable amounts of iron and carbon. To obtain a single curve on a two-dimensional plot, it was necessary to adjust the data to some arbitrary levels of iron and carbon. Levels of 0.10% iron and 0.02% carbon were selected for this purpose. The hardness of the sample was translated to the value it would have if it contained 0.10% iron and 0.02% carbon. Correction factors for this adjustment were taken from iron and carbon curves to be discussed later. In the range 100–200 BHN the oxygen + nitrogen curve is parabolic with the formula:

$$\text{Weight-per cent (O + N)} = 6.85 \times 10^{-6} (\text{BHN})^2 \quad \text{(I)}$$

Fig. 3 shows the nitrogen curve. A master alloy containing 5% nitrogen was prepared by directly nitriding sponge at 1000°C. This was homogenized by triple melting, crushed to 8–10 mesh, and added to the base sponge to yield the compositions shown. All buttons were prepared by the triple melting procedure.

With the effect of nitrogen established, it is a simple matter to convert the oxygen + nitrogen data to oxygen alone. The oxygen curve is shown in Fig. 4. The conversion is not drastic since oxygen and nitrogen have similar hardening capacities and the oxygen content is normally close to a magnitude higher than the nitrogen content. It is readily seen that nitrogen is a slightly more potent hardener on a weight basis but that up to a few hundredths of a per cent, nitrogen and oxygen can be treated as equivalent in hardening effect for all practical purposes.

### *Carbon and Iron*

Fig. 5 shows the curve for carbon. A master alloy containing 10% spectroscopically pure graphite was prepared and homogenized by triple melting. This alloy was crushed and added to sponge to yield the compositions shown; buttons were prepared by triple melting.

Fig. 6 shows the curve for iron. Specimens were prepared in the same way except that a 50–50 master alloy was used.

Data from these curves were used in making the corrections to arbitrary levels of carbon and iron in the oxygen + nitrogen curve.

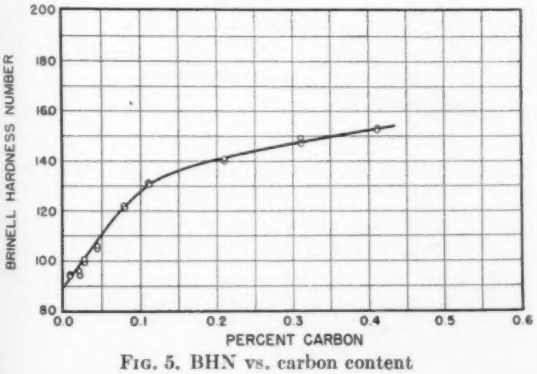


FIG. 5. BHN vs. carbon content

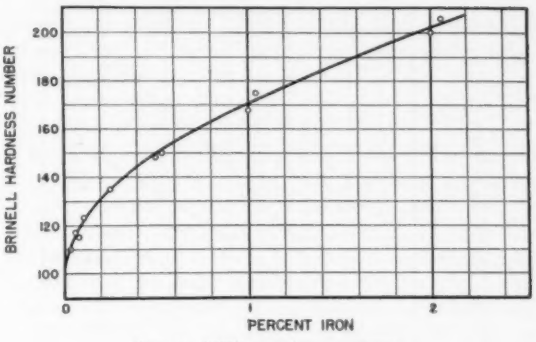


FIG. 6. BHN vs. iron content

### *Other Impurities*

The effects of silicon and of ten metallic impurities were also determined. All metals used were of the highest purity obtainable and in all cases where impurities were suspected they were checked by analysis to assure the absence of spurious results. All buttons were prepared by the triple melting technique. The sponge used in all tests was from a single lot of good quality sponge of high uniformity. The weight-per cent composition is shown in Table I. This sponge was also used in establishing the nitrogen curve. The iron and carbon curves had been determined earlier using different sponges of approximately the same composition. Data are shown in Fig. 7, 8, and and 9.

TABLE I. *Composition of sponge*

| | |
|---|---|
| Oxygen | 0.069 |
| Nitrogen | 0.004 |
| Iron | 0.045 |
| Carbon | 0.025 |
| Silicon | 0.007 |
| Chromium | <0.005 |
| Hydrogen | 0.0014 |
| BHN | 96 |

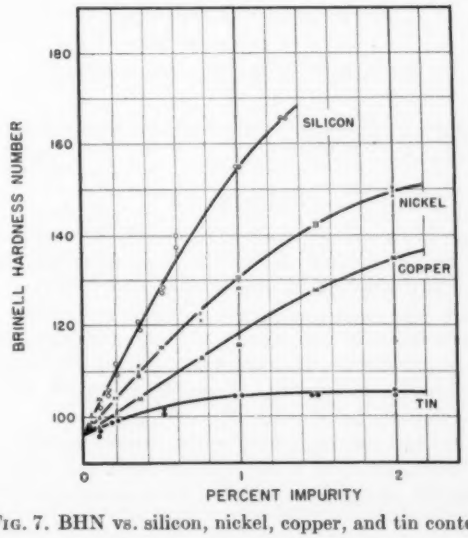


FIG. 7. BHN vs. silicon, nickel, copper, and tin content

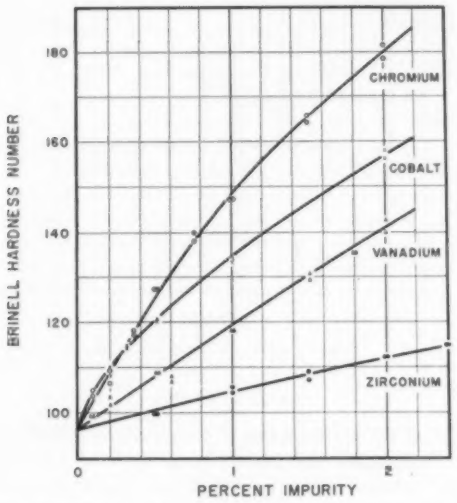


FIG. 8. BHN vs. chromium, cobalt, vanadium, and zirconium content.

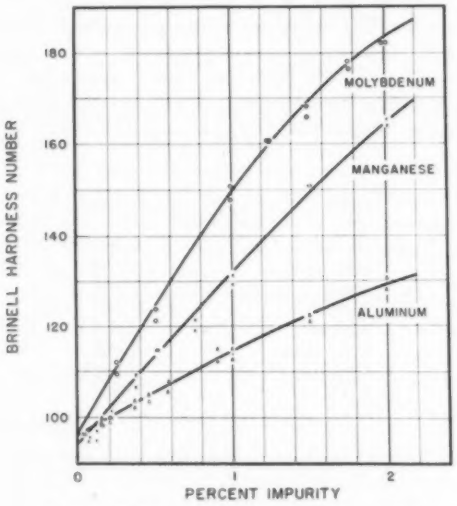


FIG. 9. BHN vs. Mo, Mn, and Al content

Methods of addition of impurities to the titanium are summarized in Table II.

TABLE II

| Element | 50-50 Master alloy, crushed | 50-50 Master alloy, drillings | Added directly |
|---|---|---|---|
| Si | X | | |
| Mo | | | X [1] |
| Cr | X | | |
| Mn | X | | |
| Co | | | X [2] |
| Ni | X | | |
| V | | X | |
| Cu | X | | |
| Al | X | | |
| Zr | | | X [1] |
| Sn | | | X [3] |

[1] Turnings of pure metal.
[2] Drillings of pure metal.
[3] Small pieces of pure metal.

*Composite Results*

Fig. 10 shows results plotted on one chart for comparative purposes. This shows the incremental hardening effect of the various impurities when added to Ti of 100 Brinell base hardness. Oxygen is shown as a dotted line since it has been transposed to the common origin. Note that in most cases the impurities maintain their relative positions over the entire range. Relationships at low concentrations are shown in Fig. 11.

Relative hardening effects of the various impurities at low levels, assuming a linear relationship, are shown in Table III. Oxygen in each case is taken as unity for reference. It should be noted that on a weight basis values vary over a range of almost two magnitudes. On an atomic basis there are some interesting twists. For example, atom for atom, iron is a more potent hardening agent than even oxygen or nitrogen.

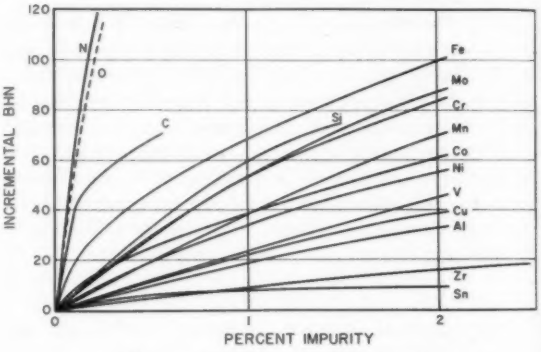


FIG. 10. BHN vs. impurity level

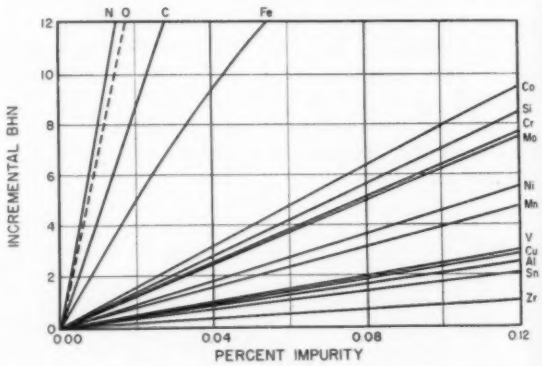


FIG. 11. BHN vs. impurity level, low concentration

TABLE III. *Relative hardening effects of small amounts of impurities added to 100 BHN* Ti

| Impurity | Weight basis | Atomic basis |
|---|---|---|
| N | 1.33 | 0.99 |
| O | 1.00 (Standard of reference) | 1.00 |
| C | 0.63 | 0.47 |
| Fe | 0.35 | 1.23 |
| Co | 0.11 | 0.41 |
| Si | 0.10 | 0.18 |
| Cr | 0.090 | 0.29 |
| Mo | 0.089 | 0.53 |
| Ni | 0.065 | 0.24 |
| Mn | 0.056 | 0.19 |
| V | 0.037 | 0.12 |
| Cu | 0.034 | 0.10 |
| Al | 0.030 | 0.05 |
| Sn | 0.025 | 0.17 |
| Zr | 0.013 | 0.08 |

## Discussion

Hardness data are shown for some 230 buttons ranging roughly from 90 to 200 BHN. The mean deviation from the best curve is less than 2 points BHN, indicating thorough homogenization. Moreover, chemical analyses of buttons invariably checked theoretical compositions within the usual limits of analytical error. On the basis of these facts, together with precautions taken to avoid extraneous contamination during preparation, it is concluded that the data presented are truly representative for conditions prescribed. The triple melting procedure is recommended for the preparation of uniform specimens of titanium containing nonvolatile impurities or alloying agents.

In attempting to duplicate these data, the most critical point perhaps would be reasonable duplication of the rate of cooling of the buttons following the melting step. In this work, buttons were prepared in a water-cooled crucible. After the power was turned off, the buttons cooled to 650°C in about 35 sec. Small deviations from such a cooling rate would not be expected to affect hardness materially. One bit of evidence substantiating this view is the fact that triple melted buttons, after removal of the small amount of metal necessary to prepare them for measurement, exhibited substantially the same hardness on top and bottom. However, greater differences might be expected to arise in the case of large ingots because of the poor heat conductivity of Ti. As mentioned earlier, mechanical working of specimens will in itself be a factor in determining the hardness of the metal.

It should be mentioned that trouble was experienced in attempting to prepare homogeneous buttons containing tungsten. Tungsten crushed to 8–10 mesh, added to the Ti sponge, and triple melted using 150% of normal power was not dispersed in the Ti. Radiographs indicated that the 8–10 mesh tungsten had been reduced to about 10–12 mesh by this treatment. Apparently the high density of tungsten forces it into the pasty region near the bottom of the molten button where solution is very slow. It would seem that tungsten must be fairly finely divided to allow uniform solution without recourse to an excessively long melting procedure. Investigations along this line were not pursued. On the other hand, radiographs of Mo alloy buttons did not show segregation.

### *Estimation of Oxygen in* Ti

One application of these data is the estimation of oxygen in unalloyed Ti without the actual performance of an oxygen analysis. As applied to Ti sponge, the sponge is melted to form a 100-g button. The Brinell hardness of the button is determined. Drillings of the button are analyzed for nitrogen, iron, and carbon by conventional methods. The Brinell hardness is adjusted to correspond to arbitrary levels of 0.10% iron and 0.02% carbon. A chart such as shown in Table IV is convenient to use in making these adjustments. Actually, this chart extends much farther than the usual range. For most commercial sponge products, the adjustment is of the order of 10 points Brinell or less. Of course, if other impurities are present in significant amounts, adjustments can be made in a similar manner. Referring again to the oxygen + nitrogen curve (Fig. 2), the oxygen + nitrogen content is found corresponding to the adjusted Brinell hardness. Subtracting the nitrogen gives the estimated figure for oxygen content. From the data on 87 specimens shown in Fig 2, the expected accuracy of a single estimation is within about 6% of the value as determined by vacuum fusion analysis.

While the accuracy of an estimation of this method is, on the average, slightly poorer than a vacuum fusion analysis by a competent analyst, it is of sufficient accuracy for most work at the present time. This method is used here in upward of 90% of the determinations of oxygen content of sponge products, reserving vacuum fusion analyses for critical or unusual samples only.

The question may reasonably be asked whether this method involves less work than an actual oxygen analysis. If oxygen content is considered as an isolated property,

TABLE IV. *Chart for BHN adjustment for iron and carbon contents*

| % Fe | BHN adjust. | % Fe | BHN adjust. | % Fe | BHN adjust. | %C | BHN adjust. | %C | BHN adjust. | %C | BHN adjust. |
|---|---|---|---|---|---|---|---|---|---|---|---|
| 0.00 | +19 | 0.20 | −10 | 0.40 | −23 | 0.000 | +9 | 0.020 | 0 | 0.040 | −8 |
| 0.01 | +16 | 0.21 | −10 | 0.41 | −23 | 0.001 | +8 | 0.021 | 0 | 0.041 | −9 |
| 0.02 | +14 | 0.22 | −11 | 0.42 | −24 | 0.002 | +8 | 0.022 | −1 | 0.042 | −9 |
| 0.03 | +12 | 0.23 | −12 | 0.43 | −25 | 0.003 | +7 | 0.023 | −1 | 0.043 | −10 |
| 0.04 | +10 | 0.24 | −13 | 0.44 | −25 | 0.004 | +7 | 0.024 | −2 | 0.044 | −10 |
| 0.05 | +8 | 0.25 | −14 | 0.45 | −26 | 0.005 | +7 | 0.025 | −2 | 0.045 | −10 |
| 0.06 | +6 | 0.26 | −14 | 0.46 | −26 | 0.006 | +6 | 0.026 | −3 | 0.046 | −11 |
| 0.07 | +4 | 0.27 | −15 | 0.47 | −27 | 0.007 | +6 | 0.027 | −3 | 0.047 | −11 |
| 0.08 | +3 | 0.28 | −16 | 0.48 | −27 | 0.008 | +5 | 0.028 | −3 | 0.048 | −11 |
| 0.09 | +1 | 0.29 | −16 | 0.49 | −28 | 0.009 | +5 | 0.029 | −4 | 0.049 | −12 |
| 0.10 | 0 | 0.30 | −17 | 0.50 | −28 | 0.010 | +4 | 0.030 | −4 | 0.050 | −12 |
| 0.11 | −1 | 0.31 | −18 | 0.55 | −31 | 0.011 | +4 | 0.031 | −5 | 0.055 | −14 |
| 0.12 | −2 | 0.32 | −18 | 0.60 | −33 | 0.012 | +4 | 0.032 | −5 | 0.060 | −16 |
| 0.13 | −3 | 0.33 | −19 | 0.65 | −35 | 0.013 | +3 | 0.033 | −5 | 0.065 | −18 |
| 0.14 | −4 | 0.34 | −19 | 0.70 | −37 | 0.014 | +3 | 0.034 | −6 | 0.070 | −20 |
| 0.15 | −5 | 0.35 | −20 | 0.75 | −39 | 0.015 | +2 | 0.035 | −6 | 0.075 | −22 |
| 0.16 | −6 | 0.36 | −21 | 0.80 | −42 | 0.016 | +2 | 0.036 | −7 | 0.080 | −24 |
| 0.17 | −7 | 0.37 | −21 | 0.85 | −44 | 0.017 | +1 | 0.037 | −7 | 0.085 | −26 |
| 0.18 | −8 | 0.38 | −22 | 0.90 | −45 | 0.018 | +1 | 0.038 | −8 | 0.090 | −28 |
| 0.19 | −9 | 0.39 | −22 | 0.95 | −47 | 0.019 | +1 | 0.039 | −8 | 0.095 | −29 |
| | | | | 1.00 | −49 | | | | | 0.100 | −31 |

the answer must be negative. However, under normal circumstances, when oxygen content is of interest, hardness of the metal, nitrogen content, iron content, and possibly even the carbon content are also of interest. These determinations are commonly made on a routine basis so that the necessary data for making an oxygen estimation are normally at hand. Therefore, an estimate of oxygen content may be made in less than a minute, whereas an actual determination of oxygen would take up to a few hours.

### *Limitations*

There are certain limitations to the use of these data that should be pointed out. In the first place the data apply only to 100-g buttons melted as prescribed. Second, the effect of impurities on hardness is not strictly additive and attempts to apply the data to grossly impure samples or samples containing a large number of impurities at significant levels may lead to serious error. However, the method was found to be reliable when applied to normal sponge products.

It should be remembered that the incremental hardening effects of the various impurities are based on Ti of 100 BHN, e.g., Ti containing 0.067% oxygen + nitrogen, 0.10% iron, 0.02% carbon. Addition of impurities at a higher base level will have a somewhat lesser effect on the numerical hardness increment. However, within the normal commercial range of hardness, the error introduced is usually insignificant.

### *Examples of Use of Data*

The usefulness of the data is illustrated by the following examples.

I. A sample of sponge has a 100-g button hardness of 120 BHN. Nitrogen content is 0.012%, iron 0.15%, carbon 0.026%. Other impurities are negligible. Estimate the oxygen content.

From Table IV the iron and carbon adjustments are −5 and −3, respectively. The adjusted BHN is then 120 − 5 − 3 = 112 (this is the hardness this specimen would have if it contained 0.10% iron and 0.02% carbon rather than the actual levels). From Fig. 2 it is found that 112 BHN corresponds to 0.086% oxygen + nitrogen. Estimated oxygen content is then 0.086 − 0.012 = 0.074%.

II. Estimate the BHN of Ti containing 0.104% oxygen, 0.008% nitrogen, 0.14% iron, and 0.015% carbon.

Oxygen + nitrogen = 0.104 + 0.008 = 0.112%. This corresponds (Fig. 2) to 128 BHN. Adjustments for iron and carbon (Table IV) are +4 and −2, respectively. (Note that the signs are reversed since the translation is away from rather than toward the arbitrary levels.) BHN = 128 + 4 − 2 = 130.

III. A sponge product containing 0.20% iron has a hardness of 130 BHN. Estimate the hardness if iron were reduced to 0.05%, other impurities remaining constant.

Table IV shows that the BHN decrease would be 18 points. 130 − 18 = 112 BHN.

IV. An impure Ti product contains 0.08% Si, 0.05% Cr, and 0.10% Mn. BHN is 115. Estimate the BHN if these impurities were eliminated. From Fig. 11 the hardness would be 115 − 6 − 3 −4 = 102 BHN.

V. A mixture of sponge of 100 BHN and 0.40% $TiO_2$ is melted to form an ingot. Estimate the BHN of the resultant ingot.

Oxygen content of $TiO_2$ is 40%. Therefore 0.16% oxygen is added to the Ti. From Fig. 2 the resultant BHN would be 183.

VI. Equal parts of sponge products A & B are mixed. Estimate the resultant BHN.

| *Sponge A* | *Sponge B* |
|---|---|
| 100 BHN | 200 BHN |
| 0.08% Iron | 0.16% Iron |
| 0.016% Carbon | 0.028% Carbon |

Adjusted BHN for sponge A is 100 + 3 + 2 = 105 BHN. Oxygen + nitrogen = 0.076%. Adjusted BHN for sponge B is 200 − 6 − 3 = 191 BHN. Oxygen + nitrogen = 0.250%.

Resultant mixture would then contain 0.163% oxygen + nitrogen, 0.12% iron, and 0.022% carbon.

Oxygen + nitrogen = 0.163% corresponds to 154 BHN.

Adjustments for iron and carbon are +2 and +1 respectively. BHN = 154 + 2 + 1 = 157.

### Acknowledgments

The author acknowledges with thanks the contributions of research personnel of the Pigments Department in various phases of the work. Among these are Andrew K. Palese who prepared the buttons and made hardness determinations, John M. Thompson who made the chemical analyses, Frederick Walls and Cortland Warrington who performed vacuum fusion analyses for oxygen content, and William Miller who prepared the line drawings.

Manuscript received December 20, 1955. This paper was prepared for delivery before the Pittsburgh Meeting, October 9 to 13, 1955.

Any discussion of this paper will appear in a Discussion Section to be published in the June 1957 JOURNAL.

### REFERENCES

1. W. J. Barth and A. L. Feild, Jr., *Metal Prog.*, **64**, 74 (1953).
2. C. I. Bradford, J. P. Catlin, and E. M. Wemple, *ibid.*, **55**, 348 (1949).
3. I. E. Campbell, R. I. Jaffee, J. M. Blocher, Jr., J. Gurland, and B. W. Gonser, *J. (and Trans.) Electrochem. Soc.*, **96**, 271 (1948).
4. C. M. Craighead, O. W. Simmons, and L. W. Eastwood, *Trans. Am. Inst. Mining Met. Engrs.*, **188**, 485 (1950).
5. C. M. Craighead, O. W. Simmons, and L. W. Eastwood, *ibid.*, **188**, 514 (1950).
6. W. L. Finlay and J. A. Snyder, *ibid.*, **188**, 277 (1950).
7. R. I. Jaffee and I. E. Campbell, *ibid.*, **185**, 646 (1949).
8. R. I. Jaffee, H. R. Ogden, and D. J. Maykuth, *ibid.*, **188**, 1261 (1950).
9. R. I. Jaffee, *Iron Age*, **171**, 162 (1953).
10. R. I. Jaffee, F. C. Holden, and H. R. Ogden, *J. Metals*, **6**, 1282 (1954).
11. A. E. Jenkins and H. W. Worner, *J. Inst. Metals*, **80**, 157 (1951–52).

12. D. J. Maykuth, *et al.*, Summary report AF 33 (038)–8344, (1953).
13. D. A. Sutcliffe, *Metal Treatment*, **21**, 191 (1954).
14. D. A. Sutcliffe and A. C. Spickett, Royal Aircraft Est. (Gt. Brit.) R.A.E. Met. 73 (N-23-199).
15. F. S. Wartman, D. H. Baker, J. R. Nettle, and V. E. Homme, *This Journal*, **101**, 507 (1954).
16. D. I. Walter, *Ind. Eng. Chem.*, **42**, 297 (1950).
17. H. W. Worner, *J. Inst. Metals*, **80**, 213 (1951–52).
18. H. W. Worner, *ibid.*, **81**, 521 (1953).

# Mathematical Studies of Galvanic Corrosion

## VI. Limiting Case of Very Thin Films

J. T. Waber

*University of California, Los Alamos Scientific Laboratory, Los Alamos, New Mexico*

ABSTRACT

The limiting case of a very thin electrolyte layer which covers a coplanar electrode arrangement has been analyzed by making the electrode dimensions infinitely larger than the corrodent depth. A Fourier integral expression for the potential throughout the corrosive medium has been derived from the Fourier series treatment of the potential pertinent to finite electrode widths. The electrolyte depth becomes the critical cell dimension. The variation of the potential along the inner and outer boundaries of the liquid are presented in two graphs with a separate curve for each value of the ratio of the liquid depth to the Wagner polarization parameter. The distribution of the corrosion current over the anode is also presented graphically as a function of this ratio.

Although the effect of thin films on minimizing the corrosion rate and concentrating the attack into the vicinity of the anode-cathode junction has been discussed (1), the case of an electrolyte film much thinner (in depth) than the electrode dimensions was not discussed. Such a film might be an adsorbed multimolecular film on a piece of commercially pure metal or a stagnant layer on a large welded structure containing gross inhomogeneities. As has been pointed out previously in this series, the actual physical dimensions of a galvanic system do not dictate the behavior of the system, but their relation to the magnitude of the polarization parameter $\mathfrak{P}$ does dictate it. It is clear from the earlier discussion of the effect of electrolyte thickness $b$ that this dimension is the critical one which most strongly affects the distribution of current density on the electrodes. Thus the systems under consideration can be characterized by the one dimensionless ratio $(b/\mathfrak{P})$.

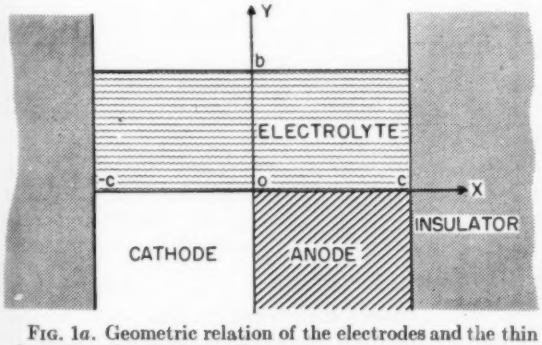


Fig. 1*a*. Geometric relation of the electrodes and the thin electrolyte. Insulating walls at $x = c$.

In previous papers, Fourier series and Fourier integrals have been used independently. One may start from the geometric arrangement of electrodes and liquid depicted in Fig. 1*a*, for which a Fourier series is appropirate, and, by increasing the distance between insulating walls to infinity, lead to the arrangement of Fig. 1*b* and to a Fourier integral. Use of this limiting process, although it is not new, may be helpful in solving similar heat transfer and diffusion problems. An independent derivation of the Fourier integral used here has been presented elsewhere (2) and will not be discussed.

### Boundary Conditions

One may assume a periodic arrangement of long narrow electrodes to determine the effects of juxtaposing an anode and a cathode in a common surface and analyze the potential distribution in terms of a Fourier series. It is sufficient, however, to examine the behavior within only one period. With the arrangement depicted in Fig. 1*a* it can be shown that only sine terms remain in the Fourier serie

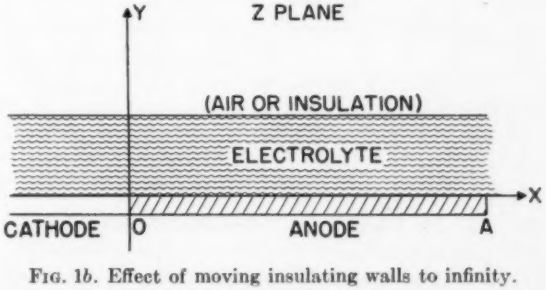


Fig. 1*b*. Effect of moving insulating walls to infinity.

since an odd symmetry about point (0, ½) has been assumed. One can ignore edge effects and concentrate on the anode-cathode junction if

$$\left.\frac{\partial P^*}{\partial x}\right|_{x=-c} = \left.\frac{\partial P^*}{\partial x}\right|_{x=c} = 0 \qquad \text{(I)}$$

Using the definition of the effective potential difference $E_a$ discussed elsewhere (3), the potential of the polarized electrode at the electrode interface, namely $P^*(x, 0)$, is

$$P^*(x, 0) - \mathfrak{L}\left.\frac{\partial P^*}{\partial y}\right|_{y=0} = E_a \qquad \text{(II)}$$

in the "anodic" region $0 < x \leq c$ and is

$$P^*(x, 0) - \mathfrak{L}\left.\frac{\partial P^*}{\partial y}\right|_{y=0} = 0 \qquad \text{(III)}$$

in the cathodic region $-c \leq x < 0$. The unpolarized interfacial potential $P(x, 0)$ takes on the values $E_a$ and 0. The relation between the two potentials is illustrated in Fig. 2.

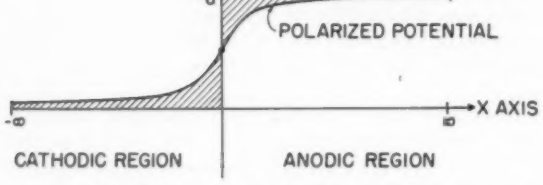


FIG. 2. Distribution of interfacial potential over the electrodes.

Since the line $y = b$ represents the upper surface of the electrolyte, an insulator type of boundary condition

$$\left.\frac{\partial P^*}{\partial y}\right|_{y=b} = 0 \qquad \text{(IV)}$$

applies. Although $P^*(x, 0)$ is a periodic function, it is not necessary to specify its behavior beyond this range $-c \leq x \leq c$.

## Potential Function

It can be established that the potential at any point is given by

$$P^*(x, y) = \frac{E_a}{2} + \frac{2E_a}{\pi}\sum_{m=0}^{\infty} \left\{ \frac{\cosh\left[\frac{(2m+1)(b-y)\pi}{2c}\right]\sin\left[\frac{(2m+1)\pi x}{2c}\right]}{(2m+1)\left\{\cosh\left[\frac{(2m+1)b\pi}{2c}\right] + \frac{(2m+1)\mathfrak{L}\pi}{2c}\sinh\left[\frac{(2m+1)b\pi}{2c}\right]\right\}} \right\} \qquad \text{(V)}$$

and that this function satisfies boundary conditions (I), (II), (III), and (IV).

It is demonstrated in the Appendix that, as $c$ becomes larger and larger, the value of the terms in (V) changes very slowly with respect to $m$ and a very large number of terms are required for even a poor approximation to the function. In the limit as $c$ approaches infinity, the summation can be replaced by integration and (V) becomes

$$P^*(x, y) = \frac{E_a}{2} + \frac{E_a}{\pi}\int_0^{\infty} \frac{\cosh\left[\frac{\omega(b-y)}{\mathfrak{L}}\right]\sin\left(\frac{\omega x}{\mathfrak{L}}\right)d\omega}{\omega\left[\cosh\left(\frac{\omega b}{\mathfrak{L}}\right) + \omega\sinh\left(\frac{\omega b}{\mathfrak{L}}\right)\right]} \qquad \text{(VI)}$$

The details of transforming the series to this aperiodic solutions are indicated in the Appendix.

The integrand becomes simpler if only the interfacial potentials are computed. The two simplified integrands are listed below.

| Interface | Integrand |
|---|---|
| Metal-solution $y = 0$ (inner) | $\dfrac{\sin\left(\frac{\omega x}{\mathfrak{L}}\right)}{\omega\left[1 + \omega\tanh\left(\frac{\omega b}{\mathfrak{L}}\right)\right]}$ |
| Solution-insulator $y = b$ (outer) | $\dfrac{\sin\left(\frac{\omega x}{\mathfrak{L}}\right)}{\omega\left[\cosh\left(\frac{\omega b}{\mathfrak{L}}\right) + \omega\sinh\left(\frac{\omega b}{\mathfrak{L}}\right)\right]}$ |

An expression different from (V) is used when $b$ is infinite, the hyperbolic cosine is replaced by a similar exponential term. Proceeding as above, the integral is

$$P^*(x, y) = \frac{E_a}{2} + \frac{E_a}{\pi}\int_0^{\infty} \frac{\exp\left(-\frac{\omega y}{\mathfrak{L}}\right)\sin\left(\frac{\omega x}{\mathfrak{L}}\right)d\omega}{\omega(1+\omega)} \qquad \text{(VII)}$$

A simplified expression can be obtained when $y$ is set equal to zero. It is

$$P^*(x, 0) = E_a - \frac{E_a}{\pi} \cdot \left[\mathrm{Ci}\left(\frac{x}{\mathfrak{L}}\right)\sin\left(\frac{x}{\mathfrak{L}}\right) - \mathrm{si}\left(\frac{x}{\mathfrak{L}}\right)\cos\left(\frac{x}{\mathfrak{L}}\right)\right] \qquad \text{(VIII)}$$

where si and Ci stand for sine and cosine integrals, namely

$$\mathrm{si}(z) = -\int_z^{\infty} \frac{\sin t\, dt}{t} \qquad \text{(IX)}$$

$$\mathrm{Ci}(z) = \int_z^{\infty} \frac{\cos t\, dt}{t} \qquad \text{(X)}$$

These functions have been tabulated, for example, by Jahnke and Emde (5). The potential at $y = \infty$ is equal to $E_a/2$ since the integral vanishes at this limit. This quantity has been referred to in earlier reports (3, 4) as the potential of the composite electrode.

## Corrosion Current Parameter

A slightly different expression must be used since both the anode and the cathode widths are infinite. The new

dimensionless quantity which represents the local variation in the corrosion attack is

$$C_b^*(x) = -\left(\frac{2b}{E_a}\right)\left.\frac{\partial P^*}{\partial y}\right|_{y=0} \qquad \text{(XI)}$$

Boundary conditions (III) and (IV) permit calculation of the normal gradient from the interfacial potential at $y = 0$. The expression is given as equation (XV) of Reference (2).

## Discussion

One practical way of minimizing the number of parameters in a problem is to discuss limiting cases, for the mathematical answers are independent of that variable or parameter taken to the limit. Specifically, it is assumed that widths of both electrodes are infinitely larger than the depth $b$ of the electrolyte. Analysis of this case would apply to adsorbed films of moisture and multiphase alloys where the film thickness is smaller than the smallest dimension of the individual grains of the microconstituent. Although there are well-known examples of precipitates forming from solid solutions, which cannot be resolved by the optical microscope, the average constituent of commercial alloys has dimensions larger than a few microns.

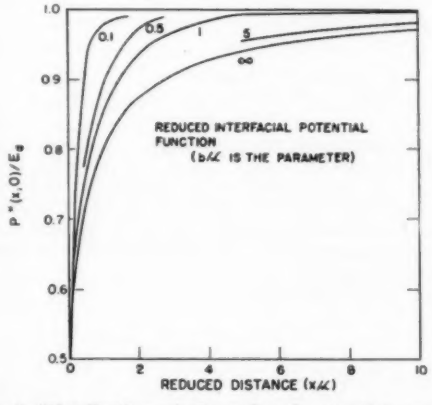


Fig. 3. Distribution of the reduced potential over the anode surface. Curves are for different values of $(b/\mathfrak{L})$.

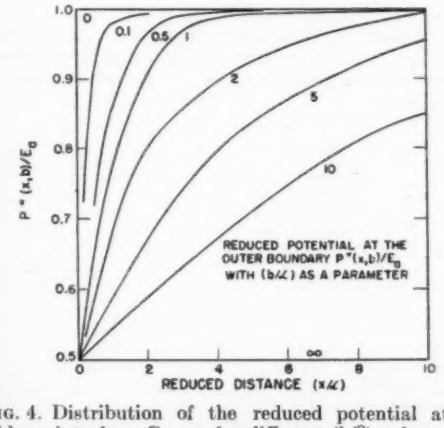


Fig. 4. Distribution of the reduced potential at the liquid-gas interface. Curves for different $(b/\mathfrak{L})$ values apply to the anodic region $(x/\mathfrak{L} > 0)$.

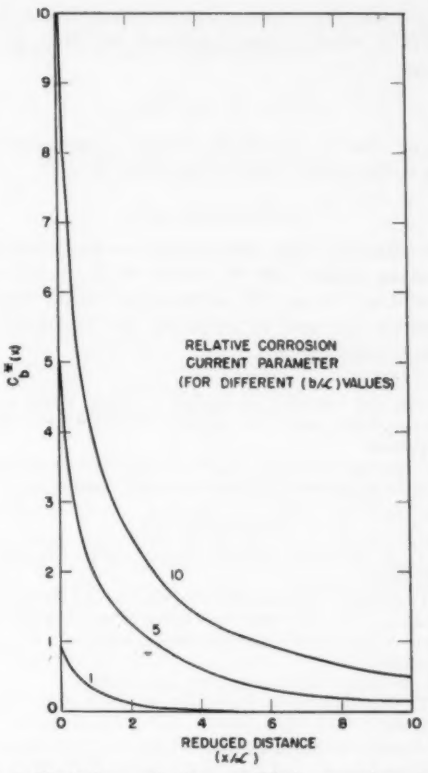


Fig. 5. Variation of the modified corrosion current parameter near the anode-cathode junction.

Values of the polarization parameter employed in previous papers (1, 3) were all larger than 0.01 cm, so for most practical cases, $\mathfrak{L}$ is much larger than the thickness of an adsorbed film.

The potentials at the interface $y = 0$ and at the outer boundary $y = b$ are shown in Fig. 3 and 4, respectively. At a given $x/\mathfrak{L}$ value, the difference between the potential at the two boundaries increases as $b/\mathfrak{L}$ increases. The potential at the outer boundary varies more rapidly with $b/\mathfrak{L}$ than it does at the other boundary.

Distribution of current over the anode is shown in Fig. 5. The corrosion current is concentrated into the immediate vicinity of the anode-cathode junction and the maximum value is reduced as $b/\mathfrak{L}$ decreases. It is evident that $b$ is the critical dimension $\lambda$ of this galvanic couple. When $b/\mathfrak{L}$ is as small as one, only small portions of the anode suffer appreciable corrosion attack. It is suggested that greatest part of the attack takes place within a distance $x/\mathfrak{L} = 2(b/\mathfrak{L})$ of the junction.

Equations (VIII) and (XI) apply as well to the potential and current distribution near the anode-cathode junction when the polarization parameter is very much smaller than any of the physical dimensions. Even though $\mathfrak{L}$ becomes very small, $y/\mathfrak{L}$ need not approach infinity simultaneously with $b/\mathfrak{L}$, since $0 \leq y \leq b$. Fig. 3 and 5 describe the situation very near the anode-cathode junction when $\mathfrak{L}$ is almost negligible. Thus, the foregoing analysis, with $b/\mathfrak{L}$ very large, can be regarded as a bridging link between

Part I in which polarization was neglected (3) and Parts II and III in which it was considered (4). Note that the relation

$$C^*(x) = a/b\, C_b^*(x) \qquad \text{(XII)}$$

must be used to correct the corrosion parameter found herein to the values previously tabulated (1, 3, 4).

ACKNOWLEDGMENT

The author is deeply indebted to Professor Carl Wagner for having pointed out the merit of the mathematical method used herein. The services of Donald Prys and Marguerite Coleman in preparing this manuscript are gratefully acknowledged.

Manuscript received December 7, 1955. Work on this paper was done under the auspices of the Atomic Energy Commission.

† Any discussion of this paper will appear in a Discussion Section to be published in the June 1957 JOURNAL.

## REFERENCES

1. J. T. WABER AND BERTHA FAGAN, *This Journal*, **103**, 64 (1956).
2. J. T. WABER, "Mathematical Analysis of Galvanic Corrosion, IX. Solution for Ultra Thin Liquid Films and Very Small Polarization Parameters" (in preparation).
3. J. T. WABER, *This Journal*, **101**, 271 (1954).
4. J. T. WABER AND M. ROSENBLUTH, *ibid.*, **102**, 344, 420 (1955).
5. E. JAHNKE AND F. EMDE, "Tables of Functions with Formulae and Curves," Table I, p. 8, 4th ed., Dover Publications, New York (1945).

## APPENDIX

Equation (V) may be written with the coefficient of the $m$-th term indicated as an integral. This is a useful form when applying the limiting process of making $c$ infinite and generating the potential function for this aperiodic case. In this form

$$P^*(x, y) = \frac{E_a}{2} + \sum_{m=0}^{\infty} \cdot\left\{\frac{2}{2c}\int_0^c P^*(x', 0)\sin\left[\frac{(2m+1)\pi x'}{2c}\right]dx'\right\} \times \sin\left[\frac{(2m+1)\pi x}{2c}\right]\cosh\left[\frac{(2m+1)(b-y)\pi}{2c}\right] \qquad \text{(XIII)}$$

Define a dimensionless frequency $\omega_m$ as an auxiliary variable

$$\omega_m \equiv (2m+1)\pi\mathfrak{L}/2c$$

The change $\Delta\omega$ between two successive terms is $(\pi\mathfrak{L}/c)$. One may rewrite (XIII) as

$$P^*(x, y) = \frac{E_a}{2} + \sum_{m=0}^{\infty} \cdot\left\{\frac{\Delta\omega}{\pi\mathfrak{L}}\int_0^c P^*(x', 0)\sin\left(\frac{\omega_m x'}{\mathfrak{L}}\right)dx'\right\} \times \sin\left(\frac{\omega_m x}{\mathfrak{L}}\right)\cosh\left[\frac{\omega_m(b-y)}{\mathfrak{L}}\right] \qquad \text{(XIV)}$$

One may substitute the values of $P^*(x, 0)$ from equations (II) and (III) and after differentiating termwise show that

$$P^*(x, y) = \frac{E_a}{2} + E_a\sum_{m=0}^{\infty}\left\{\frac{\Delta\omega}{\pi\mathfrak{L}D(\omega_m)}\int_0^c \sin\left(\frac{\omega_m x'}{\mathfrak{L}}\right)dx'\right\} \times \sin\left(\frac{\omega_m x}{\mathfrak{L}}\right)\cosh\left[\frac{\omega_m(b-y)}{\mathfrak{L}}\right] \qquad \text{(XV)}$$

since the unpolarized potential $P(x, 0)$ takes on the values of 0 and $E_a$. In this equation, the denominator

$$D(\omega_m) \equiv \cosh\left(\frac{\omega_m b}{\mathfrak{L}}\right) + \omega_m \sinh\left(\frac{\omega_m b}{\mathfrak{L}}\right) \qquad \text{(XVI)}$$

is independent of $x'$. One may integrate then with respect to $x'$ and obtain

$$P^*(x, y) = \frac{E_a}{2} + \frac{E_a}{\pi}\sum_{m=0}^{\infty} \sin\left(\frac{\omega_m x}{\mathfrak{L}}\right)\cosh\left[\frac{\omega_m(b-y)}{\mathfrak{L}}\right]\frac{1}{D(\omega_m)}\left(\frac{\Delta\omega}{\omega_m}\right) \qquad \text{(XVII)}$$

If $c$ becomes large, the frequency $\omega_m$ becomes small for any finite values of $m$ and $\mathfrak{L}$. Thus, the potential function $P^*(x, y)$ can be regarded as the sum of products of the infinitesmal $\Delta\omega$ times a function of $\omega_m$. As $c$ approaches infinity, the dense denumerable set $\omega_m$ can be replaced by a continuous variable $\omega$ and the limit of the sum of products is a definite integral.

Thus it can be shown that

$$P^*(x, y) = \frac{E_a}{2} + \frac{E_a}{\pi}\int_0^{\infty} \frac{\sin\left(\frac{\omega x}{\mathfrak{L}}\right)\cosh\left[\frac{\omega(b-y)}{\mathfrak{L}}\right]d\omega}{\omega\left[\cosh\left(\frac{\omega b}{\mathfrak{L}}\right) + \omega\sinh\left(\frac{\omega b}{\mathfrak{L}}\right)\right]} \qquad \text{(XVIII)}$$

which is identical to the expression derived (2) directly by assuming a Fourier integral with an undefined coefficient function subsequently "chosen" to satisfy the boundary conditions.

# Oxidation of Alloys Involving Noble Metals

CARL WAGNER

*Department of Metallurgy, Massachusetts Institute of Technology, Cambridge, Massachusetts*

ABSTRACT

Diffusion processes during the oxidation of alloys involving noble metals are analyzed theoretically. An oxide film of uniform thickness is stable only if diffusion in the alloy is relatively rapid compared with diffusion in the oxide of the less noble metal. Otherwise, there is the tendency to form a rugged alloy-oxide interface. The oxidation rate is calculated for the limiting case of a scale consisting of protruding sections of the oxide of the less noble metal interspersed with slender trunks of alloy rich in the more noble metal. Under these conditions, the oxidation rate of alloys containing up to 50% of noble metal is supposed to be of the same order of magnitude as the oxidation rate of the less noble metal in its pure state.

In a previous paper (1), the oxidation of alloys involving noble metals was discussed. In particular, oxidation of Ni-Pt alloys was considered in conjunction with experimental results obtained by Kubaschewski and von Goldbeck (2). At 1000°C, only nickel oxide is formed. Thus Pt is enriched in the alloy which is a substitutional solid solution without miscibility gap. Accordingly, Ni diffuses from the bulk alloy toward the alloy-oxide interface, and Pt diffuses in the opposite direction. The oxidation rate is, therefore, determined by the interplay of diffusion of Ni ions and electrons in nickel oxide, and interdiffusion of Ni and Pt in the alloy. In this analysis it has been assumed that the thickness of the nickel oxide film is uniform and the interface between the oxide and the alloy is plane. This situation, however, is not always found. It is also possible that oxidation of an alloy involving a noble metal yields a two-phase scale with the alloy consisting mostly of the more noble metal embedded in a matrix of the oxide of the less noble metal, as shown schematically in Fig. 1. Such a structure of the scale was observed in several cases discussed below.

In what follows it is shown that an oxide film of uniform thickness is stable only under certain conditions and unstable under otner conditions. In the latter case, a two-phase scale is formed. In order to understand the decisive factors which determine diffusion in a two-phase scale, calculations have been made for idealized conditions. In particular, exclusive diffusion control is assumed and effects due to space charge layers are disregarded.

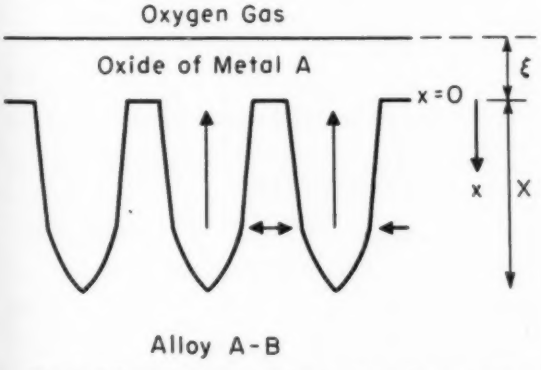


FIG. 1. Schematic cross section of the scale at the surface of an alloy $A$-$B$ with an outer layer of oxide of metal $A$ and an inner two-phase layer of oxide of metal $A$ and $B$-rich alloy. The main diffusion path of $A$ in the alloy and in the oxide is indicated by arrows.

## STABILITY OF A PLANE ALLOY-OXIDE INTERFACE

Consider an alloy $A$-$B$ in which only metal $A$ forms one oxide. To examine the stability of a plane oxide-alloy interface, inquire into the changes of a nearly plane interface involving slight perturbations. In particular, consider a sine wave profile shown in Fig. 2.

In the metallic phase, the transport rate of metal $A$ per unit area in the $x$-direction due to diffusion is given by

$$j_A'^{(x)} = -D'(\partial c_A'/\partial x) \qquad [1]$$

where $D'$ is the interdiffusion coefficient of the alloy, $c_A'$ is the concentration of $A$ in mole/cm³, and $x$ is the distance from the original surface of the alloy.

For an ideal metallic solution,

$$a_A = N_A' = c_A' V' \qquad [2]$$

where $a_A$ is the activity of $A$ referred to pure metal $A$ as the reference state, $N_A'$ is the mole fraction of $A$ in the alloy, and $V'$ is its molar volume, which is supposed to be independent of composition.

Substitution of Eq. [2] in Eq. [1] yields

$$j_A'^{(x)} = -(D'/V')(\partial a_A/\partial x) \qquad [3]$$

Analogous equations hold for transport in the $y$-direction. Fick's second law may, therefore, be formulated as

$$\partial c_A'/\partial t = (\partial a_A/\partial t)/V' = -\partial j_a'^{(x)}/\partial x - \partial j_A'^{(y)}/\partial y$$
$$= (D'/V')(\partial^2 a_A/\partial x^2 + \partial^2 a_A/\partial y^2) \qquad [4]$$

if the interdiffusion coefficient $D'$ is independent of composition.

In the oxide, diffusion is supposed to be accomplished by metal ions and electrons, whereas the oxygen ions are supposed to be virtually immobile. If the oxide exhibits

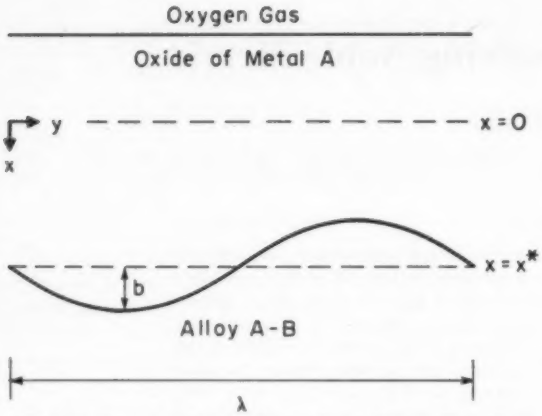


FIG. 2. Cross section of the scale at the surface of an alloy $A$-$B$ with a sine-wave profile of the interface between alloy and oxide of metal $A$.

predominant electronic conduction, the rate of transport of $A$ per unit area in the $x$-direction with respect to the original surface $x = 0$ is given by (3)

$$j''^{(x)}_A = -D'' c''_A(\partial \ln a_A/\partial x) + u_x c''_A \quad [5]$$

where $D''$ is the self-diffusion coefficient of $A$ in the oxide, $c''_A$ is the concentration of $A$ in the oxide in mole/cm$^3$, and $u_x$ is the drift velocity of the oxide toward the bulk alloy due to the recession of the alloy-oxide interface.

The dependence of the self-diffusion coefficient $D''$ is assumed to be given by

$$D'' = D''^{(o)} a_A^m \quad [6]$$

where $D''^{(o)}$ is the self-diffusion coefficient of $A$ in the oxide at unit activity of $A$, and $m$ is a constant, which is positive for an oxide with metal excess, e.g., equal to about $\frac{1}{2}$ for zinc oxide (4), and negative for an oxide with metal deficit, e.g., equal to $-\frac{1}{4}$ for nickel oxide if there are equivalent concentrations of cation vacancies and electron holes (5).

The concentration $c''_A$ is equal to the reciprocal of the volume $V''$ of the oxide involving one mole of metal $A$,

$$c''_A = 1/V'' \quad [7]$$

Substitution of Eqs. [6] and [7] in Eq. [5] yields

$$j''^{(x)}_A = -(D''^{(o)}/mV'')(\partial a_A^m/\partial x) + u_x/V'' \quad [8]$$

An analogous equation holds for transport of $A$ in the $y$-direction.

If the oxide deforms plastically and its molar volume is constant, the divergence of the flow rate of the oxide must vanish,

$$\partial u_x/\partial x + \partial u_y/\partial y = 0 \quad [9]$$

The oxide is supposed to involve only slight deviations from the ideal metal-to-oxygen ratio and, therefore, the change in the concentration of $A$ in the oxide with time virtually vanishes. Thus it follows from Eqs. [8] and [9] that

$$\partial c''_A/\partial t = -\partial j''^{(x)}_A/\partial x - \partial j''^{(y)}_A/\partial y$$
$$= (D''^{(o)}/mV'')(\partial^2 a_A^m/\partial x^2 + \partial^2 a_A^m/\partial y^2) \cong 0 \quad [10]$$

As shown in Fig. 2, the locus of the oxide-alloy interface is supposed to be given by

$$x = x^* + b \sin (2\pi y/\lambda) \quad [11]$$

where $x^*$ is the distance of the average interface from the original surface of the alloy, $\lambda$ is the wave length, and $b$ is the amplitude of the sine wave profile.

The following restrictions for the values of $b$ and $\lambda$ are assumed

$$b \ll \lambda \quad [12]$$

$$\lambda \ll x^* \quad [13]$$

At the interface moving in the $x$-direction at rate $u$, the concentration of $A$ changes discontinuously from $c''_A$ to $c'_A$. From the principle of the conservation of mass, it follows that

$$u_x(c''_A - c'_A) = j''^{(x)}_A - j'^{(x)}_A$$

at

$$x = x^* + b \sin (2\pi y/\lambda) \quad [14]$$

At the interface, also the concentration of $B$ changes discontinuously from 0 to $c'_B$. Since the transport rate of $B$ in the oxide is zero,

$$-u_x c'_B = -j'^{(x)}_B \text{ at } x = x^* + b \sin (2\pi y/\lambda) \quad [15]$$

where $j'^{(x)}_B$ is the transport rate of $B$ per unit area in the $x$-direction in the alloy.

Since the molar volume of the alloy is assumed to be independent of composition,

$$j'^{(x)}_B = -j'^{(x)}_A \quad [16]$$

and in view of Eq. [2]

$$c'_B = N'_B/V' = (1 - N'_A)/V' = (1 - a_A)/V' \quad [17]$$

Upon substitution of Eqs. [2], [3], [7], [8], [16], and [17] in Eqs. [14] and [15], it follows that

$$-u_x a_A/V' = -(D''^{(o)}/mV'')(\partial a_A^m/\partial x)_{\text{oxide}} + (D'/V')(\partial a_A/\partial x)_{\text{alloy}}$$

at

$$x = x^* + b \sin (2\pi y/\lambda) \quad [18]$$

$$u_x(1 - a_A) = D'(\partial a_A/\partial x)_{\text{alloy}}$$

at

$$x = x^* + b \sin (2\pi y/\lambda) \quad [19]$$

Combining Eqs. [18] and [19] and eliminating $u_x$, one obtains the boundary condition

$$(D'/V')(\partial a_A/\partial x)_{\text{alloy}} = (1 - a_A)(D''^{(o)}/mV'')(\partial a_A^m/\partial x)_{\text{oxide}}$$

at

$$x = x^* + b \sin (2\pi y/\lambda) \quad [20]$$

The solution of differential Eq. [4] for diffusion in the alloy may be written as the sum of two terms,

$$a_A = F(x, t) + f(x, y, t) \text{ if } x > x^* + b \sin (2\pi y/\lambda) \quad [21]$$

where $F(x, t)$ represents the known solution of Eq. [4] with $a_A = N'_A$ for a plane oxide-alloy interface, and $f(x, y, t)$ is a perturbation function, which is the difference of the solution for a sine wave profile interface and that for a plane interface.

Since $a_A = F(x, t)$ is supposed to satisfy Eq. [4],

$$\partial f/\partial t = D'(\partial^2 f/\partial x^2 + \partial^2 f/\partial y^2) \quad [22]$$

As an approximation one may use a solution $f_o$ independent of time,

$$f_o = \gamma' C' b \exp[-2\pi(x - x^*)/\lambda] \sin(2\pi y/\lambda) \quad [23]$$

where $x^*$ denotes the location of the average interface plane at time $t = t^*$, $\gamma'$ is a constant calculated below, and

$$C' = \partial F/\partial x \text{ at } x = x^*, \quad t = t^* \quad [24]$$

Thus the right-hand member of Eq. [22] is found to be

$$D'(\partial^2 f_o/\partial x^2 + \partial^2 f_o/\partial y^2) = 4\pi^2 f_o/\lambda^2 - 4\pi^2 f_o/\lambda^2 = 0 \quad [25]$$

Since $f_o$ is assumed to be independent of time and, therefore, $\partial f_o/\partial t = 0$, the function $f_o$ suggested in Eq. [23] satisfies Eq. [22].

Actually, however, the perturbation function $f$ cannot be independent of time since the interface moves at a rate $u_x$ in the $x$-direction. In order to obtain the order of magnitude of $\partial f/\partial t$, assume that the perturbation function is essentially stationary with respect to the interface and its magnitude changes only slowly. Thus the change of the perturbation function at a given distance from the interface with time is supposed to be nearly equal to zero, i.e.,

$$(\partial f/\partial t) + u_x(\partial f/\partial x) \cong 0 \quad [26]$$

Substituting the approximate solution suggested in Eq. [23] in [26], one obtains for the right-hand member in Eq. [22]

$$\partial f/\partial t \cong 2\pi u_x f_o/\lambda \quad [27]$$

The value of $\partial f/\partial t$ calculated in Eq. [27] may be compared to the individual terms in [25]. If $\partial f/\partial t$ is much less than each of the individual terms of the right-hand member of Eq. [25], i.e., if

$$u_x \ll 2\pi D'/\lambda \quad [28]$$

a relatively slight modification of the function $f_o$ will result in sufficient changes in the individual terms in Eq. [25] so that the difference of these terms becomes equal to $\partial f/\partial t$ as is required by Eq. [22]. Therefore, Eq. [28] represents a necessary condition for using the function $f_o$ in Eq. [23] as an approximation for $f$.

Transformation of Eq. [28] yields

$$\lambda \ll 2\pi D'/u_x \quad [29]$$

Use of Eq. [23] as a convenient approximation, therefore, confines the following conclusions to sufficiently small values of the wave length $\lambda$ in order to satisfy Eq. [29].

From Eq. [15] of a previous calculation (1) for a plane interface, it follows that

$$u_x \sim D'/x^* \text{ if } D' \sim (D'')_{avg} \quad [30]$$

where $(D'')_{avg}$ is the self-diffusion coefficient of the cations in the oxide averaged over the activity range occurring in the oxide layer. Under these conditions, Eq. [29] is automatically satisfied if [13] is satisfied.

The perturbation function in Eq. [23] vanishes if $(x - x^*) \gg \lambda$, i.e., is significant only in the vicinity of the interface. Therefore, as an approximation, use the first two terms of a Taylor series expansion for $F(x, t)$ as a function of $x$ and obtain for $t = t^*$ in view of Eqs. [23] and [24]

$$a_A \cong a_A^* + C' \{(x - x^*) + \gamma' b \exp[-2\pi(x - x^*)/\lambda] \sin(2\pi y/\lambda)\} \quad [31]$$

where $a_A^*$ is the average activity of $A$ at the average interface plane $x = x^*$.

Similarly, a particular solution of differential Eq. [10] is

$$a_A^m = (a_A^*)^m + C'' \{(x - x^*) - \gamma'' b \exp[2\pi(x - x^*)/\lambda] \sin(2\pi y/\lambda)\} \quad [32]$$

if $x < x^* + b \sin(2\pi y/\lambda)$

where $\gamma''$ is a constant calculated below and

$$C'' = \partial a_A^m/\partial x \text{ at } x = x^*, \quad t = t^* \text{ if } b = 0 \quad [33]$$

The last term in Eq. [32] vanishes if the distance from the interface in the negative $x$-direction is much greater than the wave length $\lambda$. In view of Eq. [13], the activity $a_A$ is, therefore, virtually independent of $y$ at the outer surface in accordance with the assumption that $a_A$ at the outer surface is determined by the oxygen partial pressure of the surrounding gas.

Next, calculate the activity of $A$ at the oxide-alloy interface from Eqs. [11] and [31]. Using a Taylor series expansion for the exponential function in Eq. [31] and disregarding terms involving higher powers of $b$,

$$a_{A(\text{interface})} = a_A^* + C'(1 + \gamma')b \sin(2\pi y/\lambda) \quad [34]$$

Likewise, it follows from Eqs. [11] and [32] that

$$[a_{A(\text{interface})}]^m = (a_A^*)^m + C''(1 - \gamma'')b \sin(2\pi y/\lambda) \quad [35]$$

Since only small deviations from a plane interface are considered, and therefore, $|a_{A(\text{interface})} - a^*| \ll a^*$, one may calculate $a_A$ at the interface approximately from Eq. [35] by using the first two terms of a series expansion for the $m$th root of the right-hand member of Eq. [35]. Thus

$$a_{A(\text{interface})} = a_A^*\{1 + [C''(1 - \gamma'')/m(a_A^*)^m]b \sin(2\pi y/\lambda)\} \quad [36]$$

Equating the right-hand members of Eqs. [34] and [36],

$$(1 + \gamma')C' = (1 - \gamma'')a_A^* C''/m(a_A^*)^m \quad [37]$$

Substituting Eqs. [31], [32], and [34] in Eq. [20], using a Taylor series expansion for the exponential function and disregarding terms involving higher powers of $b$,

$$(D'/V')C'[1 - (2\pi\gamma' b/\lambda) \sin(2\pi y/\lambda)] = (D''^{(o)}/mV'')C''\{(1 - a_A^*) - [(1 - a_A^*)(2\pi\gamma'' b/\lambda) + (1 + \gamma')bC'] \sin(2\pi y/\lambda)\} \quad [38]$$

Eq. [38] can be satisfied only if both the sum of the constant terms and the sum of the terms involving the factor $\sin(2\pi y/\lambda)$ are equal to zero. Thus

$$C'D'/V' = (1 - a_A^*)C''D''^{(o)}/mV'' \quad [39]$$

$$2\pi\gamma'C'D'/\lambda V' = [2\pi(1 - a_A^*)\gamma''/\lambda + (1 + \gamma')C']C''D''^{(o)}/mV'' \quad [40]$$

If, in accordance with Eqs. [13] and [29], the wave length $\lambda$ is sufficiently small, the first term in brackets on the right-hand side of Eq. [40] predominates and the second term may be ignored. Thus

$$\gamma'C'D'/V' \cong (1 - a_A^*)\gamma''C''D''^{(o)}/mV'' \quad [41]$$

On dividing corresponding sides of Eqs. [41] and [39], it follows that

$$\gamma' = \gamma'' \quad [42]$$

Substituting Eq. [42] in [37] and solving for $\gamma' = \gamma''$,

$$\gamma' = \gamma'' = (q - 1)/(q + 1) \quad [43]$$

where

$$q = C''a_A^*/mC'(a_A^*)^m \quad [44]$$

Eliminating the ratio $C''/C'$ with the help of Eq. [39], substituting [6] with $D''^*$ as self-diffusion coefficient of $A$ in the oxide for the activity $a_A^*$ prevailing at the average interface plane, and setting $a_A^*$ equal to the average mole fraction $N_A^*$ in the alloy at the average interface plane,

$$q = \frac{N_A^*}{1 - N_A^*}\frac{D'/V'}{D''^*/V''} \quad [45]$$

The rate of change in the position of the interface with time is equal to the drift velocity $u_x$ of the oxide. From Eqs. [3] and [15], [16], and [17] it follows that

$$u_x = D'(\partial a_A/\partial x)_{\text{alloy}}/(1 - a_A) \quad \text{at} \quad x = x^* + b\sin(2\pi y/\lambda) \quad [46]$$

Substituting Eqs. [31] and [34] in [46], using Taylor series expansions, and disregarding terms involving higher powers of $b$,

$$u_x = D'C'\frac{1 - (2\pi\gamma'b/\lambda)\sin(2\pi y/\lambda)}{(1 - a_A^*) - (1 + \gamma')bC'\sin(2\pi y/\lambda)} \cong [D'C'/(1 - a_A^*)]\{1 - [(2\pi\gamma'/\lambda) - (1 + \gamma')C'/(1 - a_A^*)]b\sin(2\pi y/\lambda)\} \quad [47]$$

If, in accordance with Eq. [13] and [29], the wave length $\lambda$ is sufficiently small, the term $2\pi\gamma'/\lambda$ prevails and the following term can be ignored. Thus the difference between the local value of $u_x$ and the average value $u_x^*$ is found to be

$$u_x - u_x^* = -u_x^*(2\pi b\gamma'/\lambda)\sin(2\pi y/\lambda) \quad [48]$$

If $q$ defined by Eq. [45] is greater than unity, $\gamma'$ calculated from [43] is positive. Then it follows from Eq. [48] that at points where the local thickness of the oxide film exceeds the average value, the local rate of change in the position of the interface is smaller than the average value. Thus, if $q > 1$, there is a tendency that deviations from a plane interface will disappear in the course of time. In other words, a plane interface is stable if $q > 1$, or if

$$\frac{N_A^*}{1 - N_A^*}\frac{D'/V'}{D''^*/V''} > 1 \quad [49]$$

Conversely, if $q < 1$, a plane interface is not stable since any irregularities tend to increase in the course of time.

A value of $q$ less than unity, however, is only a necessary but not a sufficient condition for the formation of a rugged interface since there are some factors which counteract the tendency to form a rugged interface.

First, it must be recalled that the activities of $A$ in adjacent phases are equal only in the case of a plane interface. In principle, Eq. [37] is to be supplemented by a term involving interface tension and the local radius of curvature of the interface. According to calculations omitted in this paper, such an additional term does not affect the validity of the stability criterion in Eq. [49] if the thickness of the oxide film exceeds $4 \cdot 10^{-6}$ cm. This is not a serious limitation since, in the case of thinner oxide films, the diffusion equations also must be modified in view of electrical double layers in the oxide film (6).

Second, local differences in the oxidation rate correspond to local differences in the drift velocity of the oxide lattice toward the alloy. Thus, slip of lattice planes in the oxide is required. From oxidation experiments involving cylindrical and spherical samples of pure metals (7) and observations on stressed oxide samples (8), it is known that oxides deform plastically at elevated temperatures. Certain stresses, however, may remain under quasi-steady-state conditions. Consequently, there will be additional terms in the condition for equilibrium between adjacent phases, and these terms also counteract the tendency of the formation of a rugged oxide-alloy interface.

Even if a plane alloy-oxide interface is not stable, local differences in the thickness of the oxide film may evolve rather slowly and, therefore, the over-all oxidation rate may not differ widely from that calculated for an oxide film of uniform thickness. It seems possible that irregularities in the alloy-oxide interface can be triggered by different grain orientations in the alloy. An alloy involving a small grain size may, therefore, have a greater tendency to form a rugged alloy-oxide interface and finally a structure of the scale as shown in Fig. 1 than an alloy involving coarse grains.

Eqs. [45] and [49] involve values of $N_A$ and $D''$ prevailing at the alloy-oxide interface. These values are determined by Eqs. [11] and [19] of the previous paper (1). In this paper, it has been pointed out that there are two limiting cases. First, diffusion in the oxide layer may be the rate-determining step and the concentration of $A$ at the alloy-oxide interface does not differ widely from the bulk concentration of the alloy. In this case, $D''$ at $x = x^*$ is much less than $D'$, the value of $q$ defined by Eq. [45] is much greater than unity, and accordingly a plane alloy-oxide interface is stable. Second, diffusion in the alloy may be the rate-determining step and the oxygen activity at the alloy-oxide interface is only slightly lower than the oxygen activity in the surrounding atmosphere. In the latter case, the

value of $q$ defined by Eq. [45] is much less than unity, the mole fraction of $A$ at the interface, $N_A^*$, is very low, and accordingly a plane alloy-oxide interface is not stable.

By and large, if the rate of the displacement of the boundary between two phases is controlled by diffusion or electrolytic migration of a reactant from the "forward direction," i.e., from the phase whose volume decreases, there is the tendency that deviations from a plane interface become enlarged in the course of time. This is especially true for cathodic electrodeposition of a metal from a liquid or solid electrolyte (9). But it is known that, under most conditions, the resulting roughness of the moving interface is not very distinct. Treelike growth of an electrodeposit is an exception rather than a rule.

On the other hand, if the rate of displacement of the boundary between the two phases is controlled by diffusion of a reactant from the "backward direction," i.e., from the phase whose volume increases, there is the tendency to even out irregularities of the interface as in electropolishing (10, 11) and in the high temperature oxidation of pure metals.

The inequality $q < 1$ is, therefore, only a necessary but not a sufficient condition for lack of stability of a plane alloy-oxide interface. Even if a plane alloy-oxide interface is not stable, local differences in the thickness of the oxide film may evolve rather slowly and, therefore, the over-all oxidation rate may not differ widely from that calculated for an oxide film of uniform thickness (1).

The quotient $q$ defined in Eq. (45) becomes definitely smaller than unity if the concentration of $A$ in the bulk alloy and likewise the concentration of $A$ in the alloy at the interface is small. Therefore, an oxide film of nonuniform thickness may be expected especially on alloys involving low concentrations of metal $A$ which forms an oxide. Actually, however, the oxidation rate of Pt-rich Pt-Ni alloys ($N_{Ni} = 0.15$ and 0.20) observed by Kubaschewski and von Goldbeck (2) agrees fairly well with the oxidation rate calculated under the assumption of a NiO film of uniform thickness, although $q$ is less than unity.

According to Raub and Engel (12, 13) oxidation of a Cu-Au alloy containing 5 wt % Cu ($N_{Cu} = 0.14$) yields a CuO film whose thickness is essentially uniform, whereas the oxidation of Cu-Au alloys involving higher copper concentrations ($N_{Cu} = 0.50$, 0.69, and 0.87) yields oxide layers with large local variations of the thickness as discussed below.

These observations show that alloys involving low concentrations of an oxide-forming metal may yield an oxide film of nearly uniform thickness, although the parameter $q$ is less than unity.

### Formation of a Two-Phase Scale Consisting of the Oxide of the Less Noble Metal and Alloy Rich in the More Noble Metal

The foregoing considerations have been confined to small perturbations of a plane alloy-oxide interface. Now consider the opposite case illustrated in Fig. 1. Protruding sections of the oxide of metal $A$ are supposed to alternate with slender trunks of the alloy depleted with respect to the less noble metal $A$. In addition, a compact layer of oxide is assumed on top of the original surface of the alloy because the volume of the oxide is supposed to be greater than that of the metal.

In the oxide, cations of metal $A$ and electrons are supposed to move. When atoms of metal $A$ are transferred to the oxide, voids at the alloy-oxide interface would originate if the oxygen ion lattice were at rest with respect to a reference plane inside the alloy. In the following analysis, however, it is assumed that the space initially occupied by atoms $A$ is filled concurrently by oxide which moves inward by virtue of plastic flow. No voids are supposed to occur.

If the diffusivity of the alloy is very low, atoms of component $B$ can move only over small distances. As a limiting case, it may be assumed that atoms of component $B$ move only in directions parallel to the original surface and accumulate in slender trunks of the alloy depleted with respect to $A$. Plastic flow of the alloy is assumed to be negligible.

A rigorous analysis deals with diffusion and plastic flow normal and parallel to the original surface of the alloy. In view of the geometry shown in Fig. 1, the distance to be overcome by diffusion or plastic flow is supposed to be much greater in the $x$-direction normal to the original surface than in the $y$-direction parallel to the surface. As an approximation, equations are formulated only for transport normal to the surface and thus have a one-dimensional problem. This is possible only if the trunks of the remaining alloy are so slender that diffusion equilibrium within the alloy in the $y$-direction is virtually established. Deviations from these highly idealized conditions are discussed below.

In the two-phase region of the scale, the rate of transport is determined not only by the gradient of the activity $a_A$ of metal $A$ but also by the available cross section of the oxide, i.e., by the volume fraction $\phi$ of the oxide, which is a function of distance $x$ from the original surface of the alloy and is not given but has to be calculated.

Consider a volume element $Sdx$ of the scale at distance $x$ from the original surface of area $S$. Because of oxidation of metal $A$, the mole fraction of the alloy at distance $x$ and a given time $t$ has decreased from the initial value $N_A^o$ to $N_A$. The molar volume $V'$ of the alloy is supposed to be independent of composition. The initial amount of $B$ in the volume element $Sdx$ is $(1 - N_A^o)Sdx/V'$ and must be equal to the amount in the same volume element in the scale, $(1 - N_A)(1 - \phi)Sdx/V'$ since metal $B$ is not supposed to move in the $x$-direction. Thus

$$(1 - N_A^o) = (1 - N_A)(1 - \phi) \qquad [50]$$

whence

$$\phi = (N_A^o - N_A)/(1 - N_A) \qquad [51]$$

valid for any value of $x$ in the two-phase region, with the special value $\phi = 0$ at the inside boundary of the two-phase region where $N_A = N_A^o$.

The rate of transport $j_A''^{(x)}$ of $A$ per unit total area in the $x$-direction is given by the product of the right-hand member of Eq. [5] and the fraction of the cross section of the oxide, which is equal to the volume fraction $\phi$ in view of the geometry assumed in Fig. 1. Thus, using Eq. [7],

$$j_A''^{(x)} = -\phi(D''/V'')(\partial \ln a_A/\partial x) + \phi u_x/V'' \qquad [52]$$

The rate of change in the oxide volume per unit total area in the space beyond a given value of $x$ with time is $\phi u_x$ and must be equal to the product of the molar volume $V'$ of the alloy and the amount of metal $A$ oxidized per unit area per unit time beyond the given value of $x$. This value in turn is equal to the number of moles of $A$ diffusing with respect to the oxygen ion sublattice in the oxide in the negative $x$-direction at distance $x$ per unit total area per unit time. The latter value is given by the first term on the right-hand side of Eq. [52]. Thus

$$\phi u_x = V'\phi(D''/V'')(\partial \ln a_A/\partial x) \quad [53]$$

Substitution of Eq. [53] in Eq. [52] yields

$$j_A''^{(x)} = -\phi \frac{V'' - V'}{V''} \frac{D''}{V''} \frac{\partial \ln a_A}{\partial x} \quad [54]$$

Since the activity $a_A$ increases in the direction toward the bulk alloy, i.e., $\partial \ln a_A/\partial x$ is positive and the molar volume of the oxide is supposed to exceed that of the alloy, i.e., $V'' - V' > 0$, $j_A''^{(x)}$ is negative, i.e., metal $A$ is transported outward with respect to the original surface as the reference plane.

Next, consider the movement of oxygen due to plastic flow of oxide. The average number of gram-atoms of oxygen per unit volume of the heterogeneous scale is $\nu\phi/V''$ where $\nu$ is the number of oxygen atoms per atom $A$ in the oxide. The transport rate in gram-atoms of oxygen per unit total area in the $x$-direction is $\nu\phi u_x/V''$. From the principle of the conservation of mass, it follows that the rate of change of the number of gram-atoms of oxygen per unit volume with time must be equal to the negative value of the divergence of the transport rate. Thus, omitting common factors, for the two-phase region of the scale

$$\partial\phi/\partial t = -\partial(\phi u_x)/\partial x \text{ at } 0 \leqq x \leqq X \quad [55]$$

where $X$ is the maximum distance at which oxide is found at a given time.

Substitution of Eq. [53] in Eq. [55] yields

$$\frac{\partial\phi}{\partial t} = -\frac{V'}{V''}\frac{\partial}{\partial x}\left(\phi D'' \frac{\partial \ln a_A}{\partial x}\right) \text{ at } 0 \leqq x \leqq X \quad [56]$$

Solutions of problems involving diffusion in a semi-infinite space are known to be functions of $x/t^{1/2}$. Thus, one introduces

$$z = x/2(D''^{(o)}t)^{1/2} \quad [57]$$

as independent variable where $D''^{(o)}$ is the value of $D''$ for $a_A = 1$. Hence Eq. [56] becomes

$$\frac{V'}{V''}\frac{d}{dz}\left[\phi \frac{D''}{D''^{(o)}} \frac{d \ln a_A}{dz}\right] - 2z\frac{d\phi}{dz} = 0 \text{ at } 0 \leqq z \leqq Z \quad [58]$$

where, in view of Eq. [57],

$$Z = X/2(D''^{(o)}t)^{1/2} \quad [59]$$

Likewise, introduce

$$\zeta = \xi/2(D''^{(o)}t)^{1/2} \quad [60]$$

where $\xi$ is the thickness of the compact oxide film on top of the original surface of the alloy (*see* Fig. 1).

To obtain the solution of the ordinary differential Eq. [58] of second order, two independent boundary conditions are needed. In addition, it is necessary to calculate the parameters $Z$ and $\zeta$ defined in Equations [59] and [60]. Therefore, as a whole, four conditions are to be formulated.

1. At $x = X$ or $z = Z$, the volume fraction $\phi$ of the oxide tends to zero. Thus, in view of Eq. [50],

$$a_A = a_A^o \quad \text{at} \quad z = Z \quad [61]$$

where $a_A^o$ is the activity of $A$ in the original alloy of mole fraction $N_A^o$.

2. For the front of the inward penetrating oxide, there is the relation

$$dX/dt = u_x(x = X) \quad [62]$$

Substitution of Eqs. [53], [57], and [59] in Eq. [62] yields

$$\frac{V'}{V''}\frac{D''(z = Z)}{D''^{(o)}}\left(\frac{d \ln a_A}{dz}\right)_{z=Z} = 2Z \quad [63]$$

3. In the compact oxide layer where $\phi = 1$, the transport rate of $A$ is independent of $x$. Thus, substituting Eq. [57] in Eq. [54] and letting $\phi = 1$,

$$j_A''^{(x)} = -\frac{V'' - V'}{V''}\frac{D''}{V''}\frac{1}{2(D''^{(o)}t)^{1/2}}\frac{d \ln a_A}{dz} \quad \text{at } -\zeta \leqq z \leqq 0 \quad [64]$$

where $j_A''^{(x)}$ is independent of $x$. Integrating Eq. [64] with respect to $z$ from $z = -\zeta$ to $z = 0$ and dividing through by $\zeta$,

$$j_A''^{(x)} = -\frac{(D''^{(o)})^{1/2}}{2\zeta V''t^{1/2}}\frac{V'' - V'}{V''}\int_{a_A^{(s)}}^{a_A(z=0)} \frac{D''}{D''^{(o)}}\frac{da_A}{a_A} \quad [65]$$

at

$$-\xi \leqq x \leqq 0$$

where $a_A^{(s)}$ is the activity of $A$ in the oxide coexisting with the surrounding oxidizing atmosphere.

The transport rate calculated in Eq. [65] must be equal to the transport rate at $x = 0$ calculated in Eq. [54]. Substituting Eq. [57] in Eq. [54] and omitting common factors,

$$\frac{1}{\zeta}\int_{a_A^{(s)}}^{a_A(z=0)} \frac{D''}{D''^{(o)}}\frac{da_A}{a_A} = \left[\phi \frac{D''}{D''^{(o)}}\frac{d \ln a_A}{dz}\right]_{z=0} \quad [66]$$

where the differential quotient $(\partial \ln a_A/\partial z)_{z=0}$ is to be taken as the limiting value for the region $z > 0$.

4. Next, consider the movement at the outer surface of the oxide ($x = -\xi$). The rate of change of $\xi$ with time is equal to the product of the molar volume $V''$ and the rate of formation of oxide per unit area minus the drift velocity $u_x$. The rate of formation in turn is given by the number of moles of $A$ diffusing in the oxide per unit area per unit time in the negative $x$-direction at $x = -\xi$. Thus

$$\frac{d\xi}{dt} = \left[D'' \frac{\partial \ln a_A}{\partial x} - u_x\right]_{x=-\xi} \quad [67]$$

Substituting Eqs. [53], [57], and [60] in Eq. [67]

$$\zeta = \frac{1}{2}\frac{V'' - V'}{V''}\left(\frac{D''}{D''^{(o)}}\frac{d \ln a_A}{dz}\right)_{z=-\zeta} \quad [68]$$

From Equations [64] and [65], it follows that

$$\left(\frac{D''}{D''^{(o)}}\frac{d\ln a_A}{dz}\right)_{z=\zeta} = \frac{1}{\zeta}\int_{a_A^{(s)}}^{a_A(z=0)} \frac{D''}{D''^{(o)}}\frac{da_A}{a_A} \qquad [69]$$

Substitution of Eq. [69] in Eq. [68] yields

$$\zeta^2 = \frac{1}{2}\frac{V'' - V'}{V''}\int_{a_A^{(s)}}^{a_A(z=0)} \frac{D''}{D''^{(o)}}\frac{da_A}{a_A} \qquad [70]$$

If the relation between activity $a_A$ and mole fraction $N_A$ is given, the differential Eq. [58], the boundary conditions in Equations [61], [63], [66], and [70], and the auxiliary Eq. [51] determine the activity $a_A$ and the volume fraction $\phi$ of the oxide as functions of $z$ between $z = 0$ and $z = Z$, and the parameters $Z$ and $\zeta$. Substitution of the values of $Z$ and $\zeta$ in Equations [59] and [60] yields the depth $X$ of the two-phase scale and the thickness $\xi$ of the compact oxide film at time $t$.

Finally, the oxidation rate $\dot{n}_A/S$ in gram-atom of metal $A$ oxidized per unit area per unit time may be calculated as the amount of $A$ diffusing with respect to the oxygen ion sublattice in the negative $x$-direction at $x = 0$ per unit area per unit time. Taking the first term on the right-hand side of Eq. [52] for $x = 0$ and substituting Eq. [57],

$$\frac{\dot{n}_A}{S} = \frac{1}{2V''}\left(\frac{D_A''^{(o)}}{t}\right)^{1/2}\left(\phi\frac{D''}{D''^{(o)}}\frac{d\ln a}{dz}\right)_{z=0} \qquad [71]$$

Thus a consistent set of equations has been obtained to account for diffusion processes when a two-phase scale, as shown in Fig. 1, is formed. The evaluation of the foregoing equations is the next problem to be solved.

If the relation between mole fraction and activity of $A$ in the alloy is given, the volume fraction $\phi$ of the oxide may be expressed in terms of the local activity of $a_A$ with the aid of Eq. [51]. Substitution of the relation between $\phi$ and $a_A$ in Eq. [58] gives a second-order differential equation for $a_A$, which is to be solved in accordance with Eqs. [61], [63], [66], and [70]. Even for an ideal metallic solution, the transformed Eq. [58] and the boundary conditions with two unknown parameters $Z$ and $\zeta$ are rather involved. Therefore, numerical integration is required.

Calculations are simplified by assuming equal molar volumes of alloy and oxide,

$$V' = V'' \qquad [72]$$

Thus the outer surface of the oxide coincides with the original surface of the alloy at any time, i.e., $\zeta = 0$.

Furthermore, an ideal metallic solution is assumed, i.e.,

$$a_A = N_A \qquad [73]$$

and a value of $D''$ independent of $a_A$, i.e.,

$$D'' = D''^{(o)} \qquad [74]$$

In what follows it is shown that $a_A$ and $\phi$ as functions of $z$ may be obtained by means of consecutive approximations. To this end, it is expedient to introduce the auxiliary variable

$$\eta = (z - Z)/Z \qquad [75]$$

whereupon Eqs. [58] and [63] in view of Eqs. [72] and [74] become

$$\frac{d}{d\eta}\left[\phi\frac{d\ln a_A}{d\eta}\right] + 2Z^2(1-\eta)\frac{d\phi}{d\eta} = 0 \qquad [76]$$

$$\text{at} \quad 0 \leq \eta \leq 1$$

and

$$(d\ln a_A/d\eta)_{\eta=0} = -2Z^2 \qquad [77]$$

Integrating Eq. [76] once with respect to $\eta$ with $\phi = 0$ at $\eta = 0$ as the lower limit according to Eq. [51],

$$\begin{aligned}\phi(d\ln a_A/d\eta) &= -2Z^2\int_0^\eta (1-\eta)(d\phi/d\eta)\,d\eta \\ &= -2Z^2\left[(1-\eta)\phi(\eta) + \int_0^\eta \phi\,d\eta\right]\end{aligned} \qquad [78]$$

which also satisfies Eq. [77].

Dividing through Eq. [78] by $\phi$ and integrating with $a_A = N_A^o$ at $\eta = 0$ as the lower limit,

$$\ln(a_A/N_A^o) = -2Z^2\int_0^\eta\left[1 - \eta + \phi^{-1}\int_0^\eta \phi\,d\eta\right]d\eta \qquad [79]$$

For $\eta = 1$ as the upper limit, Eq. [79] becomes

$$\ln(a_A^{(s)}/N_A^{(o)}) = -2Z^2\int_0^1\left[1 - \eta + \phi^{-1}\int_0^\eta \phi\,d\eta\right]d\eta \qquad [80]$$

Dividing corresponding sides of Eqs. [79] and [80],

$$\frac{\ln(a_A/N_A^o)}{\ln(a_A^{(s)}/N_A^{(o)})} = \frac{\displaystyle\int_0^\eta\left[1 - \eta + \phi^{-1}\int_0^\eta \phi\,d\eta\right]d\eta}{\displaystyle\int_0^1\left[1 - \eta + \phi^{-1}\int_0^\eta \phi\,d\eta\right]d\eta} \qquad [81]$$

If the absolute value of the standard free energy of formation of the oxide of metal $A$ is much greater than $RT$, the trunks of the alloy in two-phase region consist mostly of metal $B$ and, accordingly, the volume fraction of $\phi$ is close to $N_A^o$ except for the vicinity of the front of the two-phase region where $\phi$ tends to zero. Therefore, in order to obtain a first approximation, $a_A^{(1)}$, for the activity of $A$ as a function of $\eta$, substitute $\phi = N_A^o$ as a constant value in Eq. [81] and obtain

$$\ln a_1^{(1)} = \ln N_A^{(o)} - \eta\ln(N_A^o/a_A^{(s)}) \qquad [82]$$

Substituting $\phi = N_A^{(o)}$ in Eq. [80],

$$Z^{(1)} = [\tfrac{1}{2}\ln(N_A^o/a_A^{(s)})]^{1/2} \qquad [83]$$

as a first-order approximation for $Z$.

In view of Eq. [73], $a_A^{(1)}$ calculated from Eq. [82] is also a first-order approximation of the mole fraction $N_A^{(1)}$, which may be substituted in Eq. [51] in order to obtain a first-order approximation of the volume fraction, $\phi^{(1)}$. Substituting the latter value in Eqs. [80] and [81], one may calculate second-order approximations for $Z$ and $a_A$. This procedure may be repeated until differences between consecutive approximations are sufficiently small.

Numerical calculations have been made for $N_A^o = 0.5$, $a_A^{(s)} = 0.01$. The second-order approximations, $N_A^{(2)}$ and $\phi^{(2)}$, deviate from the first-order approximations by less

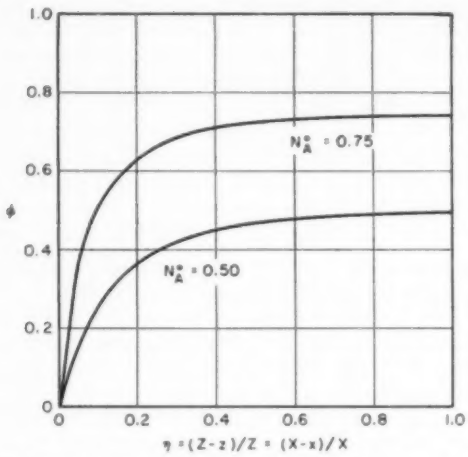


FIG. 3. Volume fraction $\varphi$ of oxide of metal $A$ as a function of the distance from the inner boundary of the two-phase scale for $a_A^{(\varphi)} = 0.01$.

than 0.015 at any value of $\eta$, and $Z^{(2)}$ is only 6% greater than $Z^{(1)}$.

The satisfactory convergence of this iteration procedure is due to the fact that the actual value of $\phi$ does not differ widely from the value $N_A^\circ$ used for the start except for the vicinity of the inner boundary of the two-phase region ($\eta = 0$). This is illustrated in Fig. 3 for two different compositions of the bulk alloy.

Upon substituting $Z^{(2)}$ in Eq. [59], the depth of the scale at any time is obtained and may be compared with the value for pure metal $A$. It follows that the depth of the scale for the alloy $N_A^\circ = 0.5$ is only 2% less than the depth of the scale on pure metal $A$.

This special result may be generalized. By and large, the depth of the scale on an alloy $A$-$B$ containing not more than 50% of a noble metal $B$ is expected to be nearly the same as on pure metal $A$ even if the special conditions formulated in Eqs. [72] to [74] do not hold.

From Eqs. [71] and [75] and the numerical values for $a_A = N_A$ and $Z$ one may also calculate the rate of oxidation of metal $A$ in moles per unit area per unit time and find that the rate for the alloy $N_A^\circ = 0.5$ is equal to 0.4 times the rate for pure metal $A$ at the same time. This decrease in rate is due essentially to the smaller fraction of the cross section available for diffusion of $A$ in the oxide corresponding to the factor $\phi$ in Eq. [71].

In the foregoing calculations, it has been assumed that diffusion equilibrium within the slender trunks of the alloy in directions parallel to the surface is established. According to Einstein (14), the time $\tau$ for a given value $b^2$ of the average square of the displacement of a particle in a given direction is

$$\tau = b^2/2D \qquad [84]$$

Diffusion equilibrium within the alloy in directions parallel to the surface will be virtually established if the time $t$ is much greater than the time $\tau$ calculated from Eq. [84] with a value of $b$ equal to the diameter of the trunks of the alloy, i.e., if

$$t \gg b^2/2D \qquad [85]$$

or

$$b \ll (2Dt)^{1/2} \qquad [86]$$

From Eq. [86] it follows that very small diameters of the trunks of the alloy are required if the diffusion coefficient for the alloy is small.

As an example, apply Eq. [86] to the oxidation of Cu-Au alloys at 750°C (10, 11). The diffusion coefficient of gold in copper is 2 to $4 \cdot 10^{-11}$ cm$^2$sec$^{-1}$ (15). For an oxidation time of 10 hr, it follows from Eq. [86] that the diameter of the trunks must be considerably smaller than $1.5 \cdot 10^{-3}$ cm, whereas the depth of the scale is about ten times greater under the same conditions. This shows that the mechanism suggested in Fig. 1 requires very slender trunks of the remaining alloy corresponding to a small diameter-to-length ratio. Further investigations are needed in order to check under which experimental conditions the irregularities of an alloy-oxide interface have a sufficiently short wave length in order to form the slender trunks presupposed in the foregoing theoretical analysis.

Among the various deviations from the presuppositions of the foregoing theoretical analysis, the occurrence of plastic flow of the alloy deserves special attention. It has been assumed that there is diffusion of atoms $B$ parallel to the original surface of the alloy but no transport of $B$ normal to the original surface. Consequently, atoms of type $B$ are supposed to stay at this location, i.e., the outer boundary of the two-phase region is supposed to be at the location of the initial surface at any time. This presupposition can be checked readily by microscopical examination of sectioned oxidized samples. Under most conditions, smaller or greater deviations may occur because diffusion in the alloy in the $x$-direction is appreciable and the alloy is not completely rigid, i.e., the alloy may deform plastically and move inward in order to fill the space left by atoms of $A$ which are transferred from the alloy to the oxide at the inner boundary of the two-phase region. Under these conditions, the volume fraction of the oxide will be greater near the surface but smaller near the front of the protruding oxide than has been assumed in the foregoing analysis, especially Eq. [51]. It can be shown, however, that in general the transport rate of $A$ in the oxide is affected only slightly by variations in the local distribution of the alloy enriched with respect to the noble metal.

The following situation is amenable to an analytical evaluation. Consider oxidation of a heterogeneous alloy $A$-$B$ so that the metal left over after oxidation is virtually pure $B$.

As case 1, assume that there is no transport of $B$ normal to the original surface from the alloy. Then it follows from Eq. [51] that the volume fraction of the oxide has a constant value in the two-phase region,

$$\phi = N_A^\circ \quad \text{if} \quad 0 \leq x \leq X \qquad [87]$$

As case 2, assume that metal $B$ has retreated from the outer region up to $x = x_0$ and is evenly distributed be-

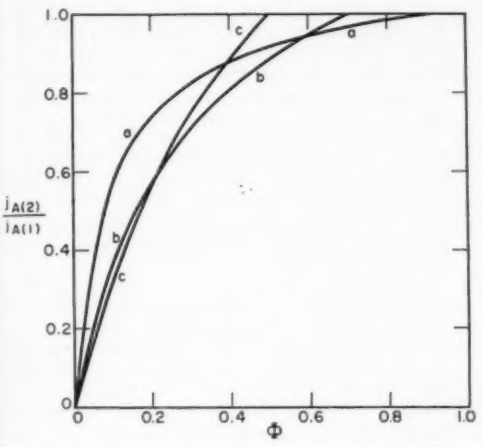


FIG. 4. Ratio of transport rates according to Eq. [90] for $N_A^0 = 0.9$ (curve a), 0.7 (curve b), and 0.5 (curve c).

tween $x = x_0$ and $x = X$,

$$\phi = 1 \quad \text{if} \quad 0 < x < x_0$$
$$\phi = \Phi \quad \text{if} \quad x_0 < x < X \qquad [88]$$

If $V' = V''$, the volume of the oxide of metal $A$ per unit area of the sample is $N_A^0 X$ in the first case, and $x_0 + \Phi(X - x_0)$ in the second case. Hence,

$$N_A^0 X = x_0 + \Phi(X - x_0) \qquad [89]$$

whereby $x_0$ is determined if the value of $\Phi$ is given.

The ratio of the transport rates of $A$ for case 1 and case 2 per unit area, $j_{A(1)}$ and $j_{A(2)}$, respectively, is given by the reciprocal of the respective diffusion resistances, $R_1$ and $R_2$, which in turn are given by the integrals $\int \phi^{-1}\, dx$. From Eqs. [87] to [89] it follows that

$$\frac{j_{A(2)}}{j_{A(1)}} = \frac{\Phi}{N_A^0(1 + \Phi - N_A^0)} \qquad [90]$$

where $\Phi$ is necessarily smaller than $N_A^0$.

The ratio of the transport rates for the two cases is plotted as a function of $\Phi$ for various alloy compositions in Fig. 4. For $A$-rich alloys, the transport rate for case 2 differs from that for case 1 markedly only if the value of $\Phi$ approaches zero, i.e., if the available cross section for diffusion of $A$ in the oxide is very narrow between $x = x_\varepsilon$ and $x = X$. Consequently, even if recession of the alloy takes place, the depth of the scale on alloys containing only 10 or 20 at. % of a noble metal is expected to be of the same order of magnitude as on a pure metal.

## Discussion

In the literature, there are the following observations which support the assumption of a composite scale as shown in Fig. 1. Raub and Engel (12, 13) have presented microphotographs of sections of the scale on Cu-Au alloys oxidized at 750°C ($N_{Cu} = 0.50, 0.69, 0.87$) which resemble the structure shown in Fig. 1. A similar structure of the scale is found on Cu-Ag alloys oxidized at 750°C (16), but in this case, diffusion of oxygen in nonoxidized Ag plays an important part. Oxygen diffusing in a Ag-rich alloy may lead to formation of $Cu_2O$ or CuO in the interior of the alloy as a "subscale" consisting of separate oxide particles without connection with the surrounding atmosphere. This process is known as internal oxidation (17). Internal oxidation may also be significant in Cu-Pd alloys (9, 19) but seems to be negligible in Au-Cu alloys in view of the very low solubility of oxygen in gold (18).

Oxidation rates of Cu-Au alloys observed by Raub and Engel (12) are listed in Table I. In accord with the foregoing analysis, the oxidation rate varies only to a minor extent between $N_{Cu}^0 = 1.00$ and 0.42 and falls off at lower Cu concentrations. Rate constants $k_{PB}$ have been calculated according to the parabolic rate law in the form suggested by Pilling and Bedworth (28),

$$k_{PB} = (\Delta m/A)^2/t \qquad [91]$$

where $\Delta m/A$ is the weight increase per unit area and $t$ is time.

Moreover, a composite scale similar to that shown in Fig. 1 has been found on a Ag-Au alloy containing 10 at. % Au after exposure to sulfur vapor at 800°C (20). In view of the size of the sulfur atom, no significant diffusion of sulfur in the alloy can be expected. The observed pattern of the scale is explainable only if the mechanism assumed in Fig. 1 is operative.

The structure of the scale shown in Fig. 1 may also occur on alloys involving two nonnoble metals both of which oxidize in their pure states. When Fe-Ni alloys (e.g., $N_{Ni} = 0.30$) are oxidized, a heterogeneous scale consisting of wüstite and Ni-rich alloy is found underneath an outer layer of iron oxides (21–25). It may be assumed that initially both iron oxide and nickel oxide nucleate at the surface of an Fe-Ni alloy. When the oxidation is continued, the faster growing iron oxide buries nickel oxide in the same manner as inert material, e.g., $Cr_2O_3$ placed on the surface of pure Fe heated in oxygen is buried (22). Buried nickel oxide, however, is not stable. Since the absolute value of the standard free energy of formation of nickel oxide is considerably less than that of wüstite, the oxygen activity at the alloy-wüstite interface is so low that nickel rather than oxidized nickel is found at this location. Thus, Ni in Fe-Ni alloys behaves in the same manner as a noble metal.

Also in the case of Fe-Ni alloys, the oxidation rate has

TABLE I. *Oxidation rate of* Cu-Au *alloys in oxygen of atmospheric pressure at 750°C according to Raub and Engel (12)*

| $N_{Cu}^0$ | $N_{Au}^0$ | Weight increase after 30 hr mg/cm² | Rate constant $k_{PB} \cdot 10^9$ (g/cm²)²/sec |
|---|---|---|---|
| 1.00 | 0.00 | 18.3 | 3.1 |
| 0.67 | 0.33 | 18.1 | 3.0 |
| 0.42 | 0.58 | 16.1 | 2.6 |
| 0.25 | 0.75 | 10.4 | 1.0 |
| 0.10 | 0.90 | 3.8 | 0.15 |
| 0.05 | 0.95 | 1.2 | 0.014 |

been found to vary only slightly with the Ni content up to 30 at. % Ni (22, 23, 27).

Likewise, oxidation of Fe-Cu alloys yields an outer scale consisting of iron oxides and an inner scale consisting of wüstite and nearly pure Cu as separate phases (23, 25).

To summarize, alloys involving noble metals may exhibit two distinct modes of oxidation, viz., (*a*) formation of an oxide layer of the less noble metal of essentially uniform thickness with a plane alloy-oxide interface, and (*b*) formation of a composite scale with an outer homogeneous oxide layer, and an inner heterogeneous layer consisting of oxide and alloy enriched with respect to noble metal. The second mode may also occur when each of the pure components of an alloy oxidizes, but the oxidation rate of the less noble component exceeds considerably that of the more noble component, and the interdiffusion coefficient of the alloy has a relatively low value.

Experimental investigations are in preparation in order to check more thoroughly the hypotheses suggested in this paper and in order to determine under which particular conditions the different modes of oxidation occur.

ACKNOWLEDGMENT

This investigation was sponsored by the Office of Ordnance Research under Contract DA-19-020-ORD-2244, Project TB2-0001 (779).

Manuscript received October 17, 1955.
Any discussion of this paper will appear in a Discussion Section to be published in the June 1957 JOURNAL.

REFERENCES

1. C. WAGNER, *This Journal*, **99**, 369 (1952).
2. O. KUBASCHEWSKI AND O. VON GOLDBECK, *J. Inst. Metals*, **76**, 255, 740 (1949).
3. C. WAGNER, "Diffusion and High Temperature Oxidation of Metals" in "Atom Movements," p. 153, American Society for Metals, Cleveland, Ohio (1951).
4. E. A. SECCO AND W. J. MOORE, *J. Chem. Phys.*, **23**, 1170 (1955).
5. H. H. VON BAUMBACH AND C. WAGNER, *Z. physik. Chem.*, **B24**, 59 (1934).
6. N. F. MOTT, *Trans. Faraday Soc.*, **43**, 429 (1947); *J. chim. phys.*, **44**, 172 (1947); *Bull. Soc. chim. France*, **1949**, D84; N. CABRERA AND N. F. MOTT, *Repts. Prog. Phys.*, **12**, 163 (1949); K. HAUFFE AND H. J. ENGELL, *Z. Elektrochem.*, **56**, 366 (1952); K. HAUFFE AND B. ILSCHNER, *ibid.*, **58**, 467 (1954).
7. W. J. MOORE, *J. Chem. Phys.*, **21**, 1116 (1953); U. R. EVANS, *Research*, **6**, 130 (1953); B. ILSCHNER AND H. PFEIFFER, *Naturwissenschaften*, **40**, 603 (1953).
8. R. F. TYLECOTE, *J. Inst. Metals*, **78**, 301 (1950).
9. H. FISCHER, "Elektrolytische Abscheidung und Elektrokristallisation von Metallen," pp. 487 ff., Springer, Berlin (1954).
10. J. EDWARDS, *J. Electrodepositors' Tech. Soc.*, **28**, 137 (1952); *This Journal*, **100**, 189*C*, 223*C* (1953).
11. C. WAGNER, *This Journal*, **101**, 225 (1954).
12. E. RAUB AND M. ENGEL, "Vorträge der Hauptversammlung der Deutschen Gesellschaft für Metallkunde 1938," p. 83, VDI Verlag, Berlin (1938).
13. E. RAUB, "Die Edelmetalle und ihre Legierungen," pp. 195–196, Springer, Berlin (1940).
14. A. EINSTEIN, *Ann. Physik*, (4) **17**, 549 (1905).
15. A. B. MARTIN, A. B. JOHNSON, AND F. ASARO, *J. Appl. Phys.*, **25**, 364 (1954).
16. J. A. A. LEROUX AND E. RAUB, *Z. anorg. u. allgem. Chem.*, **188**, 205 (1930).
17. F. N. RHINES, *Trans. Am. Inst. Mining Met. Engrs.*, **137**, 246 (1940); F. N. RHINES, W. A. JOHNSON, AND W. A. ANDERSON, *ibid.*, **147**, 205, (1942); F. N. RHINES AND H. GROBE, *ibid.*, **147**, 318 (1942); F. N. RHINES, *Corrosion and Material Protect.*, **4**, No. 2, 15 (1947).
18. F. J. TOOLE AND F. M. G. JOHNSON, *J. Phys. Chem.*, **37**, 331 (1933).
19. D. E. THOMAS, *Trans. Am. Inst. Mining Met. Engrs.*, **191**, 926 (1951).
20. J. B. WAGNER AND C. WAGNER, Unpublished results.
21. J. E. STEAD, *J. Iron Steel Inst.*, **94**, 243 (1916).
22. L. B. PFEIL, *ibid.*, **119**, 501 (1929).
23. E. SCHEIL AND K. KIWIT, *Archiv Eisenhüttenwesen*, **9**, 405 (1936).
24. J. BÉNARD AND J. MOREAU, *Rev. Métall.*, **47**, 317 (1950).
25. A. TAYLOR, Private communication.
26. F. NEHL, *Stahl und Eisen*, **53**, 773 (1933).
27. W. HATFIELD, *J. Iron Steel Inst.*, **115**, 483 (1927).
28. N. B. PILLING AND R. E. BEDWORTH, *J. Inst. Metals* **29**, 529 (1923).

# Alternating Current Bridge for Measurement of Electrolytic Conductance

F. S. FEATES, D. J. G. IVES, AND J. H. PRYOR

*George Senter Laboratory, Birkbeck College, University of London, London, England*

ABSTRACT

Various theoretical and practical aspects of the problem of attaining high accuracy in conductance measurements are discussed. A number of refinements are reported, including the use of a double conductance cell.

Jones and Josephs (1) and Shedlovsky (2) established the main conditions for minimizing errors in the a-c bridge method for measuring electrolytic conductance. A fundamental criterion of accuracy in such measurements is their complete independence of the frequency, within the audible range, of the alternating emf supplied to the bridge. This criterion has seldom, if ever, been fully satisfied (3). It is true that frequency dependence has

been reduced to limits which are negligible for many purposes, but there are certain applications of conductance measurements in which high accuracy is of critical importance and which call for further development of the a-c bridge method. No discussion of very accurate conductance measurements has appeared recently, and it is the purpose of the present paper to give consideration to various theoretical and practical aspects of this problem, and to report the development of further refinements.

The case for improving upon existing procedures may be made in two ways. The first is to indicate two applications of conductance measurements of a kind requiring the best attainable accuracy. The explicit solution of the complete conductance equation, to derive dissociation constant and equivalent conductance at zero concentration, is based on an extrapolation which must always be extremely sensitive to systematic experimental errors. This may readily be seen by reference to methods of solution of this equation (4–11). These same methods lend themselves to the second application, namely, the evaluation of the enthalpy, entropy, and heat capacity changes accompanying the ionization of weak electrolytes. Apart from the classical work of Schaller (12), no determinations of these thermodynamic functions have been based on conductance measurements until recently, when it was shown (13) that this can be done with advantage. It is clear, however, that great accuracy is needed in determining the dependence of conductance on both concentration and temperature.

## The Conductance Bridge

The second way of supporting the case that the normal bridge method has deficiencies is to direct attention to the electrodes of the conductance cell. These are commonly made of platinum and, when in contact with solutions containing no dissolved hydrogen, they must approximate the behavior of polarized electrodes (14) in which no charge is transferred across the metal-solution interface (15). The alternating current is therefore carried through the conductance cell less by reversible ion-discharge processes occurring at the electrodes than by the very large capacitance of the electrical double layers which reside there. On this view, the conductance bridge approximates a Wien bridge of the type shown in Fig. 1, where $R_3$ and $R_4$ are identical, purely ohmic ratio arms, $R_1$ is the resistance of the electrolyte in the conductance cell, $C_1$ the double-layer capacitance at the electrodes, $R_2$ the standard, noninductive resistance box, and $C_2$ the variable parallel capacitance invariably required to produce a sharp bridge balance. Thus, with $R_3 = R_4$, conditions for balance may be expressed by the relations,

$$f = 1/2\pi\sqrt{R_1R_2C_1C_2} \qquad \text{(I)}$$

where $f$ is frequency

and

$$C_2/C_1 = 1 - R_1/R_2 \qquad \text{(II)}$$

which is true at any frequency.

It is clear that the assumption that $R_2 = R_1$ when the bridge is balanced requires $C_2/C_1$ to be zero, and this can never be the case in practice. The use of black-platinized electrodes greatly increases the value of $C_1$ and, for a given cell and solution, increase of frequency reduces $C_2$. By these devices the error is reduced to a magnitude normally regarded as insignificant, but the approximation remains. That this approaches a correct electrical model of the conductance bridge is supported by the usual experience that an increase of frequency requires a decrease in $C_2$ to restore bridge balance, and this simultaneously proves that the measurements cannot be independent of frequency. It is perhaps more serious that $C_1$ is a function of ionic concentration (16), so that the effect of frequency dependence varies along the concentration scale, thus producing the kind of systematic error particularly to be avoided in extrapolation methods. On this simple bridge model, which is not new (17), the true value of $R_1$ may be obtained by an extrapolation to infinite frequency. For values of the measured resistance, $R_2^A$ and $R_2^B$, determined at the two frequencies $f^A$ and $f_*^B$, the true value of the cell resistance is given by

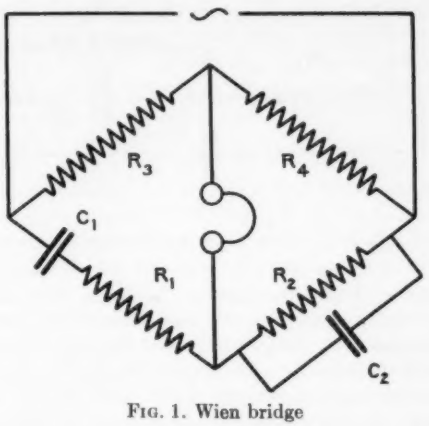


Fig. 1. Wien bridge

$$R_1 = \frac{(f^A)^2R_2^A - (f^B)^2R_2^B}{(f^A)^2 - (f^B)^2} \qquad \text{(III)}$$

There is, however, an important respect in which the conductance bridge differs from the simple Wien model and which invalidates this extrapolation. This has been shown by a study of frequency dependence, using a bridge capable of measuring purely ohmic resistance with an accuracy of better than 0.001% over the full frequency range and a conductance cell, entirely free from Parker effect, with gray-platinized electrodes. In this study it has been found that impossible values of $C_2/C_1$ are required to express the observed frequency dependence in terms of equations (I) and (II). Further, values of $C_1$, the double-layer capacitance at the electrodes, on this basis have been found to be less by orders of magnitude than those reasonably to be expected in the light of existing knowledge of the double layer and the superficial area of the electrodes. This leaves no doubt that the Wien bridge of Fig. 1 is not a satisfactory approximation to the conductance bridge.

In seeking a closer approximation, consideration was given to the fact that the conductance cell electrodes are unlikely to be ideally polarized, for the methods of conductance measurement preclude rigorous deoxygenation.

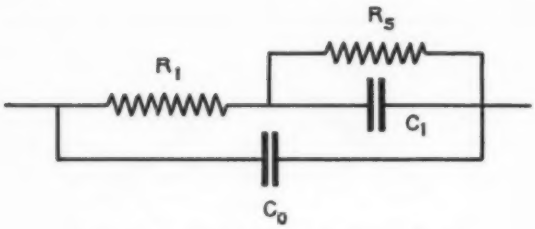


FIG. 2. Cell arm of the conductance bridge

Reference to the literature on hydrogen overpotential shows the stringency of the requirements to avoid depolarization and the practical impossibility of meeting them in conductance work. Even if depolarization is not significant, which is regarded as very unlikely, the occurrence of a faradaic process, involving charge transfer across the electrode-solution interface, cannot be excluded, and will provide an additional admittance in parallel with that due to the double-layer capacitance.

On this basis, a closer approximation to the cell arm of the conductance bridge is represented in Fig. 2, which is identical with the model proposed by Grahame (18) for a metal-solution system, except that the Warburg impedance has been set at zero, and an additional capacitance, $C_0$, has been added to represent "stray capacitance" due to the dielectric properties of the cell solution, capacitance between cell connections and the like. $R_5$ represents the faradaic "leakage" of the double-layer capacitance, and is assumed, to all intents and purposes, to be purely resistive.

This assumption can be justified in two ways. First, $R_1$ is overwhelmingly large in conductance measurements, and the total frequency dependence of $R_2$ is small; attempts to analyze this frequency dependence beyond conceivable limits of experimental error would lead to fruitless complexities. The present task is to find a sufficiently close approximation for the particular purpose. Second, in the extremely dilute solutions which are of interest, it is more than probable that the small portion of the current which is faradaic is concerned with the reversible electrodeposition of hydrogen from water molecules. Whether this is depolarized by traces of dissolved oxygen or not, the reactants belong to Grahame's Class I (18), and there will be no Warburg impedance. Further, the voltage swing across the cell in conductance measurements will not normally exceed 100 mv, so that current will remain proportional to voltage. In the present work, linearity between observed resistance and the reciprocal of the square root of frequency, as recorded by Jones and Christian (19), has not been observed. It may be suggested that perhaps this relation appears under conditions where the frequency dependence is relatively high and where the Warburg impedance is considerable. It may be noted that Wien (17) suggested this model, although his physical ideas on how it arose are not now acceptable.

Conditions for balance of this bridge model are

$$4\pi^2 f^2 (C_2 - C_0) C_1 R_1 R_2 R_5 = R_1 + R_5 - R_2 \qquad \text{(IV)}$$

and

$$C_1 R_5 (R_2 - R_1) = (C_2 - C_0)(R_1 R_2 + R_2 R_5) \qquad \text{(V)}$$

An approximation, based on the likely assumptions that $C_0 \ll C_2$ and $R_5 \ll R_1$, allows some check to be made of this bridge model. Although separate quantities cannot be evaluated, substitution of known or reasonably assessed data in the equation

$$C_1 R_5 = \frac{C_2 R_1 R_2}{R_2 - R_1} \qquad \text{(VI)}$$

indicates values of $C_1$ in the range 200–2000 $\mu$F for corresponding values of $R_5$ from 1 to $10^{-1}$ ohm. These are physically reasonable for a very dilute solution in a cell with gray-platinized electrodes. No more quantitative data in support of this model can be advanced, but it can be said with confidence that the kind of frequency dependence of $R_2$ which is observed in practice is inconsistent with the simple Wien model (Fig. 1), but is in agreement with the suggested model (Fig. 2).

Equations (IV) and (V) show that, as the frequency is increased to very high values, both $(C_2 - C_0)$ and $(R_2 - R_1)$ tend to zero; but the form of these equations is such that no simple extrapolation method can be devised. If, by black platinization of the electrodes, frequency dependence has been largely reduced, use of equation (III) may be a justifiable approximation. Black platinization, however, is open to objection for a number of reasons[1] and, although it makes the extrapolation shorter by increasing $C_1$, it also makes equation (III) less applicable by reducing $R_5$. Where gray-platinized or bright electrodes are used, there is little doubt that significant error arises from the use of this formula.

## DOUBLE CELL PROCEDURE

Ives and Pryor (13) used a double-cell method in an attempt to achieve increased accuracy in conductance measurements, a device similar in principle to that suggested by Shedlovsky (20). Two conductance cells were made as closely similar as possible except for the distances between the electrodes, which stood in the ratio 4:1. With both cells filled with the same solution, it was hoped that the difference between their apparent resistances ($R_2$ values) would be free, by cancellation, of any errors due to electrode effects, whether these were due to "transfer resistance," specific ion adsorption, or any other cause. It can be seen from equation (IV) that as frequency tends to zero (excluding the onset of finite electrolysis) $R_2$ tends to $(R_1 + R_5)$. If $R_5$ can be assumed to be the same for each cell, then it is clearly cancelled out in the difference method. It is also clear that the method involves no error when frequency tends to infinity. Between these frequency limits, however, it can be shown from equations (IV) and (V) that the difference method is not strictly valid; furthermore, it is impossible in practice to construct absolutely identical electrodes. For these reasons, it was found that the resistance differences, $\Delta R_2$, were dependent on frequency, though to an order of mag-

[1] Instability, adsorbent properties, catalytic action, facilitation of undesired electrode reactions.

TABLE I. *Cell constant determinations*

| Concentration (g mole/liter × 10⁴) | Ω | Constants from $R_2$ at 1150 cps | | Constant from $\Delta R_1$ |
|---|---|---|---|---|
| 106.299 | 141.08 | 0.46502 | 0.11802 | 0.34749 |
| 74.5656 | 142.34 | 0.46496 | 0.11799 | 0.34745 |
| 49.1596 | 143.64 | 0.46475 | 0.11754 | 0.34748 |
| 36.6060 | 144.44 | 0.46470 | 0.11740 | 0.34750 |
| 14.9472 | 146.32 | 0.46449 | 0.11705 | 0.34744 |
| 13.0958 | 146.54 | 0.46449 | 0.11703 | 0.34747 |
| 5.85475 | 147.62 | 0.46444 | 0.11696 | 0.34745 |
| 4.31205 | 147.94 | 0.46448 | 0.11695 | 0.34748 |
| | | Mean: | | 0.34747 ± 0.00002 |

nitude less than the separate $R_2$ values. This residual effect was eliminated by extrapolating the resistance differences to infinite frequency, involving an adjustment of the order of 0.01% in the case of solutions not exceeding 0.005 g equiv/liter in concentration. The extrapolation was carried out by means of the empirical equation

$$\Delta R_1 = \frac{f^A \Delta R_2^A - f^B \Delta R_2^B}{f^A - f^B} \qquad \text{(VII)}$$

two standard frequencies, 3880 and 1150 cps ($f^A$ and $f^B$), being used. This equation, which is supported by the work of Wien (17) on this type of bridge, may be justified by Table I which relates to a set of determinations of cell constant. Potassium chloride solutions at 25°C were used for these calibrations, the extended Onsager equation (21), with values of coefficients due to Gunning and Gordon (22), being used to interpolate conductance values appropriate to the concentrations used. Table I shows the constants for each cell, based on the values of $R_2$ determined at 1150 cps, and the constant for the double cell based on the corresponding values of $\Delta R_1$ calculated from equation (VII).

The mean deviation of the values of the constant derived from $\Delta R_1$ is only 0.005% and it is entirely random over the concentration range. It is well within the limits of error associated with the primary data and the preparation of the solutions. Since they are referred to conductance standards obtained by a high-precision d-c method (22), these results may be taken to give strong support to the validity of the double-cell method, which may therefore be advocated as a means of attaining the highest accuracy.

## Experimental Procedures

It is apparent that these considerations, concerned as they are with extending accuracy to a further significant figure, are supererogatory unless all sources of error are reduced to appropriate limits. It is for this reason that some reference must be made to certain practical aspects of conductance technique in which there is some improvement to be reported.

*Leads resistance.*—The usual method of making electrical contact to the conductance cell involves the use of mercury cups and copper wires of large cross section. This is open to many objections, apart from its clumsiness and inconvenience, especially when elevated temperatures are to be used. These difficulties may be absolutely avoided, and all uncertainties about the "leads correction" to be applied to measured resistances may be removed, by adoption of the "four-leads" system which is invariably used in modern platinum resistance thermometry. The advantages to be gained are so great that it would appear desirable to outline the principle involved. Two connecting leads are attached to each electrode of the conductance cell, and these are led to a switch box arranged in such a way that, by means of a mercury-contact switch of negligible resistance, reversals of connections may be made as shown in Fig. 3. The resistances $a$, $b$, $c$, and $d$ represent the four contact leads, $X$ is the resistance between the cell electrodes, and $R_3$ and $R_4$ have the same significance as in Fig. 1; $R_2'$ and $R_2''$ are the values of $R_2$ in the alternative bridge arrangements. When the bridge is balanced with equal ratio arms ($R_3 = R_4$) the connections represented in Fig. 3 require that

$$a + X = d + R_2' \qquad \text{(VIII)}$$

and

$$d + X = a + R_2'' \qquad \text{(IX)}$$

so that the mean of the two values $R_2'$ and $R_2''$ gives the true value of $X$, all extraneous resistances being cancelled out. This device at once allows greater flexibility of cell design, and the elimination of thermal disturbance of the cells by the use of thin leads of any length; it also removes all objection to the inclusion of selector switches of the normal radio type in the cell circuit. The same circuitry may be used to include a platinum resistance thermometer in the equipment of the bridge, thus facilitating precise temperature control of the cells and investigation over a temperature range. This arrangement is, in fact, regarded

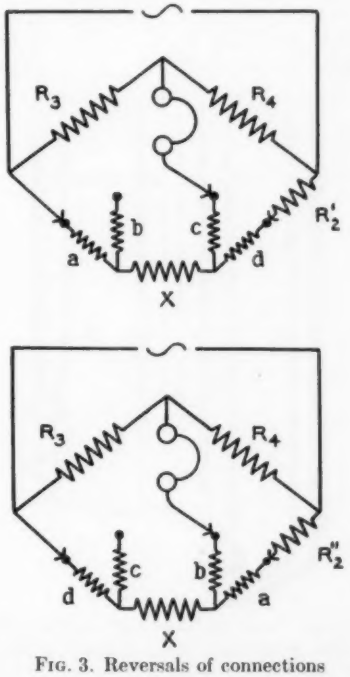


Fig. 3. Reversals of connections

as practically essential for use in conjunction with the double-cell method.

*Cell design and use.*—The first requirements in the design of a completely satisfactory cell are absolute rigidity of the electrodes and the absence from the cell of any dead space containing enclaves which do not readily mix with the bulk of solution in washing and filling operations. These conditions are difficult to satisfy because of the properties of platinum and borosilicate glasses; leakage of solution past imperfect seals is likely to be troublesome unless the functions of electrode support and electrical connection are separated. "Graded seals" and electrodes fused bodily to the glass cell envelope have their peculiar difficulties and disadvantages. These problems have been satisfactorily solved in the design used to construct the double cell, which is shown in Fig. 4. The electrodes were formed from platinum hemispheres, a shape offering maximum rigidity with minimum weight, and these were drilled in the center to allow free flow of solution and near the edges to permit the insertion of Pyrex anchoring "rivets," which were subsequently fused to the inside of the Pyrex envelope. Two fine tags of platinum foil, 0.001 cm thick, were welded to each electrode at opposite edges of the central drilling. These were taken through the envelope by means of thin-walled Pyrex pinch seals, which are known to be vacuum-tight (23, 24). The contact tags, which are destructively amalgamated if mercury is used, were welded to platinum contact wires which were in turn connected to coned brass terminals sealing the upper ends of the contact tubes. It may be noted that the leads resistance arising from this method of construction, from flexible connections and from the selector switch-gear amounted to some 2–3 ohms, but that measurements reproducible to $10^{-4}$ ohm could be made with certainty on account of the properties of the "four-leads" system.

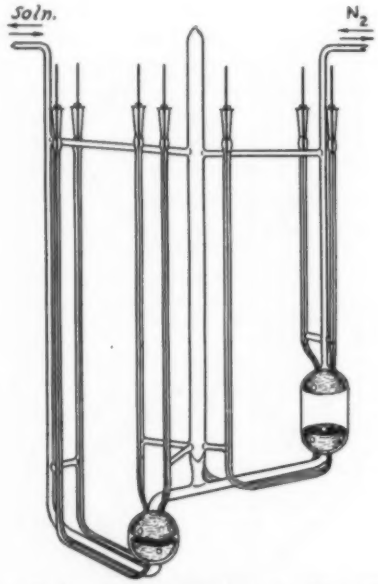


FIG. 4. Design used to construct double cell. (Figure published with permission of the Journal of the Chemical Society, London.)

The double cell was permanently mounted in an oil-filled thermostat and was filled, emptied, rinsed, and washed by the manipulation of solutions under pressure of highly purified nitrogen in a totally enclosed, all-glass apparatus. After the initial cleaning of the cell, following gray platinization of the electrodes *in situ*, it was not again subjected to drastic chemical cleaning agents. Scrupulous care was taken to be certain that only solutions for measurement or water of ultimate purity were ever admitted to the cell; this procedure proved to be entirely satisfactory. The opinion is held that the repeated use of cleaning mixture and steam is deleterious to conductance cells.

*Bridge design and use.*—It is well known that the oscillator supplying the bridge must provide a sinusoidal wave symmetrical about earth potential. This is not the case in many otherwise suitable commercial oscillators, one side of the output often containing an actual or "reflected" earth connection. This difficulty may be obviated by inserting a phase-splitting valve, with symmetrical anode and cathode loads, between the oscillator and the bridge input.

It has been found advantageous to feed the oscillator output first into a simple network consisting of two potentiometers of 1000 ohms each arranged in parallel. From this feeder circuit a signal of any desired amplitude and degree of asymmetry about earth potential may be supplied to the bridge. Sufficient stability of adjustment over the time interval required for a bridge measurement is provided by ordinary radio potentiometers and no complications have been found to occur as a result of using wire-wound types. In principle, this unit is capable of performing, if somewhat crudely, the functions of a Wagner earth; a conventional Wagner earth circuit was, however, used in the present work. In any case, tests of symmetry of input signal to the bridge can be made in the usual way by adjusting the bridge output to zero when taken alternatively from opposite bridge points, or from one bridge point and earth.

Finally, two points concerning standard resistance boxes call for comment. The authors have found that their resistance box (by Cambridge Instrument Co.), which has negligible temperature coefficient and frequency dependence, undergoes a slow change in resistance and requires recalibration at intervals of six to twelve months. It is also found that contact resistance develops over the course of a day or two, and is only countered by frequent routine cleaning of all contacts. For this operation, polishing alumina suspended in benzene has been found to be the ideal medium. So-called "contact lubricants" have been found to be deleterious.

ACKNOWLEDGMENTS

The authors are indebted to the Chemical Society for permission to reproduce Fig. 4. One of the authors (F. S. F.) thanks Birkbeck College for a research studentship, during the tenure of which part of this work was carried out.

Manuscript received November 17, 1955.

Any discussion of this paper will appear in a Discussion Section to be published in the June 1957 JOURNAL.

## REFERENCES


1. G. Jones and R. C. Josephs, *J. Am. Chem. Soc.*, **50,** 1049 (1928).
2. T. Shedlovsky, *ibid.*, **52,** 1793 (1930).
3. G. Jones and G. M. Bollinger, *ibid.*, **53,** 411 (1931).
4. R. M. Fuoss and C. A. Kraus, *ibid.*, **55,** 476 (1933).
5. D. J. G. Ives, *J. Chem. Soc.*, **1933,** 731.
6. T. Shedlovsky and H. H. Uhlig, *J. Gen. Physiol.*, **17,** 594 (1934).
7. R. M. Fuoss, *J. Am. Chem. Soc.*, **57,** 488 (1935).
8. T. Shedlovsky, *J. Franklin Inst.*, **225,** 739 (1938).
9. D. Belcher, *J. Am. Chem. Soc.*, **60,** 2744 (1938).
10. M. L. Kilpatrick, *J. Chem. Phys.*, **8,** 306 (1940).
11. D. J. G. Ives and K. Sames, *J. Chem. Soc.*, **1943,** 511.
12. R. Schaller, *Z. Physik. Chem.*, **25,** 497 (1898).
13. D. J. G. Ives and J. H. Pryor, *J. Chem. Soc.*, **1955,** 2104.
14. A. Slygin and A. Frumkin, *Acta Physicochim.*, **3,** 791 (1935).
15. D. C. Grahame, *Chem. Rev.*, **41,** 441 (1947).
16. J. D. Ferry, *J. Chem. Phys.*, **16,** 737 (1948).
17. M. Wien, *Ann. Phys., Lpz.*, **58,** 37 (1896).
18. D. C. Grahame, *This Journal*, **99,** 370*C* (1952).
19. G. Jones and S. M. Christian, *J. Am. Chem. Soc.*, **57,** 272 (1935).
20. T. Shedlovsky, *ibid.*, **52,** 1806 (1930).
21. T. Shedlovsky, A. S. Brown, and D. A. MacInnes, *Trans. Electrochem. Soc.*, **66,** 165 (1934).
22. H. E. Gunning and A. R. Gordon, *J. Chem. Phys.*, **10,** 126 (1942).
23. W. B. Campbell, *J. Amer. Chem. Soc.*, **51,** 2419 (1929).
24. G. J. Hills and D. J. G. Ives, *J. Chem. Soc.*, **1951,** 305.

# Technical Feature

# Alaska's Power Resources in Relation to Mineral Development[1]

IVAN BLOCH

*Ivan Bloch and Associates of North Pacific Consultants, Portland, Oregon*

ABSTRACT

A large number of potential Alaskan hydropower sites appear feasible of development. Some of them are favorably situated to facilitate the utilization of the Territory's mineral resources such as Fe, Cu, Ni, chromites, and possibly others. With decreasing availability of abundant, low-cost supplies of hydroelectricity in the 48 States, Alaska's power potential warrants immediate consideration, especially in the southeastern and central portion accessible to tidewater for electroprocess industry establishment.

The enormous expansion of electroprocess industries in the United States combined with equally enormous consumption of electric power for other industrial, residential, and commercial purposes, has resulted in a rapid exhaustion of large, low-cost hydroelectric power supplies. Although the utilization of large coal properties for mine-mouth electric steam-generating plants in various parts of the United States will provide large blocks of comparatively low-priced electricity for electroprocess industries, it will not be adequate for the electric furnace and electrolytic cell treatment of many mineral substances located long distances from consuming markets.

In the North Pacific region of America there are enormous hydroelectric potentials, largely unexplored and of great logistic importance for the processing of mineral ores known to exist in those areas. The tremendous development of hydroelectric power in the Kitimat-Nechako, Kemano area of northern British Columbia is clear evidence of the interest of industry in the North Pacific region.

This paper deals in summary with Alaska and its various hydro potentials. In exemplary manner, it points to the potential utilization of some mineral ores as well as to the positive establishment of electroprocess industries in the Territory.

## GENERAL DESCRIPTION OF ALASKA BASINS

The hydroelectric potential of Alaska, now believed to be in excess of 16 million kw, is examined in terms of major regions and subareas. These are:

*Southeastern Alaska Region:* (potential—over 2¼ million kw) (*a*) Ketchikan area, (*b*) Wrangell area, (*c*) Sitka area, (*d*) Angoon area, (*e*) Juneau area.

*Southwestern Alaska Region:* (potential—over 4¼ million kw) (*f*) Gulf of Alaska area, (*g*) Matanuska Valley area, (*h*) Susitna Basin area, (*i*) Kenai Peninsula area, (*j*) Bristol Bay, Alaska Peninsula, Aleutian and Kodiak Island area.

*Central Alaska Region:* (potential—over 10 million kw) (*k*) Kuskokwim Basin area, (*l*) Upper Yukon Basin area, (*m*) Middle and Lower Yukon Basin area, (*n*) Tanana Basin area.

*Northern Alaska Region:* (potential—over ¼ million kw) (*o*) Seward Peninsula area, (*p*) Arctic Region area.

In each of these areas will be found physiographic and climatic characteristics which generally will control the type of eventual hydroelectric development (*see* Fig. 1).

Both the Southeastern Alaska and Kenai Peninsula areas have a substantial number of lakes emptying into short, rapid streams providing considerable hydraulic head. The major portion of potential hydroelectric sites in these two regions, therefore, entail the tapping of lakes by means of tunnels, pipelines, and penstocks to high-head turbine installations. A few streams in those regions are susceptible of development by means of low-head dam installations and transmountain diversion.

On the other hand, the Yukon, Kuskokwim, Susitna, Tanana, and Copper rivers—each with very large drainage basins and consequent large stream flows—will be developed by means of substantial reservoirs, created by large dams, and providing very large individual generating capacity potentials.

Most of the proposed installations at Southeastern Alaska and Kenai Peninsula power sites involve lakes containing little or no sediment. Contrariwise, most of the large rivers are heavily laden with the products of erosion and glacial action and contain substantial sedimentary materials carried as bed load.

The Southeastern Alaska region is one of very heavy rainfall at lower elevations and substantial snowfall in the mountains. Temperatures are moderate and not unlike those which occur in the Puget Sound area, increasing in severity with distance from the coastal areas and altitude of the land masses. The Southwestern Alaska region contains a number of different climatic regions. The Kenai

[1] Paper delivered before the San Francisco Meeting, April 29 to May 3, 1956.

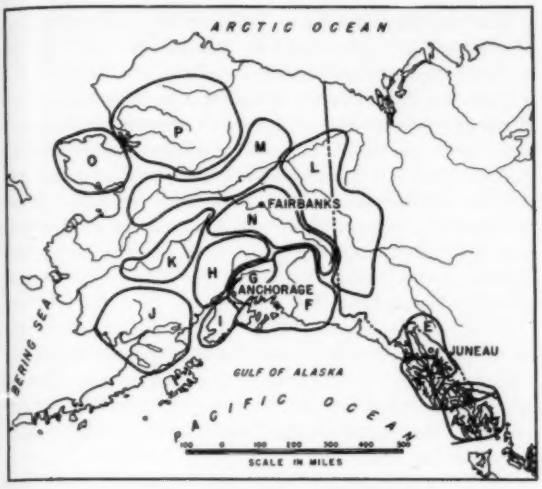


FIG. 1. Hydro power regions of Alaska

Peninsula, Coastal Gulf of Alaska and Bristol Bay areas which adjoin ocean and tidal waters are characterized by somewhat more rigorous but still moderate climate. Rainfall and snowfall are heavy along coastal areas, but decline in interior areas, with much lower winter temperatures. The regions which contain the Yukon, Kuskokwim, Tanana, Seward Peninsula, and Arctic drainages are subject to extremely low and long-duration winter temperatures, sometimes surprisingly high summer temperatures, with moderate annual precipitation.

Although long visualized as a region of forbidding physical and climatic aspects, remote from civilization, even the farthest reaches no longer are considered beyond the possibility of development. Recent experience gained in Arctic operations of both the military and civilians tempers the awe naturally stimulated by past account of long periods of subzero temperatures, and boundless areas of mountainous or tundra terrain. The very physiographic and climatic characteristics which have presented barriers to general development in the past may well be turned to advantage in large-scale development of hydroelectric resources.

Alaska's population, estimated at some 225,000, is largely concentrated in the Southeastern, Kenai Peninsula, and Fairbanks areas. Anchorage, at the head of Kenai Peninsula, at the upper end of Cook Inlet, is the largest city and modern in every sense. The Greater Anchorage area which includes Anchorage and its immediate environs stretching into the famed Matanuska Valley, now has a population well in excess of 100,000. Fairbanks, to the north, is also a completely modern city, serving an area with a population of close to 50,000. It is served by the Alaska Railroad from the ports of Seward, Whittier, and Anchorage. Southeastern Alaska contains a number of communities. The capital of the Territory, Juneau, has an area population of 16,000. Other communities include Ketchikan, Wrangell, Sitka, and Petersburg.

Transportation is well developed for all of the Territory. The airplane is possibly the most important means of transportation and it serves every area of Alaska with modern equipment operating both on regular schedules or by charter. Four major scheduled airlines operate in the inter-Alaska service, and a European airline is scheduled for Trans-Polar service between Europe, the Orient, and West Coast cities. Ocean vessel as well as ocean-going barge services are well established to major ports of the Territory. Sea-train service is projected from Puget Sound points to Gulf of Alaska terminals. The Alaska Railroad serves an area from the Gulf of Alaska, via Anchorage to Fairbanks. An excellent network of good, surfaced highways serves major points. These highways interconnect with the Alaska Highway, and traffic of all kinds, including modern trucking, is continuous the year around. A new type of transportation in the areas north of the Arctic Circle is now established. This consists of "Cat-trains" and the specially built "snow-trains."

Alaska's economy is undergoing a transition of considerable importance. The tremendous increase in population during the past ten years, especially in the Greater Anchorage and the Fairbanks areas, in very large measure has been due to construction activities required in the establishment of large military bases. However, a noticeable stabilization of population and of the related economy is taking place. The pattern seems to parallel that observable in the historical development of the West, which centered about the establishment of military outposts and garrisons. That is to say, people drawn to Alaska in the main by construction activity are putting down their roots in the Territory, building and purchasing modern homes, engaging in commercial and service establishments, and gradually building a sizeable agricultural economy in the Matanuska and Tanana River valleys.

Although it is common to view Alaska as an area of very high labor costs, this is not the case in enterprises with steady all-year employment activity. The most striking example is in the well-established contract between the U. S. Smelting, Refining and Mining Co. in Fairbanks, and the local A.F.L. Union, which sets forth rates comparable with those prevailing in the Puget Sound area.

In an area of about one-fifth that of the 48 states, which until recent years has been considered remote and inaccessible, it follows that much of the area is unexplored. There is a dearth, for example, of reliable, long-term information on stream-flows, hydrologic data, and on the geology of potential water power sites. Although the geologic literature on mineral discovery and development is substantial, it remains sketchy for many large areas. Further, it reflects traditional interest in precious metals such as gold. The analysis, therefore, of mineral potential in relation to hydroelectric power development must be of most preliminary nature.

In the following sections, an attempt is made to sketch some principal possibilities of development. It is believed that, with the passage of time, the importance of many developments will be much greater than can be anticipated.

### SOUTHEASTERN ALASKA

*Total Potential Installed Kilowatts: Over 2¼ Million*

This region comprises the large archipelago and the land strip which is the southern Panhandle of Alaska. It is bordered on the east by British Columbia, and on the west

by the Pacific Ocean. The region is very mountainous, with long inland fjords. One of the greatest rain forests of the world cloaks the area which, as a consequence, is now well on the way to becoming a principal producer of pulp and other forest products. Major communities include Ketchikan, Wrangell, Petersburg, Sitka, Juneau, Haines, and Skagway.

The hydroelectric potential (for units in excess of 5,000 kw installed capacity) is estimated at a total of over 2 million kw.[2] As previously noted, most sites involve relatively small individual units, from 10,000 to 70,000 kw, usually involving the tapping of lakes at moderate altitudes. Power costs from these plants are conservatively estimated as 5 to 12 mills/kwhr averaging 6 to 7 mills/kwhr.

One outstanding potential project is the Yukon-Taiya project located near Skagway. It involves utilization of seven Canadian (Yukon Territory) lakes on the Yukon river above Whitehorse, Y. T., by diverting these flows across the Alaska-Canadian border near Skagway and dropping them to sea level at the head of deep-water Lynn Canal. The project's main features involve tapping Sloko Lake into Atlin Lake, thence into Taku Arm Lake, Marsh, and Tagish Lakes, into Bennett Lake, reversing the flow of Lindeman Lake, and dropping 2,800 $ft^3$/sec of water through the Coast Mountains by means of a 14-mile tunnel to the power house. An ultimate power capacity ranging from 900,000 to as high as 2 million kw has been indicated. Estimates of possible power costs from this huge project have varied, but are all in the general range of 2 mills/kwhr. The Taiya project's projected power plant is at the head of Lynn Canal near Skagway and Haines, with industrial plant site areas within less than 25 miles.

Because of the international character of the project, its construction poses substantial problems. On the one hand, diversion of the Canadian water of the upper Yukon drainage basin would affect navigation and power potentials of the Yukon river further downstream in Alaska, a matter of grave concern to the United States. On the other hand, diversion by means of this project would, in effect, utilize Canadian waters for power production in Alaska, a matter which the Canadians look upon with some disfavor.

As a consequence, other schemes have been recently investigated by Canadian industrial interests. One scheme in particular would involve utilization of approximately the same watershed of the upper Yukon as for the Taiya project, but diverting the flows to the head of Taku Inlet (in Canada), a tidal body to the east of Juneau. Power capabilities for this scheme would be substantially less than for Taiya. Power production would be all-Canadian, but access to deep-draft navigation would necessitate crossing the American Panhandle of Alaska. In addition, there are sizeable physiographic limitations regarding plant sites and access thereto.

Therefore, development of either project must await resolution of some rather difficult international problems between the United States and Canada. It appears, however, that the Taiya project is far superior in every respect to alternative suggestions so far made for the use of this section of the Yukon watershed.

[2] This total includes the Taiya project with a potential listing of 1,600,000 kw.

The possibilities of interconnecting the potential hydroelectric sites of Southeastern Alaska by high-voltage transmission networks are limited because of the rugged topography and the relative isolation of individual sites. Some grouping by a combination of overland transmission lines and submarine cables is indicated as warranting further consideration. Suggested groupings are the following: (*a*) Ketchikan area—Grace, Mirror, Ella, Manzanita, and Swan Lakes; (*b*) Wrangell area—Cascade and Scenery Creeks; (*c*) Sitka area—Green, Blue, and Takatz Lakes; (*d*) Juneau area—Long, Crater, and Dorothy Lakes, Speel River.

Thus, development of most of these sites will be for utilization in generally close proximity to power plants. Suitable areas for industrial or processing plant location are limited or will require very careful consideration because of the sharply rising nature of the terrain from tidewater.

There are at least three possibilities of interest regarding the utilization of Southeastern Alaska's power potential for mineral beneficiation and processing. These include the utilization of the very large quantities of magnetites in the Klukwan area near Haines in the Chilkat Mountain range. There are also apparently extensive nickel-bearing ores in the Takobi-Chichagof-Baranof Island area, and copper-bearing areas in various parts of the Archipelago, especially on Prince of Wales Island and in the Ketchikan area. Considerable exploration of these principal minerals has taken place within the last few years. Tonnages are great, with grades quite variable. Should the Yukon-Taiya hydroelectric project be built, a sizeable portion of its output would be consumed by electric furnace treatment of the Klukwan magnetites. Similarly, processing of the relatively low-grade nickel-bearing ores by electric furnace means (possibly by the low density carbon or dry-top method developed by the U. S. Bureau of Mines at Albany, Oreg.) appears worthy of considerable attention. Regarding the copper-bearing materials of the area, electric-matte smelting might provide a satisfactory economic answer to their exploitation. These possibilities are within the foreseeable future, and promising hydroelectric sites (in addition to Taiya) are favorably situated with respect to major ore bodies. Companies most prominent in evincing interest in the location of electroprocess industries in this area are the Aluminum Co. of America, Reynolds Metals Co., and the Frobisher interests of Canada.

### Southwestern Alaska Region

*Total Potential Installed Kilowatts: Over 4¼ Million*

This enormous region contains some of the most interesting power potentials for mineral and electroprocess industry development. The hydroelectric possibilities of the Gulf of Alaska, the Matanuska Valley, Susitna and Kenai Peninsula area are susceptible of eventual interconnection by means of a high-voltage and high-capacity electric transmission system. It is in this general area that the major portion of Alaska's population resides, and therefore it is the principal center of economic activity in the Territory. Physiographic conditions are such that major land communication routes are well developed, and there exist numerous areas accessible to tidewater which offer facilities for industrial plant establishment.

The largest individual hydroelectric potential is that of the Copper River. The principal project is at Wood Canyon, a few miles below the confluence of the Copper and Chitina rivers, at which point the combined run-off of two valleys, draining an area of 24,000 square miles, flows through a deep rock-walled canyon. About 35 miles below Wood Canyon is a site which appears favorable for the construction of another large dam. Conservative estimates place the potential installed capacity of these two dams in excess of 1,500,000 kw and prime power capabilities of over 1,100,000 kw. A preliminary appraisal of power costs at the two plants is around 3 mills/kwhr, although this figure is very conservative.

Of particular importance with regard to the Wood Canyon and Peninsula site projects is that the upper dam would create a reservoir about 100 miles long. This reservoir would extend into the Chitina Valley to the abandoned site of the famous Kennecott operations (Kennecott Copper Co.), and up the Copper river into the Copper Center-Gulkana area. This reservoir would provide an excellent possibility for the establishment of barge transportation to highly mineralized areas now inaccessible except by air or very arduous surface trails. Industrial plant site areas in the vicinity of Chitina or the upper end of the proposed reservoir near Copper Center would have access to the Edgerton Cut-off Highway and the Richardson Highway into Valdez, with its all-year ocean port. Considerable headway is being made toward the building of a highway along the right-of-way of the abandoned Copper River and Northwestern Railway, built by Kennecott in the early 1900's, from the Cordova area, with its all-year port, up the Copper river past the Peninsula dam and the Wood Canyon sites to Chitina. A highway has been built from Cordova to the Copper river; the route from this area up-river will require some modification, depending on the possible construction of the Copper river dams.

There are many other power sites on various tributaries of the Copper in its head waters such the Nizina, Kennecott, and Tebay in the Chitina drainage; The Tonsina, Klutina, and Tazlina in the upper Copper drainage; and the Bremner and Tiekel rivers below the Wood Canyon site. Preliminary estimates show power costs in ranges between 9 and 15 mills/kwhr. However, as will be the case with most Alaska power sites, investigations have been meager and on a bare reconnaissance basis. It would appear that additional investigations will lead to the development of construction plans for much lower power rates than now estimated.

The Matanuska Valley area has interesting hydroelectric potentials. The largest of those involves a most unusual scheme of development proposed by Reuben Hack, an engineer with the U. S. Corps of Engineers in Alaska. Considerable reconnaissance work carried out by Mr. Hack on his own responsibility shows remarkable possibilities for a power scheme having an installed potential capacity of between 120,000 and 190,000 kw with high prime power capabilities.

The Hack scheme for the Lake George project contemplates using the Knik Glacier as a permanent dam to make possible the full use of waters impounded intermittently in back of the glacier. Under present conditions, Lake George represents the annual accumulation of run-off from an area of approximately 870 square miles, of which 40% comprises glaciers and perennial ice fields Each year, in July or August, the lake overflows the ice barricade across the valley, cutting a channel which widens as it undercuts the glacier front, and empties into the Knik river below the glacier in a torrential flow which lasts only 8–10 days. After the lake empties, the glacier continues its advance and again blocks the channel to repeat the annual cycle. The estimated annual run-off is in excess of 3½ million acre-feet.

In the Hack scheme, one or two large tunnels would be driven through the valley wall (ahead of the glacier front) from the lake to a power plant below the glacier. The tunnels would act both as spillways to pass excess waters below the glacier and as penstocks to the power plant. As a consequence, the Knik glacier would advance against the valley wall, permanently closing the gap or channel which is now cut each year by the overtopping waters of Lake George. Although several questions come to mind, sufficient reliable information is available to indicate that the Hack scheme merits careful consideration.

Power costs from the Hack scheme would range from slightly over 3 mills to slightly under 4 mills for various load factors at the power plant, and between 3½ and slightly over 4 mills transmitted to the Anchorage area, approximately 50 miles distant.

Other power potentials of the Matanuska Valley include the Matanuska river itself, Caribou Creek, and others. The Eklutna project, constructed by the U. S. Bureau of Reclamation, began operations in 1955. This project involves the tapping of a high mountain lake by means of a long tunnel driven through a mountain massif, dropping the waters to the power plant at near tidewater elevation on Knik Arm. The output of this 30,000 installed kilowatt project is transmitted to the Matanuska Valley communities and to the Anchorage area by means of a 115-kv transmission line.

Until the Eklutna project began operations, the Anchorage and Matanuska Valley area depended entirely on thermal power generation. A substantial portion of this generation is obtained by means of modern steam-electric plants in Anchorage and immediate environs utilizing coal from the fields in the lower Matanuska Valley.

The Kenai Peninsula contains a number of relatively small hydro sites. Their development is of considerable importance, not only for the rapidly growing population of the Anchorage area, as well as of the Matanuska Valley and Peninsula area, but also in terms of potential mineral development. It is significant that active planning is under way for the construction of a regional high-voltage, high-capacity transmission network by the Central Alaska Power Association, Inc. (*see* Fig. 2).[3] This network would interconnect the various sites of the Kenai Peninsula, starting with the extremely interesting Bradley Lake at the southwestern extremity of the Peninsula, picking up Kasilof and Kenai river development sites, and then the sites involving the tapping of mountain lakes including Cooper, Crescent, Juneau, Ptarmigan, and Grant. Under preliminary design also is a single-span transmission line crossing of Turnagain Arm to interconnect into the present

[3] A local power agency at present composed of a number of aggressive rural electric cooperative corporations.

FIG. 2. Hydroelectric system of Kenai Peninsula-Anchorage-Matanuska valley.

Anchorage-Matanuska Valley power systems; this single span, if determined feasible of construction, will be the world's largest, or approximately 12,500 ft long.

At present, a detailed engineering report has been completed on Cooper Lake,[4] and engineering studies are under way on Crescent Lake.[5] It is possible that construction will start on Cooper Lake in the summer of 1956. This project would have an installed capacity of 15,000 kw and will tap Cooper Lake by means of a short tunnel, pipeline, and penstock dropping some 740 ft to a power house on Kenai Lake.

With the exception of Bradley Lake, most of the Kenai Peninsula power projects involve estimated power costs ranging from slightly over 5 mills (for Cooper Lake) to around 11 mills/kwhr.

In terms of potential mineral development, Bradley Lake appears to offer the most significant opportunities, especially when considered as a part of the regional transmission network proposed by the Central Alaska Power Association. Present reconnaissance investigations by the U. S. Corps of Engineers and U. S. Geological Survey show that power installations of 30,000 kw may provide costs of between 3 and 4 mills/kwhr depending on load factor. Capacity available on better than 90% load factor would be in the neighborhood of 40,000 to 50,000 kw.

The Susitna Basin, almost directly north of Anchorage, contains some sizeable potential hydroelectric sites. Reconnaissance surveys indicate at least three of them with prime power capabilities of around 200,000 kw. Cost estimates for these are somewhat high, probably about 9 mills/kwhr, but such estimates undoubtedly err on the "high side." These sites lie along the general route thought feasible for interconnection by means of the transmission network discussed later.

Draining into Cook Inlet from the northwest are two important rivers, the Beluga and the Chakachatna. Three possible sites have been reconnoitered for a prime power total of around 150,000 kw. These might have some future importance, with reference particularly to the development of the Beluga coal fields.

Along the base of the Alaska Peninsula and into the Bristol Bay area are a number of streams and lakes. These are generally of small individual hydro potential, and costs are roughly estimated at 8–15 mills/kwhr, and upward. The same situation prevails generally along the Aleutian Peninsula.

Attention has been given to the desirability of constructing a large-capacity and high-voltage transmission system to interconnect the Copper and Chitina, Matanuska, Anchorage, and Kenai Peninsula projects, thence northward up the Susitna Basin to the drainages in which

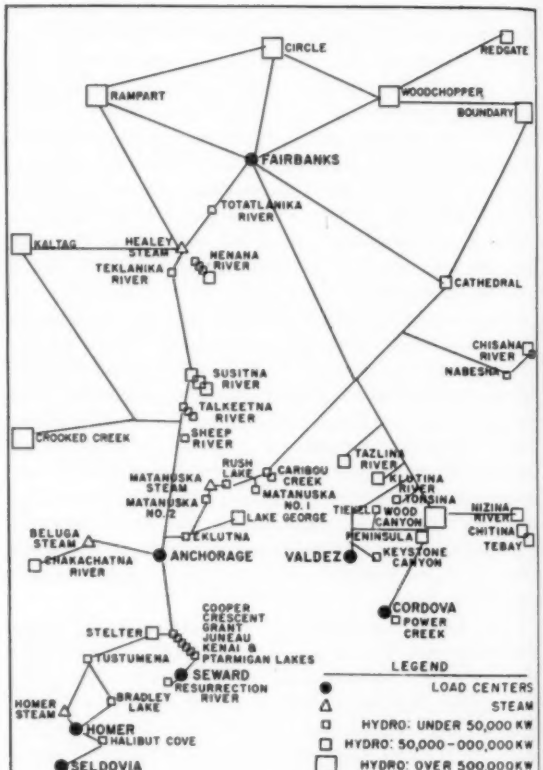


FIG. 3. Generalized scheme showing ultimate high capacity, high voltage electric power transmission network for the Central Alaska region. No attempt has been made to show transmission line routes nor to indicate potential operating voltages. Engineering and economic feasibility of several generating plants is yet to be determined.

[4] Under the auspices of the Central Alaska Power Association.

[5] Under the auspices of the City of Seward.

Fairbanks may be considered centrally located. Preliminary studies have been made by various governmental agencies, by the Central Alaska Power Association, Inc., and by North Pacific Consultants of what would be one of the nation's largest power grid systems (*see* Fig. 3). There appears to be sufficient hydrologic diversity between the various drainage basins to provide definite advantages for large-scale interconnection. Such a power network would make possible the large-scale utilization of the coal resources of the Matanuska, Beluga, and Healy fields by means of steam-electric plants located at mine-mouth. At this juncture, the economics of such a system are not sufficiently clear to warrant an opinion as to ultimate feasibility, but the national power situation urges immediate study and consideration for the portions interconnecting the Copper river areas with those centering about Anchorage and the Kenai Peninsula.

The area described above is immense, and portions are known to be highly mineralized. There is not much question, for example, that the Copper and Chitina drainages contain very large reserves of copper-bearing ores. The abandonment of the Copper River and Northwestern Railroad in the 1930's withdrew the Chitina river area from access; most of the rest of the area is incredibly rugged. The combination of a reservoir such as would result from the construction of the Wood Canyon Dam together with large blocks of low-cost power would not fail to open up a territory rich in mining possibilities. The extent to which electric copper-matte smelting could be conducted near the Wood Canyon site, with ores or concentrates being barged to a plant site in that area, is of course subject to considerable study. However, it would appear to be a logical way to provide high-value matte which could then be trucked down to Valdez or Cordova for transhipment to ocean-going vessels.

The possibility of opening up the area to barge transportation over the reservoir would no doubt stimulate exploration and development so far frustrated by access difficulties. Occurrences of nickel, lead, zinc, and other ores have been reported over the years, but relatively little has been done to explore the area with modern means.

The possibilities of establishing large units of electroprocess industries based on water-borne imports from Pacific Basin countries in the Valdez-Cordova areas, served by means of an appropriate transmission system from the various large hydroelectric sites in the Copper and Chitina basins, are also worthy of attention. To date, Harvey Aluminum, Inc., has obtained a preliminary permit to investigate the Wood Canyon site for precisely that type of power utilization.

As mentioned before, the Bradley Lake potential hydro site also has much merit for investigation with relation to mineral development. The proposed power plant is at the head of Kachemak Bay. At the mouth of the bay, in the Seldovia area, are the well-known chromites of the Kenai Peninsula. Mining operations, which have been under way on portions of the deposits, have been for the purpose of shipping metallurgical, lump chromite. Reserves of other chromites suitable for simple concentration are known to be substantial. The possibilities of an electric furnace operation for the production of various grades of ferrochrome should be considered as good, especially with low-cost power from Bradley Lake and its interconnection with the proposed transmission grid system of the Central Alaska Power Association. Plant sites which might be suitable for the establishment of concentrating and furnace operations would have access to all-year ocean-going transportation.

Of some interest also are possibilities of calcium carbide furnace operations in the same general area, possibly centering at Homer on Kachemak Bay. In this respect, limestones of varying quality are available on Kachemak Bay, and it appears worth investigation to utilize some of the better seams of the Homer area coals for the production of a metallurgical char. Some investigations of this possibility as well as of the ferrochrome operation are under way in a preliminary manner. There is also much discussion of the feasibility of establishment in that area of an ammonium nitrate plant similar to that now operating in Iceland.

The eventual development of power resources in this entire area would have beneficial effects on the expansion of mining activities for gold, platinum, and possibly for other materials such as molybdenum. As pointed out previously, the area is vast and relatively unexplored, so that appraisal of mineral utilization potential cannot be more than sketchy beyond the examples cited.

### Central Alaska Region

*Total Potential Installed Kilowatts: Over 10 Million*

The principal rivers of this tremendous land mass are the Yukon, the Kuskokwim, and the Tanana. Remote and enormous, these rivers until recent years were not considered as having much hydroelectric potential. For the most part, they flow sluggishly with great volume, meandering across great areas of uninhabited country. However, reconnaissance, particularly by the U. S. Corps of Engineers, is changing the former appraisal greatly. It now appears that their hydroelectric potential may be among the world's largest. Three sites have potentials ranging from 1½ to over 3 million kw each of installed capacity, and estimates of the prime power capabilities of these are on the order of 75% of installed capacity. Information so far available does not permit indicating possible power costs, but they may be surprisingly low and suitable for industrial utilization.

Obviously, the development of industrial interest in these sites must be related to accessibility. In that regard, the Kaltag site on the lower Yukon is about 275 miles up the river from Norton Sound on the Bering Sea. Past experience with river boat and barge commerce along the Yukon for almost its entire length would lead one to conclude that this method of transportation is worthy of consideration when open-water navigation is possible during the summer. The same observation regarding water transportation might be applied for the Rampart Circle and Woodchopper sites. Obviously, these are items necessitating careful analysis.

Interconnection of the hydro sites of this area by an extension of the power system described in the previous sections may be desirable and feasible ultimately.

It is not possible to sketch any specific examples in which the development of the water power resources of this area would be advantageous to mineral development. Substantial placer mining for gold is continuing, and possibly the availability of system electric power would assist in its expansion. The immensity of the area and its isolation still place it in the general category, mineral-wise, of "terra incognita." However, there are a number of operations in the area for a variety of minerals. Among those known to exist in variable quantity are silver, zinc, lead, antimony, barite, tungsten, tin, bismuth, mercury, and others. In addition, the Healy coal fields near Fairbanks have been operated for many years. The availability of high-quality limestones in the Windy area on the Alaska Railroad about ⅔ rds of the way from Anchorage to Fairbanks has also stimulated some interest in the establishment of a cement plant to meet the substantial needs for that material in Alaska.

### Northern Alaska Region

*Total Potential Installed Kilowatts: Over ¼ Million*

Most of this area adjoins and is above the Arctic Circle. Several of the large rivers possess substantial summer flows. Surveys have been limited to reconnaissance with interest developing to the point where previous examinations are in the process of revision. The potential susceptible of development may exceed 400,000 kw of prime power. The Noatak river, for example, which empties north of Kotzebue, may possess well in excess of 250,000 kw of prime power. The Colville, which empties into the Arctic Ocean east of Barrow, is by far the largest river of the entire area, but its potential is unevaluated.

Mining operations at present are centered in the Seward Peninsula in the vicinity of Nome. Minerals of interest include gold, silver, lead, zinc, antimony, bismuth, graphite, platinum, mercury, and tin. Most operations depend on captive diesel-generated electric power at high costs. Eventual development of the hydro potential of the area might facilitate expansion of mining activity.

### General Notes

As noted above, there are at least two areas of immediately promising hydroelectric development: Southeastern Alaska with the Taiya-Yukon project, and Southwestern Alaska with the Cooper river (Wood Canyon and Peninsula sites), and the Matanuska-Anchorage, Kenai Peninsula, Susitna areas (Lake George, the Central Alaska Power Association developments and Bradley Lake). These areas combine potentially large blocks of power at costs competitive with those projects remaining in the Pacific Northwest, with access to deep-draft ocean transportation and available population with a substantial labor force. Although mineralization is known to be extensive, the outstanding possibilities are in the electroprocess utilization of iron, nickel, copper, and chromites of the two areas.

In the development of some of the enormous hydro potential of such rivers as the Yukon and Kuskokwim, much work of an investigatory nature must be performed. In this, new engineering approaches must be devised to make feasible lowest cost design and construction of dam and control structures. That is, it is within reason that climatic and soil conditions which appear at first to provide obstacles may well be turned to advantage. For example, considerable thought is being given to permanently frozen earthen structures.

High-voltage, high-capacity networks to transmit huge blocks of hydroelectric power are not unusual in the modern world. Their construction and operation under conditions prevailing in Alaska, however, will require adept use of engineering principles. A promising start is being made in the plans of the Central Alaska Power Association for interconnecting the power potentials of the Matanuska-Anchorage-Kenai Peninsula area.

It is also quite probable that the hydro potential of Alaska, especially southwestern, central, and northern regions, will be developed in concert with the establishment of large coal mine-mouth steam-electric plants, as well as of nuclear reactor power plants. Regarding the latter, preliminary discussions are now under way for two reactors of approximately 10,000 kw capacity.

# Current Affairs

## News Notes in the Electrochemical Field

### New Patron Member

Aluminum Co. of Canada Ltd., Montreal, Que., Canada, recently became a Patron Member of the Society.

### New Sustaining Members

Cramet, Inc., Chattanooga, Tenn.; Titanium Metals Corp. of America, Henderson, Nev.; and Westvaco Chlor-Alkali Division, Food Machinery & Chemical Corp., South Charleston, W. Va., recently became Sustaining Members of the Society.

### Palladium Medal Award for 1957

The fourth Palladium Medal of The Electrochemical Society will be awarded at the Fall Meeting of the Society in Buffalo, N. Y., October 6–10, 1957. The medal was established in 1951 by the Corrosion Division for distinguished contributions to fundamental knowledge of theoretical electrochemistry and of corrosion processes. It is awarded biennially to a candidate selected by a committee appointed by the Society's Board of Directors. This year the Committee members are H. A. Laitinen, J. P. Fugassi, E. B. Yeager, P. Delahay, T. P. May, and N. Hackerman, Chairman.

The Committee requests Sections, Divisions, and members of the Society to send suggestions for candidates, accompanied by supporting information, to *Norman Hackerman, Dept. of Chemistry, University of Texas, Austin 12, Texas.* Candidates may be citizens of any country and need not be members of the Society. Previous medallists are Carl Wagner, Massachusetts Institute of Technology; N. H. Furman, Princeton University; and U. R. Evans, Cambridge University.

### Two Rare Metals Contracts to Horizons Inc.

Horizons Inc., Cleveland industrial research organization, has been engaged by the Kennecott Copper Co. of New York as consultants in the design, erection, and operation of a pilot plant to produce zirconium in the Cleveland area.

The work results from a contract between Kennecott and the Horizons' affiliate, the Horizons Titanium Co. of New York. The pilot plant marks the first non-Government sponsored piloting of this critically important nuclear metal. The facilities will be located on property leased from the Ferro Corp. in the Cleveland suburb of Bedford.

Horizons recently was awarded a $200,000 development contract by the Navy Bureau of Aeronautics for the development of a commercial method for producing virgin titanium metal by an improved electrolytic process.

### NSF Science Grants

The National Science Foundation has announced 289 grants, totaling $3,504,227, awarded during the quarter ending June 30, 1956, for the support of basic research in the sciences, for conferences in support of science, for exchange of scientific information, for training of science teachers, and for the support for attendance of scientists at scientific meetings abroad. This is the fourth and final group of awards to be made during fiscal year 1956. Since the beginning of the program in 1951, 2495 such awards have been made totaling almost $30,000,000.

Grants were made to institutions and scientists in 42 of the States, and Hawaii, Puerto Rico, Great Britain, and France. The research fields included are anthropology, astronomy, chemistry, biology, physics, earth sciences, engineering sciences, mathematical sciences, and socio-physical sciences.

### National Bureau of Standards to be Relocated

A tract of approximately 550 acres of land near Gaithersburg, Md., has been selected for relocation of the Washington laboratories of the National Bureau of Standards. The move will permit the Bureau to plan new buildings to replace present research facilities, which over the past 50 years have become inadequate for current needs. Transfer of operations to the new location is expected to be completed in about five years.

The Bureau occupied its present site on Connecticut Ave. in Washington in 1903. Since that time its responsibilities have greatly increased, largely as a result of the rapid expansion of technology and the growth of scientific research. The new site will enable the Bureau to plan for a more up-to-date plant consistent with its continually increasing responsibilities; and the rural location will remove the Bureau's work from the variety of mechanical, electrical, and atmospheric disturbances present in a city.

In addition to its Washington laboratories, the Bureau maintains a major research center in Boulder, Colo., and 20 widely scattered field stations. The Boulder Laboratories are concerned with radio propagation research, radio standards, and cryogenic engineering. Most of the field stations are engaged in gathering data on radio propagation.

### Manufacturing Chemists' Association Science Education Program

A nationwide education program designed to encourage more of America's youth to follow a career in science was announced recently by the Manufacturing Chemists' Association, Inc.

According to General John E. Hull (U.S.A. ret.), MCA President, the program for a five-year period will cost an estimated $1,000,000 and will include work at elementary, high school, and college levels.

During 1956–57, emphasis will be placed on work with junior high schools. Pilot tests have been conducted in 50 school systems. Printed materials for both students and teachers plus visual aids, such as charts, will be offered science classes of 3600 separate junior high schools during the year.

Simultaneously, a pilot program will be conducted at the senior high school level using a demonstration manual, teaching chart, and film strip. On completion of the pilot study, the program will be offered to the 11,700 high schools in the United States now teaching chemistry. This will cover an estimated 400,000 students.

To promote recognition of the science teacher, the MCA program contemplates the granting of awards to college teachers who have done outstanding instructional work.

### Ultrapure Silicon

Commercially available silicon, even of the highest purity, contains significant amounts of impurities which must be removed if the material is to be used for semiconductor devices. Of these impurities, the most difficult to remove is boron.

H. C. Theuerer of Bell Telephone Labs. has found that boron can be removed from molten silicon by reaction with water vapor. A liquid silicon zone supported only by surface tension is caused to traverse a vertical silicon rod around which flows a mixture of hydrogen and water vapor. This technique prevents contamination from crucibles and provides a large interface between the silicon and the atmosphere.

This method, used together with the zone refining technique developed at Bell Telephone Labs., makes possible the production of silicon containing boron at a concentration below one part in ten billion and having a resistivity greater than 3000 ohm-cm. Improved transistors and other semiconductor devices may result from this ultrapure material.

### Pennsalt Plans Industrial Chemicals Plant in Mexico

To broaden the scope of its operations in Latin America, Pennsalt Chemicals plans early construction of its third plant in Mexico. The new component will be known as Industrial Quimica Pennsalt, S. A. de C. V., and will operate in conjunction with Pennsalt International Corp.

The new installation, located near the company's agricultural chemicals plant in Mexico City, will produce chlorine, caustic soda, muriatic acid, and hydrogen, and is expected to become the first in Mexico to manufacture technical DDT. Robert P. Ogden, former manager of Pennsalt's Riverview, Mich., plant will direct its operations.

### Bound Vol. 102 Available

Copies of bound Vol. 102 (1955) of the JOURNAL are available from Society Headquarters, 216 W. 102 St., New York 25, N. Y.

The Price is $12.00 to members of the Society and $18.00 to nonmembers.

## DIVISION NEWS

### Electric Insulation Division

The officers of the Division for the 1956–57 term are:

*Chairman*—D. A. Lupfer
*Vice-Chairman*—L. J. Frisco
*Secretary-Treasurer*—A. J. Sherburne, 907 Walnut St., Coshocton, Ohio

L. J. FRISCO, *Vice-Chairman*

## SECTION NEWS

### Boston Section

The following programs have been scheduled for the 1956–57 meeting year:

*October 15*—H. H. Uhlig, M.I.T., "Electrochemistry of Corrosion."

*November 15*—President Hans Thurnauer, Minnesota Mining & Mfg. Co., "Recent Advances in Ceramics."

*January 9, 1957*—R. C. Wade, Metal Hydrides, Inc., "Metal Hydrides."

*March 21, 1957*—F. J. Biondi, Bell Telephone Labs., "New Sources of Electrical Energy."

*May 6, 1957*—R. M. Bowie, Sylvania Electric Products Inc., "Color Television."

All meetings will be held at the M.I.T. Graduate House, 305 Memorial Drive, Cambridge, Mass. All interested persons are invited to attend.

CHARLES LEVY, *Secretary*

### Midland Section

The officers of the Section for 1956–57 are:

*Chairman*—P. R. Juckniess
*Vice-Chairman*—H. W. Schmidt
*Secretary-Treasurer*—P. F. George, Dow Chemical Co., Midland, Mich.
*Representatives on Council of Local Sections*—F. W. Koerker and R. C. Kirk

P. R. JUCKNIESS, *Chairman*

### Ontario-Quebec Section

The spring meeting of the Section was held on May 11 at McGill University, Montreal, Canada. The program consisted of a symposium on "Power Resources of Canada" under the chairmanship of Dr. A. O. Dufresne, Deputy Minister, Quebec Dept. of Mines. The speakers were:

H. Massue, Shawinigan Water and Power Co.—"Hydroelectric Resources of Quebec and Eastern Canada"

W. Preston, Hydroelectric Power Commission of Ontario—"Hydroelectric Resources of Ontario and Midwest Canada"

R. M. Bibbs, British Columbia Electric Co. Ltd.—"Hydroelectric Resources of British Columbia and the Yukon"

C. E. Baltzer, Dept. of Mines and Technical Surveys of Canada—"Power from Other Energy Sources in Canada."

Only three countries produce more electric power than Canada. Each of these countries, the United States, Russia, and the United Kingdom, has 3 to 14 times as large a population as Canada, and their electric power is derived mostly from coal-fired steam plants. At the present time 95% of the power produced in Canada is from hydroelectric sources. However, this situation can be expected to change since the reserves of natural gas, crude

### 1956 Extended Abstracts

The Electronics Division has available copies of the "Enlarged Abstracts" booklet, "printed but not published," containing 1000-word abstracts of papers presented at the Division's symposia on Luminescence and Semiconductors at the San Francisco Meeting of the Society, April 29–May 3.

The booklets are available at $2.00 each from:
Martin F. Quaely
Research Dept., Lamp. Div.
Westinghouse Electric Corp.
Bloomfield, N. J.

* * *

The Theoretical Electrochemistry Division also has available copies of the extended abstracts booklet of papers presented at the sessions of the Theoretical Division at the San Francisco Meeting of the Society. The booklet also contains abstracts of papers presented at the Symposium on "Adsorption Phenomena at Electrode Surfaces" sponsored jointly by the Theoretical Electrochemistry and Corrosion Divisions.

Copies can be obtained at $2.00 each from:
Ernest Yeager
Dept. of Chemistry
Western Reserve University
Cleveland 6, Ohio

oil, and particularly coal, are very great compared to the amount of water power which can be produced.

It is apparent that, of the energy sources available, coal is by far the most abundant. While water power is only a small fraction of the total, its importance in Canada's economy is considerable. This is due to its availability and its renewable characteristic in the otherwise energy-deficient area of the "St. Lawrence Lowlands." This relatively small area supports as much as 60% of Canada's total population and the bulk of the secondary industries, and requires (with minor exception) import of all its fuel energy, either from distant points in Canada or from the United States. On the other hand, the proven oil and gas reserves in Canada, although not large in comparison with coal, are increasing at a phenomenal rate. One authority recently estimated that by 1980 the proven oil reserves will be about 5 times greater than they are today.

The situation with regard to atomic power was summarized by calling attention to statements in the press by Mr. J. A. Fuller, President, Shawinigan Water and Power Co., and Sir John Cockcroft, Director, Atomic Energy Research Establishment, Harwell, England, who indicated that there was little likelihood of any widespread use of atomic power in countries like Canada where abundant supplies of hydroelectric power and fossil fuel resources exist.

The way in which much of this Canadian power is being utilized has been described in an excellent series of articles.*

R. R. ROGERS,
*Secretary-Treasurer (1955–56)*

The officers of the Ontario-Quebec Section for 1956–57 are:

*Honorary Chairman*—A. H. Whitaker, Jr.

*Chairman*—John Sumner

*Vice-Chairman (Membership)*—R. R. Rogers

*Vice-Chairman (Programs)*—T. S. Gamble

*Chairman Junior Membership Committee*—J. U. MacEwan

*Secretary-Treasurer*—H. A. Timm, Dominion Magnesium Ltd., Haley, Ont., Canada

H. A. TIMM, *Secretary-Treasurer*

*A. C. HOLM AND V. G. BARTRAM, *This Journal*, **100**, 295*C* (1953); **101**, 7*C*, 41*C*, 67*C* (1954).

## Proposed Mohawk-Hudson Section

On July 25, a meeting was held at the Edison Club, Rexford, N. Y., to initiate the Mohawk-Hudson Section of the Society. The Section is proposed to serve the interests of the Tri-City area, a 50-mile radius from Troy, Schenectady, and Albany.

The meeting was conducted by Dr. Harold R. Schmidt. A nominating committee was appointed. Dr. Norman Hackerman spoke on "Streaming Current Measurements on Metals." A resumé of his talk follows.

A method for measuring streaming currents in small radius metal capillaries was described. It depends largely on using a measuring circuit which effectively "shorts" the current caused by moving a solution by the metal wall so that the current cannot return through that wall. In distilled water ($K = 2 \times 10^{-6}$ ohms$^{-1}$ cm$^{-1}$) the zeta potentials for Pt, Au, and Hg were $61.0 \pm 1.0$, $60.8 \pm 1.0$, and $49.0 \pm 4.0$ mv, respectively. The values were rationalized in terms of the solubilities of the oxides, and predictions of the effects of adding small quantities of electrolytes were shown to be satisfactory.

Plans are being made for a September meeting. Tentative copies of the constitution and bylaws will be distributed at that time.

C. B. MURPHY, *Acting Secretary*

## PERSONALS

L. H. JUEL, manager of research and development for the Electrode Division of Great Lakes Carbon Corp., Niagara Falls, N. Y., recently served as a guest lecturer at a refractories symposium held by State University of New York College of Ceramics at Alfred University, Alfred, N. Y. His topic was "Carbon and Graphite Refractories."

EDGAR L. ECKFELDT has been appointed Assistant Division Chief of the Chemical Division of the Research and Development Dept., Leeds & Northrup Co., Philadelphia, Pa. Dr. Eckfeldt has been with Leeds & Northrup since 1942.

MORRIS EISENBERG, of Palo Alto, Calif., has joined Thermo Materials, Inc., as Vice-President in charge of research. The firm manufactures high temperature industrial ceramics. Dr.

*Faster, easier, better*

HEAT

CONTROL

AGITATION

*at the Turn of a Dial*

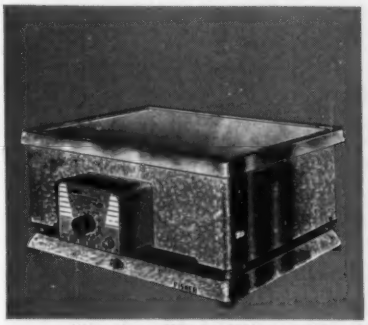

Dimensions: 8½" h., 18½" w., 14½" d.

**FISHER OSCILLATING HOT PLATE**

The Fisher Oscillating Hot Plate assures rapid and complete mixing, dissolving, precipitation or evaporation without spattering at a constant 216 rpm, with or without heat. 2000 watt cast-in-aluminum heating element, operating at 200° F to 700° F surface temperatures, gives faster, more uniform heat distribution. Stepless control allows operator to dial and duplicate the exact heat every time, all the time, for maximum effectiveness with minimum attention. Heater and oscillator operate independently or together.

**Send for details**

The new Fisher Catalog Supplement, page 53, gives specifications on the Fisher Oscillating Hot Plate. Send for your copy.

Write: 110 Fisher Bldg., Pittsburgh 19, Pa.

**FISHER SCIENTIFIC**

Boston, Buffalo, Chicago, Cleveland, Detroit, New York, Philadelphia, Pittsburgh, St. Louis, Washington, Montreal, Toronto

*America's Largest Manufacturer-Distributor of Laboratory Appliances and Reagent Chemicals*

8-1-A

Eisenberg previously was with Stanford Research Institute in Menlo Park.

ROBERT H. CHERRY has been named to the position of Associate Director of Research and Development, in charge of research, Leeds & Northrup Co., Philadelphia, Pa. Mr. Cherry, who joined the company in 1929, has been Chief of the Chemical Division of the Research and Development Dept. since 1951.

## BOOK REVIEWS

VAPOR-PLATING by C. F. Powell, I. E. Campbell, and B. W. Gonser. Published by John Wiley & Sons, Inc., New York, N. Y., 1955. vi + 158 pages, $5.50.

The preparation of supported films must still be regarded as a highly specialized art as well as a science. "Vapor Plating" is concerned with film formation, both metallic and nonmetallic, by the chemical reaction of a suitable vapor and substrate. As such, it is a valuable supplement to other methods in film technology such as vacuum evaporation, sputtering, electrodeposition, and solution deposition. Films which cannot easily be produced by other methods are often prepared with ease by vapor plating.

This book is an outgrowth of work at the Battelle Memorial Institute, which was concerned with the evaluation of metallic and refractory coatings. The subject matter of the book is, accordingly, divided into the preparation of films of metals, carbides, nitrides, borides, silicides, and oxides.

While the book is not intended to be a comprehensive and detailed reference course on the properties of vapor-plated materials, physical and chemical properties of the above-prepared coatings are enumerated in considerable detail. The techniques of the art which are described in the Introduction will no doubt be of interest to workers in film technology.

S. LEVINSON

DIELECTRIC BEHAVIOR AND STRUCTURE by Charles P. Smyth. Published by McGraw-Hill Book Co., Inc., New York, N. Y., 1955. 441 pages, $9.00.

In the years since Debye put forward the now accepted theory of the dielectric constant and dielectric loss, the literature on these subjects has grown steadily. Professor Smyth, who has contributed so much to this field himself, has organized this literature in a useful and systematic way. The presentation of a unified discussion of the theory and experimental results is a substantial contribution to the subject.

The coverage is intended to be broad rather than deep, comprehensive rather than exhaustive. The theory, which is still actively developing, is treated more thoroughly elsewhere. The tabulated data are not all inclusive. Details of experimental techniques are not presented. On the other hand, the discussion of the relation between structure and dipole moment is the best available anywhere.

The style is straightforward, the format satisfactory, and the price a bit too high.

This book is highly recommended to chemists, teachers, and students.

BENSON R. SUNDHEIM

CHROMIUM, Vol. I. Chemistry of Chromium and its Compounds. Edited by Marvin J. Udy. Published by Reinhold Publishing Corp., New York, N. Y., 1956. xiii + 433 pages, $11.00.

In this ACS monograph, the attempt is made to present a critical compilation of the best data and knowledge currently available relating to the history, mineralogy, geology, toxicology, and analytical chemistry of chromium, the chemical and physical properties of its compounds, and the manufacture and industrial use of chromium compounds. Of particular interest to readers of this JOURNAL will be Chap. 6, Physical and Chemical Properties of Compounds of Chromium (138 pp.); Chap. 12, Chromium Chemicals in Corrosion Prevention (14 pp.); and Chap. 14, Chromium Chemicals in the Graphic Arts (21 pp.).

S. Z. LEWIN

GAS CHROMATOGRAPHY by Courtenay Phillips. Published by Academic Press, Inc., New York, N. Y., 1956. x + 105 pages, $3.80.

This slim volume presents an extremely lucid account of the relatively new and rapidly expanding field of gas-liquid partition chromatography. In brief but comprehensive fashion it describes basic theoretical principles, apparatus and detection devices, types of results that have been obtained, and the relative advantages and disadvantages of gas-liquid partition vs. gas adsorption, elution vs. displacement analysis. This book should be read by all who wish to become familiar with the subject of chromatography in the vapor phase.

S. Z. LEWIN

## 1956 Directory

The 1956 Directory of Members of the Electrochemical Society is now available. The Directory contains an alphabetical and geographical list of members of the Society as of March 1, 1956, and a list of Patron and Sustaining Members, Past Presidents, and winners of Society prizes and awards.

Members who wish to receive the Directory are requested to fill in and return the order form below, accompanied by check, to Society Headquarters, 216 West 102 St., New York 25, N. Y.

Please send_____copy(ies) of the 1956 Membership Directory to:

Name_____

Company_____

Street_____

City_____ Zone____ State_____

Attached is check for $_____ for Directory. (Single copies cost $2.00.)

## ANNOUNCEMENTS FROM PUBLISHERS

1952–1953 BIBLIOGRAPHIC SURVEY OF CORROSION. Publication No. 56-11. Compiled by A. Irene Humphrey. Published by National Association of Corrosion Engineers, 1061 M & M Bldg., Houston 2, Texas, 1956. 382 pages, hard cloth binding. Price:

nonmembers NACE, $12.50; members NACE, $10.00.

Summaries of 3344 corrosion and corrosion prevention articles, books, and brochures published in 1952–1953 are compiled in this volume. Material was selected from bulletins published by more than 30 abstracting agencies representing international literature coverage.

Abstracts are arranged topically according to the NACE Abstract Filing Index, dividing the literature into eight main groups: general, testing, characteristic corrosion phenomena, corrosive environments, preventive measures, materials of construction, equipment, and industries. Each main group is subdivided. Topical cross references are appended to each section.

The subject index, in addition to terms in the NACE Abstract Filing Index, lists many metals and alloys by trade name and indexes them as to specific properties and to behavior in specific media. An author index is included. All referencing is to classification and serial numbers of abstracts for ease in searching. An appendix has been included to aid the user in locating and obtaining copies of unfamiliar foreign or domestic journals.

ASTM Standards on Metallic Electrical Conductors. Published by American Society for Testing Materials, 1916 Race St., Philadelphia 3, Pa. 300 pages, heavy paper cover, $3.50.

All of the ASTM Standards pertaining to metallic electrical conductors, which were developed by ASTM Committee B-1 on Wires for Electrical Conductors, and related standards from other committees of the ASTM have been compiled in compact, readily useable form. The December 1955 edition of ASTM Standards on Metallic Electrical Conductors includes in their latest form 52 ASTM standards—43 specifications, 7 test methods, 1 recommended practice, and 1 classification of coppers. Of the material included in this compilation, 20 of the specifications have been revised and one of the standards is new since the previous edition.

## NEW PRODUCTS

Tubeless d-c Source. A new tubeless d-c source, providing 6vdc and 2vdc output voltages regulated to within ± 0.01%, has been introduced. The transistorized circuit employed in the unit, Model MA6501, combines reliability with rugged construction and precise performance. A silicon diode is used as reference element, and a transistor amplifier provides the control current for the magnetic amplifier. The transistor amplifier is temperature-compensated for small ambient room changes. Complete specifications and performance data available. *Sorensen & Co., Inc.*, Fairfield Ave., Stamford, Conn.

Zone Electrophoresis Apparatus. An apparatus completely furnished with all accessories required for operation and designed for processing either paper strips or starch blocks is available. Using the free horizontal suspension of strips, the apparatus overcomes a number of drawbacks previously associated with this system. Rapid and complete moisture saturation of the strips, assured by a tight sealing cover and no waste space above the paper, provides uniform electrical resistance. The ability to transfer the strips directly to a drying oven by insertion of the entire paper carrier is an added feature. Electrodes are made of platinum and electrolytic decomposition products are effectively screened from the buffer chambers. The detailed instruction book which accompanies the instrument includes a comprehensive and indexed bibliography of all research papers in the field of paper and zone electrophoresis published to date. *Laboratory Glass & Instruments Corp.*, 514 W. 147th St., New York 31, N. Y.

Computing Telemetering System. A new system of telemetering instruments which will totalize several flow measurements, correct for such factors as temperature, pressure, specific gravity, and supercompressibility in fluids, and which will provide a corrected flow value, is available. This system of telemetering tramsmitters and receivers, and electronic self-balancing instruments, can be used wherever corrected flow values are vital for proper operation. *The Bristol Co.*, Waterbury 20, Conn.

Mercury Lamp. A new, 1000-watt mercury lamp with an interior phosphor reflector which directs ⅔ of the light downward has been announced. The lamp, designated G-E H1000 RC 15, is in the same group of lamps which includes the H1000 A15, a clear

## MANUSCRIPTS AND ABSTRACTS FOR SPRING MEETING

Papers are now being solicited for the Spring Meeting of the Society, to be held at the Statler Hotel in Washington, D. C., May 12, 13, 14, 15, and 16, 1957. Technical Sessions probably will be scheduled on Electric Insulation, Electronics (including Luminescence, Semiconductors, Oxide Cathodes, Instrumentation, and possibly Screen Applications), Electrothermics and Metallurgy, Industrial Electrolytics, and Theoretical Electrochemistry (including a special symposium on electrolytes).

To be considered for this meeting, triplicate copies of abstracts (*not to exceed 75 words in length*) must be received at Society Headquarters, 216 West 102nd St., New York 25. N. Y., *not later than January 2, 1957. Please indicate on abstract for which Division's symposium the paper is to be scheduled.* Complete manuscripts should be sent in triplicate to the Managing Editor of the Journal at the same address.

* * *

The Fall 1957 Meeting will be held in Buffalo, N. Y., October 6, 7, 8, 9, and 10, 1957, at the Statler Hotel. Sessions will be announced in a later issue.

glass 1000-watt mercury lamp, and the H1000 RC 15, a phosphor coated, 1000-watt mercury lamp with improved color. The new lamp is $15\frac{1}{16}$ in. long, has a mogul base, is rated at 53,000 lumens, and will cost $56 list. It will be used in medium and high mounting in industrial installations. *General Electric Co.*, Lamp Division, Nela Park, Cleveland 12, Ohio.

## LITERATURE FROM INDUSTRY

CORROSION PROOFING MANUAL. A revised edition of Pennsalt Chemicals' reference manual on corrosion proofing provides information on the latest developments in this field. Included are descriptions of the application of Corlok, an entirely new type chemical-resisting mortar recently introduced by Pennsalt. Corlok is a special silicate bonding material which is resistant to sulfation and highly concentrated acids at temperatures up to 1900°F for long periods of time. *Pennsalt Chemicals*, Corrosion Engineering Dept., 3 Penn Center Plaza, Philadelphia 2, Pa.

CHLORINE AND CAUSTIC SODA CHARTS. Two illustrated wall charts presenting up-to-date instructions for the safe handling of chlorine and caustic soda have been prepared. The chlorine chart describes proper procedures for unloading tank cars and ton containers, what to do in case of a leak, and first aid measures to be followed in the event of exposure to chlorine. The caustic soda chart presents steps for unloading tank cars of 50% and 73% caustic, and a list of safety Do's and Don't's to be observed in handling the material. *Olin Mathieson Chemical Corp.*, Industrial Chemicals Div., Baltimore 3, Md.

STANDARD AND SIMPLIFIED DRAFTING. A 56-page booklet on "Standard and Simplified Drafting Practices" is being offered. The first section contains a speech on this provocative subject as given by Jay H. Bergen, AMF Standards Administrator, before the American Society for Engineering Education. The remaining 44 pages are devoted to the details of AMF standards on Drafting Room Practice and Simplified Drafting. For free copy, write on company letterhead to *American Machine & Foundry Co.*, Public Relations Dept., 261 Madison Ave., New York 16, N. Y.

AMERICAN POTASH PRODUCT BULLETINS. American Potash & Chemical Corp. has issued informational product bulletins on the series of electrochemicals produced at its Henderson, Nev., plant, including sodium and potassium chlorate, ammonium and potassium perchlorate, and manganese dioxide. The bulletins include analysis, description, and applications in various manufacturing processes. *Robinson-Hannagan Associates, Inc.*, 6671 Sunset Blvd., Los Angeles 28, Calif.

## ADVERTISERS' INDEX


Allis-Chalmers Manufacturing Company ..... 224C
American Brass Company .. 234C
Baker & Adamson Products, General Chemical Division, Allied Chemical & Dye Corporation ..... 225C
Enthone, Incorporated ... Cover 4
Fisher Scientific Company ... 231C
Great Lakes Carbon Corporation ..... Cover 2
E. H. Sargent & Company ... 226C



# "Plus-4" Anodes make better boot molds too!

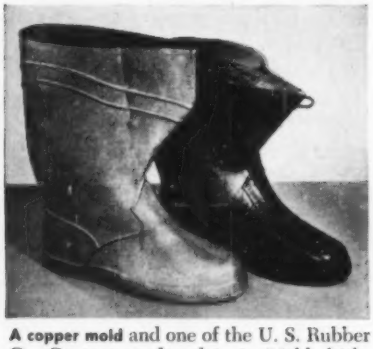

**A copper mold** and one of the U. S. Rubber Co. Gaytees produced in it. Mold thicknesses vary from .035" to .090", depending on size and type of boot.

**Each electroforming tank can** plate 10 molds —uses standard acid-plating solution and 35 "Plus-4" Rolled Anodes, ½" x 8" x 20" —300 amps power input.

IN ELECTROFORMING—as in acid electroplating and electrotyping—ANACONDA "Plus-4" (Phosphorized Copper) Anodes are turning in superior performance records.

The Shoe Hardware Div. of U. S. Rubber Co. electroforms the copper molds used in the production of rubber and plastic rainwear known as Gaytees®. With ordinary anodes, they had been troubled with porosity and "treeing."

Nearly two years ago, they turned to "Plus-4" Anodes and report the following advantages: 1. Extremely smooth plating, without "treeing." 2. Good grain build-up. 3. No porosity. 4. Uniform anode corrosion with consequent scrap reduction. 5. Savings in solution correction due to reduction of sludge and copper build-up. 6. All-round cleaner plate.

You have everything to gain and nothing to lose by setting up one acid-copperplating tank to test "Plus-4" Anodes. Send in the coupon today. 5814

The American Brass Co., Waterbury 20, Conn.
*In Canada:* Anaconda American Brass Ltd., New Toronto, Ont.

Give me details on how I can get a test supply of "Plus-4" Anodes sufficient to fill one tank.

NAME.....
COMPANY.....
ADDRESS.....
CITY.....ZONE....STATE.....

"Plus-4" Anodes
(Phosphorized Copper)
*A product of*
ANACONDA®
Made by The American Brass Company
For use under Pat. No. 2,689,216


**To receive further information on any New Product or Literature from Industry listed write directly to the company at the address given in each item.**

# The Electrochemical Society

## INSTRUCTIONS TO AUTHORS OF PAPERS

Address all correspondence to the Editor, JOURNAL OF THE ELECTROCHEMICAL SOCIETY, 216 W. 102nd St., New York 25, N. Y.

### FORM

***Manuscripts*** submitted for publication should be in triplicate to expedite review. They should be typewritten, double-spaced, with 2½–4 cm (1–1½ in.) margins.

***Title*** should be brief, followed by the author's name and his business or university connection.

***Abstract*** of about 100 words should state the scope of the paper and give a brief summary of results.

### ILLUSTRATIONS

***Drawings*** will be reduced to column width, 8 cm (3⅛ in.), and after reduction should have lettering at least 0.15 cm (1/16 in.) high. Original drawings in India ink on tracing cloth or white paper are preferred. Curves may be drawn on coordinate paper only if the paper is ruled in blue. All lettering must be of lettering-guide quality. See sample drawing on reverse page.

***Photographs*** must be glossy prints and mounted flat.

***Captions*** for all figures must be included on a separate sheet. Captions and figure numbers should not appear in the body of the figure.

***General***—Figures should be used only when necessary. Omit drawings or photographs of familiar equipment. Figures from other publications are to be used only when the publication is not readily available, and should always be accompanied with written permission for reprinting.

### REFERENCES

Literature and patent references should be listed at the end of the paper on a separate sheet, in the order in which they are cited. They should be given in the style adopted by *Chemical Abstracts*. For example:

R. Freas, *Trans. Electrochem. Soc.*, **40,** 109 (1921).

H. T. S. Britton, "Hydrogen Ions," Vol. **1,** p. 309, D. Van Nostrand Co., New York (1943).

H. F. Weiss (To Wood Conversion Co.), U. S. Pat. 1,695,445, Dec. 18, 1928.

### UNITS OF MEASUREMENT

Metric units should be used throughout but, where desirable, English units may be given in parentheses.

Corrosion rates in the metric system should preferably be expressed as milligrams per square decimeter per day (mdd), and in the English system as inches penetration per year (ipy).

As regards algebraic signs of potentials, the standard electrode potential for $Zn \rightarrow Zn^{++} + 2e$ is negative; for $Cu \rightarrow Cu^{++} + 2e$, positive.

## ABBREVIATIONS

Abbreviations should conform with the American Standards Association's list of "Abbreviations for Scientific and Engineering Terms."

## GENERAL

Authors should be as brief as is consistent with clarity, and must omit all material which can be regarded as familiar to specialists in the particular field.

The use of proprietary names, trade-marks, and trade names should be avoided if possible. If used, these should be capitalized so that the owner's legal rights are not jeopardized

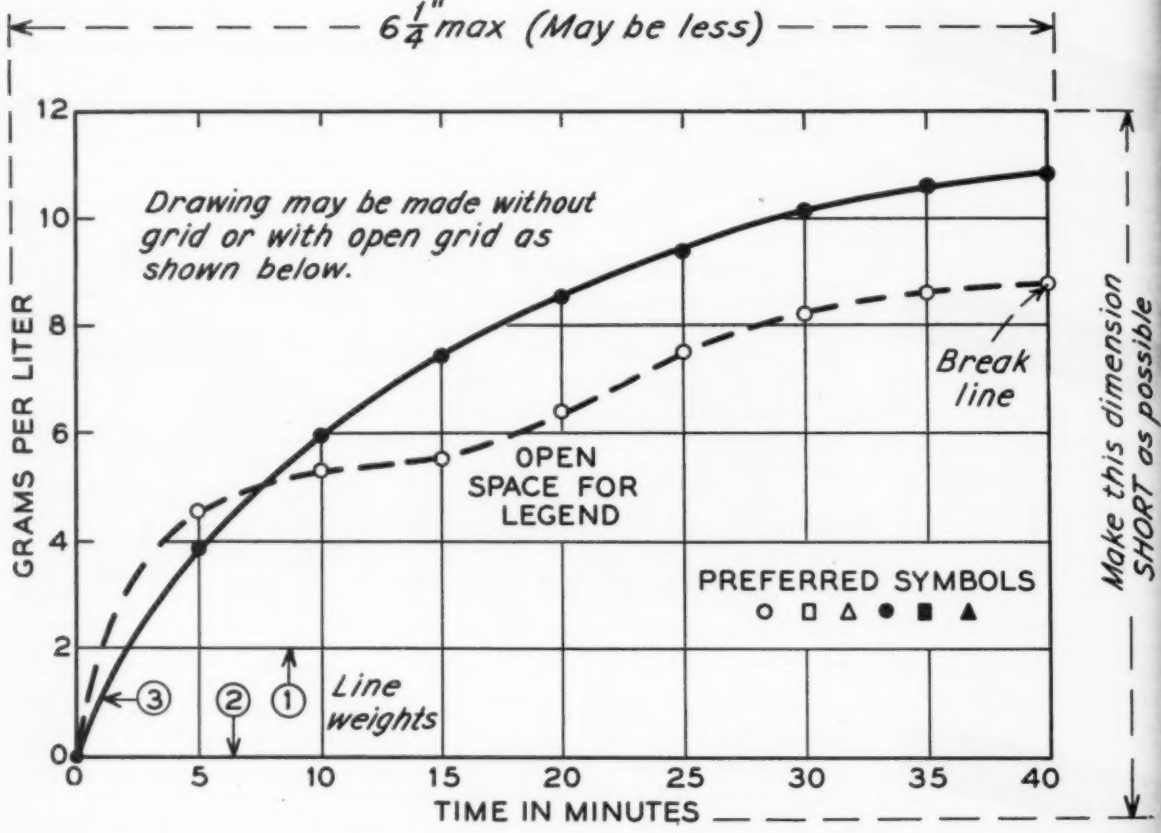
6 1/4" max (May be less)
Drawing may be made without grid or with open grid as shown below.
Break line
OPEN SPACE FOR LEGEND
PREFERRED SYMBOLS
○ □ △ ● ■ ▲
③ ② ① Line weights
GRAMS PER LITER
TIME IN MINUTES
0 2 4 6 8 10 12
0 5 10 15 20 25 30 35 40
Make this dimension SHORT as possible

*Remarks: Line weight ② is used for borders and zero lines. When several curves are shown, each may be numbered and described in the caption. Lettering is approx. 1/8".*

SAMPLE CURVE DRAWING FOR REDUCTION TO $\frac{1}{2}$ SIZE

n's list

ll ma-
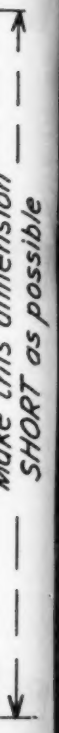
voided
ts are